Percorso dottorale sviluppato con il sostegno finanziario di NextGenerationEU:

Missione 4, Componente 2, Investimento 3.3, CUP B63C22000980008

Borsa MUR ex DM 352/2022

Dipartimento di Scienze della Vita

Dottorato in Scienze della Vita – Life Sciences

38° Ciclo

Coordinatrice: Prof.ssa Simona Maccherini

Development and characterization of viral pseudotypes as safe tools for investigating WHO Priority Pathogens

Settore scientifico disciplinare: MEDS-24/B

Candidata

Dr. ssa Vittoria Forconi

Università di Siena – VisMederi Srl

Firma digitale della candidata

09/03/2026 08:56:52
VITTORIA FORCONI

Vittoria Forconi

Supervisore

Prof. Emanuele Montomoli

Dipartimento Medicina molecolare e dello sviluppo – Università di Siena

Co-supervisore

Dr. ssa Silvia Grappi

Project Director – VisMederi Srl

Anno accademico di conseguimento del titolo di Dottore di ricerca

2024/2025

Università degli Studi di Siena

Dottorato in Scienze della Vita – Life Sciences

38° Ciclo

Data dell'esame finale

24 marzo 2026

Commissione giudicatrice

Prof. ssa Sara Epis

Dipartimento di Bioscienze – Università statale di Milano

Prof. ssa Elena Pariani

Dipartimento di Scienze Biomediche per la Salute – Università statale di Milano

Prof. Emanuele Montomoli

Dipartimento Medicina molecolare e dello sviluppo – Università di Siena

INDEX

INDEX OF FIGURES

INDEX OF TABLES

1 ABBREVIATION LIST

ACE-2	Human Angiotensin I converting enzyme 2
BSL	Biosafety Level
CEPI	Coalition for Epidemic Preparedness Innovations
CHICKV	Chikungunya Virus
COVID-19	Coronavirus disease 2019
DMEM	Dulbecco’s modified essential medium
DPP-4	Dipeptidyl peptidase-4
EBOV	Ebola Virus
EBOVD	Ebola virus disease
EMA	European Medicines Agency
F&T	Freezing and thawing
FBS	Fetal Bovine Serum
FDA	Food and Drug Administration
GP	Glycoprotein
HCoV-HKU1	Human coronavirus HKU1
HCoV-OC43	Human coronavirus OC43
HEK	Human embryonic kidney

HIV-1	Human Immunodeficiency virus-1
IC_{50}	Half maximal-inhibitory concentration
ICTV	International Committee on Taxonomy of Viruses
LASV	Lassa Fever virus
L-GLUT	L-Glutamine
mAb	Monoclonal antibody
MARV	Marburg Virus
MARVD	Marburg virus disease
MCMs	Medical countermeasures
MERS-CoV	Middle East Respiratory Syndrome Coronavirus
MLV	Murine Leukemia virus
NiV	Nipah Virus
NP	Nucleoprotein
pAb	Polyclonal antibody
PAC	Prioritization Advisory Committee
PBNA	Pseudotype-Based Neutralization Assay
PEN-STREP	Penicillin-streptomycin
PES	Polyethersulfone

PHEICs	Public Health Emergencies of International Concern
PV	Viral pseudotype
R&D	Research and Development
RdRp	RNA dependent RNA polymerase
RLU	Relative Light Unit
SARS-CoV-1	Severe Acute Respiratory Syndrome Coronavirus 1
SARS-CoV-2	Severe Acute Respiratory Syndrome Coronavirus 2
TMPRSS2	Transmembrane protease serine 2
VSV	Vesicular Stomatitis virus
WHO	World Health Organization
Z	Zinc

2 ABSTRACT

Recent outbreaks of highly pathogenic human RNA viruses have highlighted the importance of epidemic and pandemic research preparedness within society. Due to their biological risk, authentic viruses require handling by experienced personnel in high containment level laboratories; therefore, research efforts for the establishment of therapeutic and prevention strategies are hindered and slowed down. Pseudotyped viruses, which are surrogate, non-pathogenic recombinant viral particles bearing the envelope protein of the virus of interest, represent a safe alternative to circumvent the drawbacks highlighted by “live” viruses.

Aims of this work are threefold: provide a library of viral pseudotypes for selected World Health Organization (WHO) priority pathogens, compare practical workflow and production yields across the three applied packaging platforms (lentiviral two/three-plasmids platforms and VSV based system) and validate each construct through pseudotype based neutralization assays using appropriate controls in order to support evaluation of vaccines and antiviral agents in practice.

Viral pseudotypes are produced in HEK293T/17 cells under standardized transfection and harvest conditions. Lentiviral systems use pNL4-3 (two-plasmid platform) or p8.91 with pCSFLW (three-plasmid platform) alongside pathogen-specific envelopes; VSV based particles are generated by transient glycoprotein expression followed by VSV-ΔG-LUC*G infection. Titration and neutralization assays are based on luciferase readout and employ target cells that match viral entry requirements. Three-plasmid lentiviral and VSV based platforms generally out-performed the two-plasmid lentiviral system.

Most pseudotypes achieved the titer threshold needed for their application in neutralization assays. In case of Nipah pseudotypes, where titers lagged, process refinements (freeze-thaw cycles and subsequent concentration) improved performance. Neutralization behaved as expected: positive controls neutralized pseudotypes (observed as a suppression of luciferase signal), whereas negative controls did not provide a protective titer. Overall, the work delivers reproducible routes to generate functional pseudotypes as a shareable resource that strengthens vaccine and antiviral testing for pandemic preparedness.

3 INTRODUCTION

3.1 Background on WHO Priority Pathogens and prioritization process

The WHO, founded in 1948, is a specialized agency of the United Nations with a broad mandate to act as a coordinating authority on international health issues, including helping countries mount responses to public health emergencies (Kaiser Family Foundation, 2024). Since 2015, WHO R&D Blueprint for Epidemics has a primary goal to accelerate the development of medical countermeasures (MCMs) for diseases with epidemic and pandemic potential, thereby contributing to the prevention of Public Health Emergencies of International Concern (PHEICs).

The WHO R&D Blueprint for Epidemics functions as a global platform for R&D collaboration, stressing the significance of international cooperation in expediting the R&D of MCMs to respond to epidemics and pandemics (World Health Organization, 2024). The first WHO priority pathogen list was published in 2017 and is routinely updated; this is because novel pathogens can exploit current weaknesses of healthcare systems, while re-emerging pathogens may evolve to resist previously effective treatments and preventive methods (Polgreen PM *et al*., 2017).

Regarding the 2024 list, an initial review was conducted on 28 viral families and one main group of bacteria, for a total of 1652 pathogens. Following this, the Prioritization Advisory Committee (PAC) analyzed evidence from 8 DNA virus families, 19 RNA virus families, and five bacterial families. As a result, the final 2024 list includes a minimum of 27 viral families and five bacterial families. The viral families were originally collected based on the classifications by the International Committee on Taxonomy of Viruses (ICTV), with a focus on those associated with human pathogens that could lead to outbreaks. Families that were unlikely to pose an epidemic or pandemic threat were excluded from consideration. For the remaining families, experts evaluated the pathogens based on their transmission, virulence, the availability of MCMs, and the potential to evolve into a future threat which is referred to as Pathogen X. This assessment used a questionnaire that looked at the pathogen's spread, disease severity, available treatments, and the possibility of an outbreak. The selection

focused on pathogens with the potential to cause a PHEIC, considering both current knowledge and possible future risks (Ukoaka BM *et al*., 2024). Table 1 shows Families and Pathogens that were prioritized by the WHO R&D Blueprint for Epidemics in the 2024 updated version, compared with the 2017 and 2018 prioritizations.

Within the list, the viral families of concern related to this work are: *Arenaviridae*, *Coronaviridae*, *Filoviridae*, *Paramyxoviridae*, and *Togaviridae*. In particular, the viruses of interest belonging to the listed families are: Lassa Fever Virus (LASV) (family *Arenaviridae*), Middle East Respiratory Syndrome Coronavirus (MERS-CoV), Severe Acute Respiratory Syndrome Coronavirus 1 and 2 (SARS-CoV-1 and SARS-CoV-2) (family *Coronaviridae*), Ebola Virus (EBOV) and Marburg Virus (MARV) (family *Filoviridae*), Nipah Virus (NiV) (family *Paramyxoviridae*) and Chikungunya Virus (CHIKV) (family *Togaviridae*).

	2017	2018	2024		
Family	**Priority Pathogens**	**Priority Pathogens**	**PHEIC risk**	**Priority Pathogens**	**Prototype Pathogens**
Adenoviridae			Low-Medium		Recombinant Mastadenovirus
Adenoviridae			Low-Medium		Mastadenovirus blackbeardi serotype 14
Anelloviridae			Low		
Arenaviridae	Arenaviral hemorrhagic fevers including Lassa Fever	Lassa Fever virus	High	Mammarenavirus lassaense	Mammarenavirus lassaense
Arenaviridae			High		Mammarenavirus juninense
Arenaviridae			High		Mammarenavirus lujoense
Astroviridae			Low		Mamastrovirus virginiaense
Bacteria			High	*Vibrio cholerae serogroup 0139*	
Bacteria			High	*Yersinia Pestis*	
Bacteria			High	*Shigella dysenteriae serotype 1*	
Bacteria			High	*Salmonella enterica non typhoidal serovars*	
Bacteria			High	*Klebsiella pneumoniae*	
Bornaviridae			Low		Orthobornavirus bornaense
Coronaviridae	Middle East Respiratory Syndrome Coronavirus	Middle East Respiratory Syndrome Coronavirus	High	Subgenus Merbecovirus	Subgenus Merbecovirus
Coronaviridae	Other highly pathogenic coronaviral diseases such as Severe Acute Respiratory Syndrome	Severe Acute Respiratory Syndrome	High	Subgenus Sarbecovirus	Subgenus Sarbecovirus
Filoviridae	Filoviral diseases Ebola	Ebola virus disease	High	Orthoebolavirus zairense	Orthoebolavirus zairense
Filoviridae	Filoviral diseases Marburg	Marburg virus disease	High	Orthomarburgvirus marburgense	
Filoviridae			High	Orthoebolavirus sudanense	
Flaviviridae	Zika virus	Zika virus	High	Orthoflavivirus zikaense	Orthoflavivirus zikaense
Flaviviridae			High	Orthoflavivirus denguei	Orthoflavivirus denguei
Flaviviridae			High	Orthoflavivirus flavi	
Flaviviridae			High		Orthoflavivirus encephalitidis
Flaviviridae			High		Orthoflavivirus nilense
Hantaviridae			High	Orthohantavirus sinnombreense	Orthohantavirus sinnombreense
Hantaviridae			High	Orthohantavirus hantanense	
Hepadnaviridae			Low		Orthohepadnavirus hominoidei genotype C

	2017	2018	2024		
Family	**Priority Pathogens**	**Priority Pathogens**	**PHEIC risk**	**Priority Pathogens**	**Prototype Pathogens**
Hepeviridae			Low		Paslahepevirus balayani genotype 3
Herpesviridae			Low		
Nairoviridae	Crimean Congo Haemorrhagic Fever	Crimean Congo Haemorrhagic Fever	High	Orthonairovirus haemorrhagiae	Orthonairovirus haemorrhagiae
Orthomyxoviridae			High	Alphainfluenzavirus Influenzae H1	Alphainfluenzavirus Influenzae H1
Orthomyxoviridae			High	Alphainfluenzavirus Influenzae H2	
Orthomyxoviridae			High	Alphainfluenzavirus Influenzae H3	
Orthomyxoviridae			High	Alphainfluenzavirus Influenzae H5	Alphainfluenzavirus Influenzae H5
Orthomyxoviridae			High	Alphainfluenzavirus Influenzae H6	
Orthomyxoviridae			High	Alphainfluenzavirus Influenzae H7	
Orthomyxoviridae			High	Alphainfluenzavirus Influenzae H10	
Papillomaviridae			Low		
Paramyxoviridae	Nipah and related henipaviral diseases	Nipah and henipaviral diseases	High	Henipavirus nipahense	Henipavirus nipahense
Parvoviridae			Low		Protoparvovirus carnivoran
Peribunyaviridae			Low		Orthobunyavirus oropoucheense
Phenuiviridae	Severe Fever with Thrombocytopenia Syndrome		High	Bandavirus dabieense	Bandavirus dabieense
Phenuiviridae	Rift Valley Fever	Rift Valley Fever	High		Phlebovirus riftense
Picobirnaviridae			Low		Orthopicobirnavirus hominis
Picornaviridae			Medium	Enterovirus coxsackiepol	
Picornaviridae			Medium		Enterovirus alphacoxsackie 71
Picornaviridae			Medium		Enterovirus deconjucti 68
Pneumoviridae			Low-Medium		Metapneumovirus hominis
Polyomaviridae			Low		
Poxviridae			High	Orthopoxvirus variola	
Poxviridae			High		Orthopoxvirus vaccinia
Poxviridae			High	Orthopoxvirus monkeypox	Orthopoxvirus monkeypox
Retroviridae			Medium	Lentivirus humimdef1	Lentivirus humimdef1
Rhabdoviridae			Low		Genus Vesiculovirus
Sedoreoviridae			Low		Genus Rotavirus
Spinareoviridae			Low		Orthoreovirus mammalis
Togaviridae			High	Alphavirus chikungunya	Alphavirus chikungunya
Togaviridae			High	Alphavirus venezuelan	Alphavirus venezuelan
Pathogen X	Pathogen X	Pathogen X		Pathogen X	

Table 1. *WHO Research and Development (R&D) Blueprint for Epidemics list of high priority pathogens from unpublished report of June 2024 (World Health Organization, 2024).*

3.2 Overview of viral families and target viruses

3.2.1 The *Arenaviridae* Family

The *Arenaviridae* family is composed of 4 genera: *Hartmanivirus*, *Antennavirus*, *Reptarenavirus* and *Mammarenavirus*. This last one can be divided into Old World and New World complexes (Hastie KM *et al*., 2023).

LASSA VIRUS

LASV is an enveloped, segmented RNA virus, classified as an Old World arenavirus (Yun NE *et al*., 2012) belonging to the family *Arenaviridae*, genus *Mammarenavirus* (Raabe V *et al*., 2022). Virion structure (Figure 1), protein functions, and replication strategies appear to be conserved across multiple lineages of LASV (Garry RF, 2023).

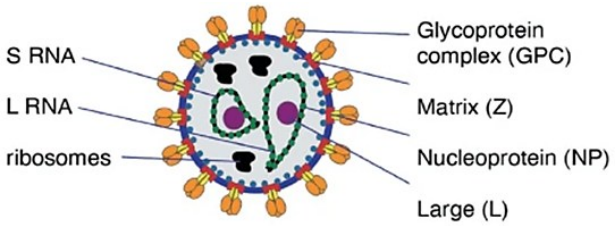

***Figure 1**. Illustration of LASV virion where major structural proteins are highlighted (Garry RF, 2023).*

The glycoprotein (GP) complex mediates viral entry into the host cell and is the major target for neutralizing antibodies (Perrett HR *et al*.,2023). In particular the GP complex (Figure 2) is a trimer composed of GP 1 (interacts with host cell receptor), GP 2 (responsible for membrane fusion) and a stable signal peptide (senses pH changes to prompt fusion under appropriate conditions) (Pennington HN *et al*., 2022).

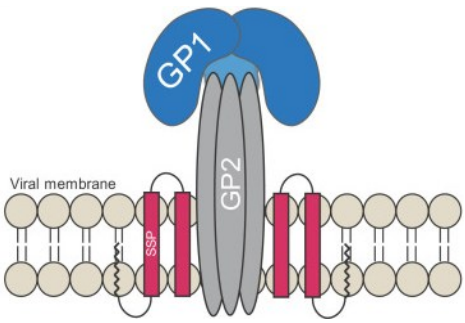

***Figure 2**. Schematic representation of LASV GP complex (Pennington HN et al., 2022).*

LASV circulates in West and Central Africa (Figure 3) where a total of 7 lineages have been identified (Forni *et al*., 2020). The natural host species of LASV are rodents, and human transmission occurs through contamination of food and water by rodents' excreta (Figure 4) (Günther S *et al*., 2004), however human to human spread is also possible (Garry RF, 2023). In West Africa, outbreaks of LASV persist with an estimated $5x10^5$ reported cases per year. Even though the case fatality rate is around 2%, it can reach up to 50% in hospitalized patients (Asogun *et al*., 2019). The number of individuals at risk of LASV infection is projected to increase due to human populations enlargement, land-use changes and climate change (Simons D, 2023).

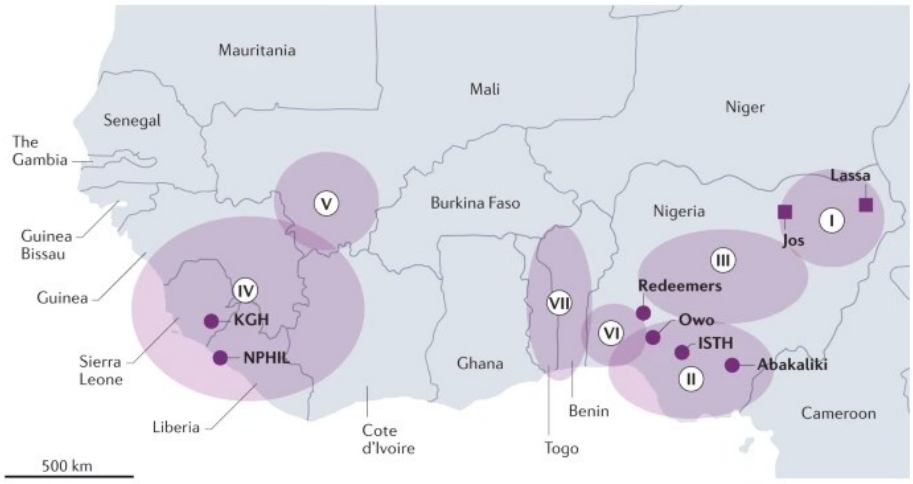

***Figure 3**. The seven lineages (I-VII) of LASV in endemic zones of West Africa (Garry RF, 2023).*

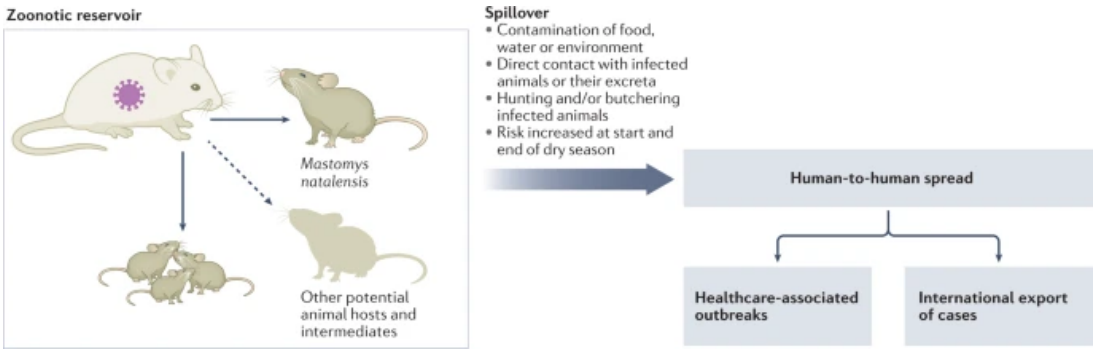

***Figure 4**. LASV ways of transmission (Garry RF, 2023).*

Even though 80% of infections are asymptomatic, LASV can cause Lassa Fever, a viral hemorrhagic disease in humans (Figure 5): the initial symptoms are nonspecific (fever, weakness, myalgia, chest and abdominal pain) followed by headaches, sore throat vomiting

and diarrhea. This general clinical picture may often cause misdiagnoses (Besson ME *et al.*, 2024). In severe cases, the clinical course evolves to hemorrhages, multi-organ impairment and hypovolemic shock. Among survivors a range of *sequelae* can be observed: sensorineural hearing loss, hair loss, impairment of balance and speech (Grant DS *et al*., 2023). Studies on pregnant women revealed adverse fetal outcomes including miscarriage, stillbirth and intrauterine death associated with maternal death (Chaudhary M et al., 2024).

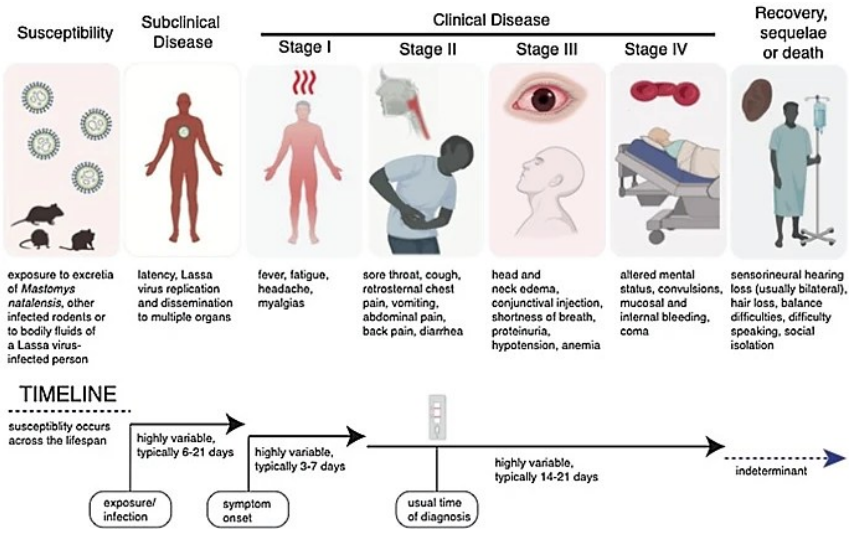

***Figure 5**. Symptomatic course of Lassa fever disease (Grant DS et al.,2023).*

LASV mainly targets blood vessels and replicates within endothelial cells, ultimately leading to capillary damage; hemorrhaging may occur in various organs (Rezaverdinejad M, 2024). Administration of ribavirin is the standard protocol for LASV prophylaxis (Salam AP *et al*., 2022). To date, no specific therapeutic option nor vaccine against LASV are available and their development is impaired by the classification of LASV as a Category A pathogen to be handled in Biosafety Level 4 (BSL-4) laboratories. For all these reasons LASV is listed by the WHO R&D Blueprint for Epidemics and by the Coalition for Epidemic Preparedness Innovations (CEPI) as a priority pathogen, with the aim to boost LASV control in at-risk countries (Antonelli R *et al*., 2024).

3.2.2 The *Coronaviridae* Family

The ICTV classifies coronaviruses as: *Nidovirales* order, *Cornidovirineae* suborder, *Coronaviridae* family, *Orthocoronavirinae* subfamily (Figure 6). Coronaviruses infecting

animals are further subdivided into 4 genera, *Alphacoronavirus*, *Betacoronavirus*, *Deltacoronavirus* and *Gammacoronavirus* (Gonzalo AS *et al*., 2023). Human coronavirus HKU1 (HCoV-HKU1), Human coronavirus OC43 (HCoV-OC43), MERS-CoV, SARS-CoV-1 and SARS-CoV-2 are betacoronaviruses infecting humans (Raaban AA *et al*., 2020).

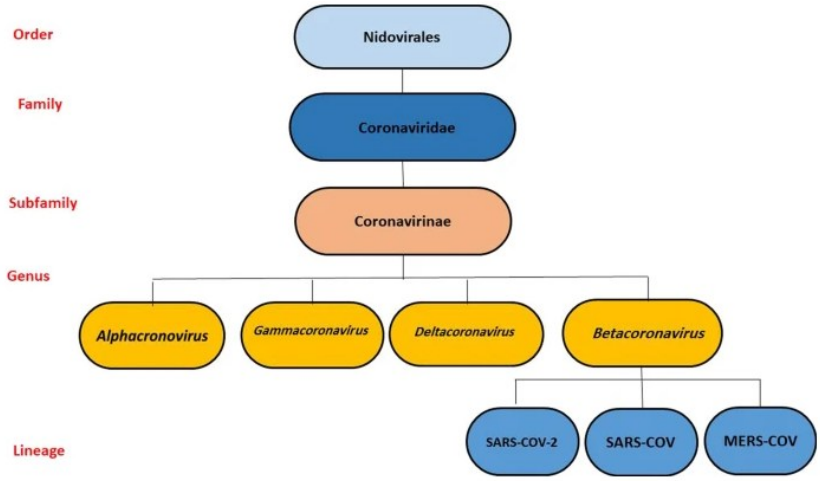

***Figure 6**. Phylogenetic structure of Coronaviruses (Saberiyan M et al., 2022).*

Coronaviruses are enveloped RNA viruses with spike proteins forming projections on their surface. The spike proteins are the first to interact with the host cell mediating virus entry, as well as the main inducer of immune response and are important for tissue tropism, their variations allow viral engagement with a broad array of receptors (Verma J *et al*., 2021). Figure 7 highlights the structure of Coronavirus with a focus on the spike protein: the S1 subunit contains the host receptor-binding domain and the S2 subunit makes up the stalk of the spike (Kannan S *et al*., 2020).

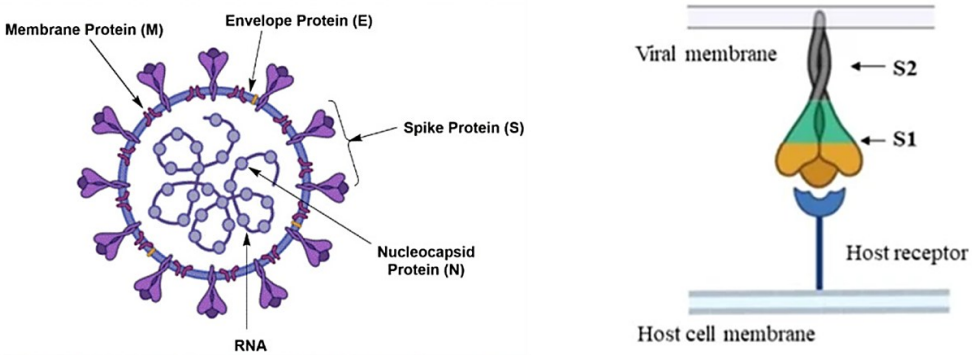

***Figure 7**. On the left a graphic representation of coronavirus highlighting major structural components is reported (Goyal R et al., 2022). On the left the spike protein is schematized showing the two subunits and the interaction with host cell receptor (Verma J et al., 2021).*

MERS-CoV, SARS-CoV-1 and SARS-CoV-2

Human coronaviruses have emerged sporadically in different regions and have been associated with significant outbreaks of deadly pneumonia since the start of the 21st century (Wu C *et al*., 2020). MERS-CoV, SARS-CoV-1 and SARS-CoV-2 are three of the most common pathogens that primarily affect the human respiratory system with a range of symptoms that variate from mild respiratory sickness to acute pneumonia and/or failure of the respiratory system (Abdelrahman *et al*., 2020). Indeed, these viruses are the only ones in their family that have caused human epidemics (Rothan HA *et al*., 2020). SARS-CoV-2 is named after SARS-CoV-1 since their genetic sequence is more than 80% identical (Zhang L *et al*., 2020). Additionally, SARS-CoV-2 shares around 50% sequence similarity with MERS-CoV at the total genome level (Muratov EN *et al*., 2021). The possible routes of transmission of coronaviruses are described in Figure 8.

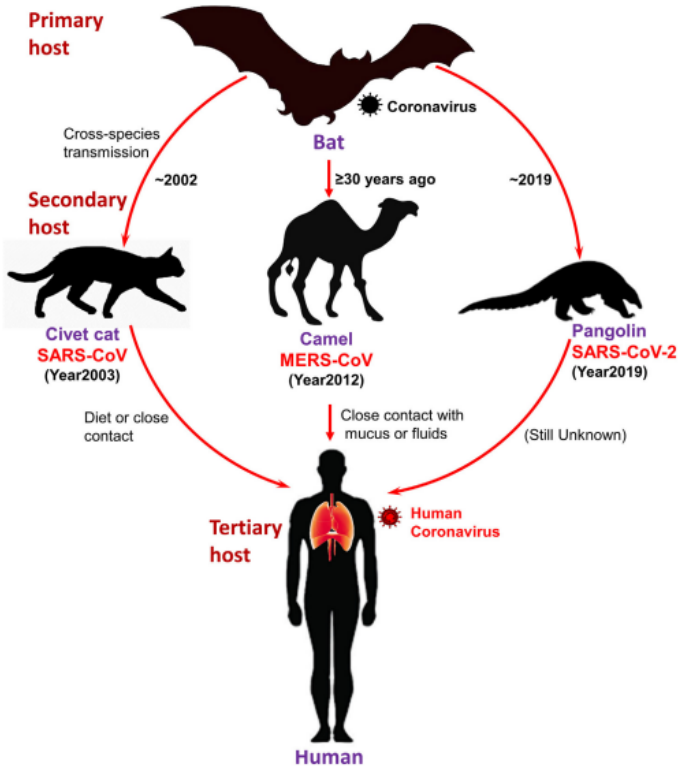

***Figure 8**. Coronavirus zoonotic transmission to humans (Kirtipal N et al., 2020).*

MERS-CoV is a zoonotic virus firstly discovered in Saudi Arabia in 2012 (Zaki AM *et al*., 2013). Alpacas and bats are possible reservoirs for the virus, but the spill over for human infections mainly occurs through infected dromedary camels (Mohd HA *et al*., 2016). Human

to human transmission can occur in hospital settings (Assiri A *et al*., 2013). Since its discovery, 2605 MERS-CoV confirmed cases resulting in 937 associated deaths have been addressed (Salomon I *et al*., 2024). The case fatality rate is around 36% (Al-Tawfiq JA *et al*., 2024).

SARS-CoV-1 first case was identified in November 2002 in Foshan, China (Xu RH *et al*., 2004). Primary hosts are found in horseshoe bats and palm civets are intermediate hosts (Fung TS *et al*., 2019). From the latter, SARS-CoV-1 is transmitted to humans through diet or close contact in poor hygienic conditions (Kirtipal N *et al*., 2020). Person to person spread is the result of inhalation of respiratory droplets (Golke A *et al*., 2021). The 2002 epidemic caused by SARS-CoV-1, ended with 8098 laboratory verified cases, resulting in 774 death cases and a case fatality rate of 9,6% (Rabaan AA *et al*., 2023). SARS-CoV-1 is the causative agent of severe acute respiratory syndrome; the disease initially presents itself with fever, myalgia, malaise, chills and cough, later in the course of the illness, shortness of breath and tachypnea are prominent. Between 20 and 30% of patients are hospitalized in intensive care units (Peiris JS *et al*., 2003). After the acute phase of SARS-CoV-1 and MERS-CoV infection, the main long-term manifestation is damage to the respiratory system with reduced pulmonary function and lung lesions (Løkke *et al*., 2023).

In December 2019 a large number of pneumonia cases were reported in hospitals located in Wuhan, China. The causative agent was later identified as SARS-CoV-2, the etiological agent of coronavirus disease 2019 (COVID-19) (Chung YS *et al*., 2024). On 11th March 2020 the WHO declared COVID-19 outbreak a global pandemic (Cucinotta *et al*., 2020). Bat is the original reservoir of this virus, while pangolin is most likely the intermediate host (Gupta SK *et al*., 2022). The main person to person contagion of SARS-CoV-2 occurs through respiratory droplets and aerosol (Arienzo A *et al*., 2023). COVID-19 can be characterized by mild symptoms or can evolve to severe acute respiratory distress syndrome, multi organ failure and death (Panahi et al., 2023). The severity of COVID-19 is strictly related to the SARS-CoV-2 induced host immune response: the virus leads to a dysfunctional response with an excessive production of inflammatory factors impairing viral clearance and leading to cytokine storm and disease progression (Li X *et al*., 2024). A cytokine storm can be defined as a dysregulated inflammatory response with extensive cytokine release and immoderate activation of immune cells leading to self-reinforcing feedback (Jarczak *et al*.,

2022). Additionally, neurological involvement in COVID-19 patients has been investigated: the most observed neurological symptoms are headaches and anosmia (Hingorani KS *et al*., 2022). From the beginning of COVID-19 pandemic until April 2023, a total of $7{,}6x10^8$ infections had been reported with $6{,}8x10^6$ associated deaths (Du J *et al*., 2024). The case fatality rate is consistently lower than that of SARS-CoV-1 and MERS-CoV. Although 13-14billion people have been vaccinated globally, SARS-CoV-2 breakthrough infections continue to occur, often leading to long term complications among those with pre-existing medical conditions (Zhang X *et al*., 2024). In fact, approximately 65 million people suffer from the so-called long COVID: a series of post-acute *sequelae* that impede the patient from returning to the normal pre-infection status within 12 weeks of the illness. The emergence of SARS-CoV-2 variants with significant phenotypic mutations poses a major public health concern in efforts to control the disease. These variants differ in terms of their transmissibility, disease severity, and ability to evade the humoral immune response in infected individuals. In particular, mutations in the spike (S) protein are most likely to affect the virus's ability to recognize and bind to host cell receptors. A key concern regarding these mutations is their potential impact on the effectiveness of existing vaccines (Artik Y *et al*., 2022).

The pathogenesis of human coronaviruses (Figure 9) is mainly given by binding of the virus to specific host cell receptors: SARS-CoV-1 and SARS-CoV-2 recognize as cellular target Human Angiotensin I converting enzyme 2 (ACE-2), whereas MERS-CoV binds to Dipeptidyl peptidase-4 (DPP-4) receptor (Pustake M *et al*., 2022). Despite their similarity, the receptor binding domain of the spike protein of SARS-CoV-2 shows greater affinity for binding to ACE2 as compared to the one of SARS-CoV-1, this may explain the higher intra-host replication and inter-host transmission efficacy of SARS-CoV-2 (Tai W *et al*., 2020). The transmembrane protease serine 2 (TMPRSS2) plays an important role in SARS-CoV-2 infection as it is involved in spike protein priming (Hoffmann M *et al*., 2020).

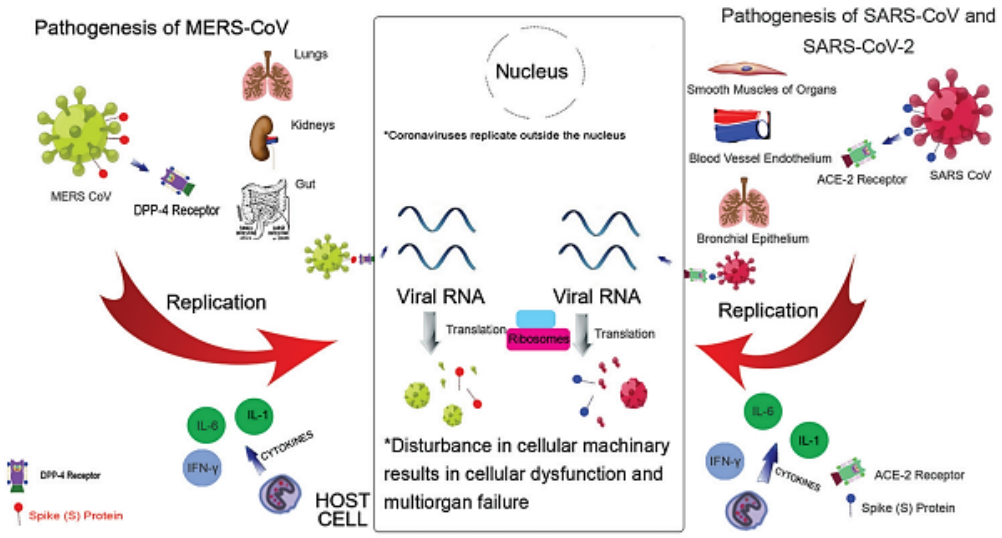

***Figure 9**. Comparison of pathogenesis within different betacoronaviruses (Pustake M et al., 2022).*

To date there are no available antiviral therapies nor vaccine against MERS-CoV infection (Te N *et al*., 2022). Even for SARS-CoV-1 there are no fixed treatments other than supporting care and infection control measures (Keshta AS *et al*., 2021). Instead, the emergence of SARS-CoV-2 with a global population of immunologically naive individuals, led to a fast response in terms of vaccine development. Normally vaccine generation occurs over multiple years, but in the case of COVID-19 it took less than a year to obtain vaccines ready for administration (Figure 10): by early 2021 mRNA vaccines by Pfizer-BioNTech and Moderna and adenovirus-based vaccines by Johnson & Johnson and AstraZeneca were available (Harne R *et al*., 2023).

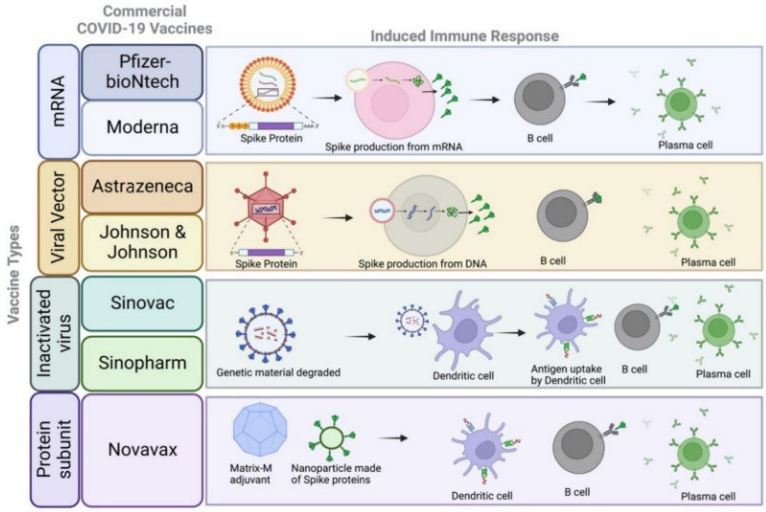

***Figure 10**. SARS-CoV-2 commercial vaccines and their induced immune response (Harne R et al., 2023).*

3.2.3 The *Filoviridae* Family

The *Filoviridae* family (Figure 11) belongs to the *Mononegavirales* order (Languon S *et al*., 2021) and it includes, among others, *Orthoebolavirus* and *Orthomarburgvirus* genera (Groseth A *et al*., 2024).

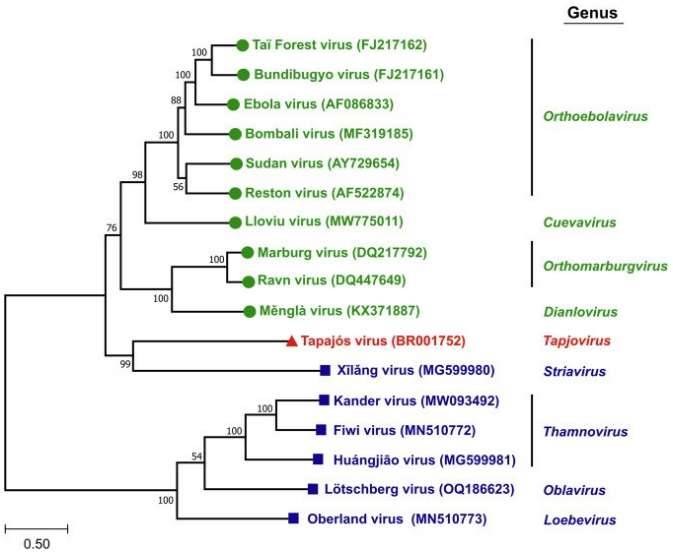

Figure 11. *Phylogenetic relationship among filoviruses (Groseth A et al., 2024).*

Filovirus virions (Figure 12) are enveloped and filamentous viruses with linear, non-segmented, negative sense RNA genome (Kuhn JH *et al*., 2019). The NP enclosing the viral genome concurs, together with RNA dependent RNA polymerase (RdRp), to the formation of the nucleocapsid involved in viral transcription and replication (Dupuy LC *et al*., 2023).

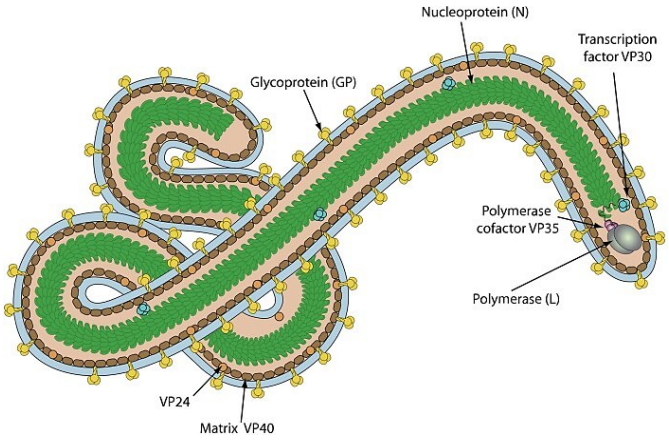

Figure 12. *Filovirus virion structure (Dupuy LC et al., 2023).*

The envelope GP of filoviruses (Figure 13) mediates host cell receptor attachment, viral entry and membrane fusion. This molecule is a homotrimer composed of disulfide-linked subunits GP1 and GP2. GP1 contains the receptor-binding site, while GP2 contains the fusion loop and transmembrane domain (Igarashi M *et al*., 2021). The trimeric GP is the target for neutralizing antibodies and is the major focus of vaccine development (Rutten L *et al*., 2020).

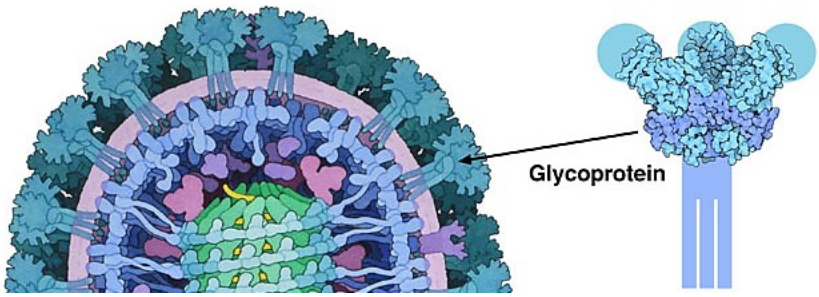

Figure 13. *Structure of glycoprotein of filoviruses (Goodsell DS, 2014).*

Ebola Virus and Marburg Virus

The first case of EBOV was reported in 1976 in the Democratic Republic of Congo (Breman JG *et al*., 2016). EBOVs have zoonotic origin, they are found in primates, but fruit bats are most likely the primary reservoir (Ahmad B *et al*., 2024). Spillover is observed when humans are in contact with wildlife, direct contact with an infected individual and body fluids exchange are responsible for viral spread within humans (Ohiman EI *et al*., 2021). Since its discovery, over 25 outbreaks of EBOV have happened (Figure 14), mainly in central Africa (Tomori O *et al*., 2021). More than $1{,}5x10^4$ people died due to EBOV infection (Barbiero VK *et al*., 2020). The most recent outbreak was announced in September 2022 and by the end of it 164 cases were traced with 55 deaths (Bwire G *et al*., 2023). The deadliest outbreak goes back between 2014 and 2016 with $2{,}8x10^4$ laboratory confirmed cases and nearly $1{,}1x10^4$ deaths (Kamorudeen RT *et al*., 2020). The case fatality rate of EBOV infection ranges from 25% to 90% (Izudi J *et al*., 2024).

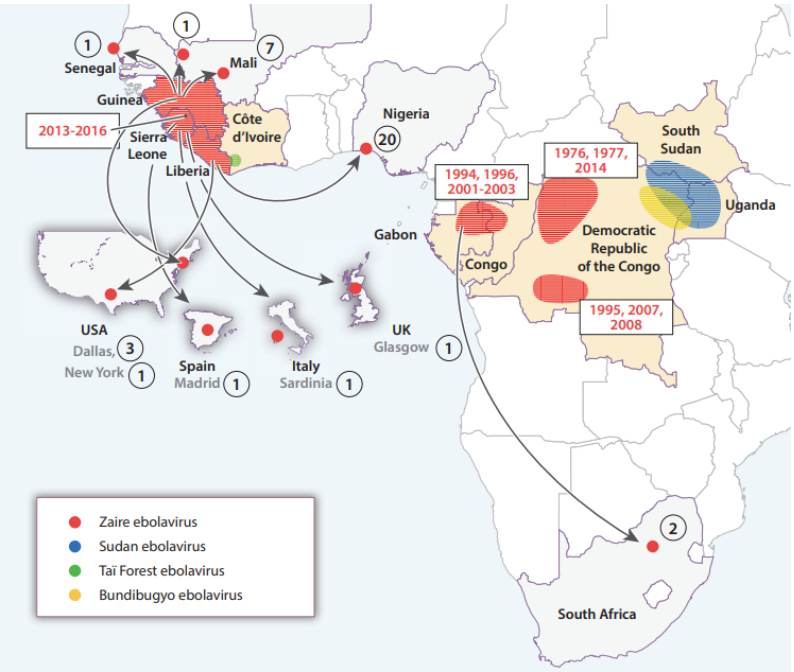

***Figure 14**. Geographical distribution of EBOV outbreaks (Baseler et al., 2017).*
The map illustrates the locations of all documented human outbreaks linked to four distinct EBOV strains across the equatorial region of Africa. The numbered circles represent cases of Ebola Virus Disease (EBOVD) that originated from individuals infected with EBOV during the 2013–2015 West African outbreak.

EBOVs are the etiological agent of EBOVD. People affected by EBOVD present with sudden fever, headache and myalgias; these symptoms are followed by nausea, vomiting, diarrhea and hemorrhagic features, with the progression of the disease neurologic symptoms are observed (Hollingshead CM *et al*., 2024). Clinical *sequelae* in two thirds of survivors include uveitis, arthralgia and fatigue; EBOV persists in selected body compartments, especially in semen (Nicastri E *et al*., 2019). EBOVD in pregnancy is associated with high maternal and perinatal mortality (Kayem ND *et al*., 2022).

Two U.S. Food and Drug Administration (FDA) approved therapeutics are available for the treatment of Ebola virus disease: Ebanga, a monoclonal antibody that targets EBOV GP, and Inmazeb, a combination of human immunoglobulins each targeting a distinct GP epitope (El Ayoubi LW *et al*., 2024). Regarding prevention strategies, vaccines approved by the European Medicines Agency (EMA) and the U.S. FDA, are: Ervebo and Zabdeno, the latter is administered as a two doses regimen with Mvabea (Kuehn R *et al*., 2024).

MARV was firstly characterized in 1967 when laboratory workers in Marburg and Frankfurt (Germany) and in Belgrade (Serbia) were infected with a previously unknown pathogen

(Brauburger K *et al*., 2012). The Egyptian rousette bat is the only known host reservoir of MARV (Guito JC *et al*., 2024), humans can contract the virus through direct contact with the reservoir or contaminated fruit consumption. Human to human transmission occurs via direct contact and body fluids (Figure 15) (Srivastava S *et al*., 2023).

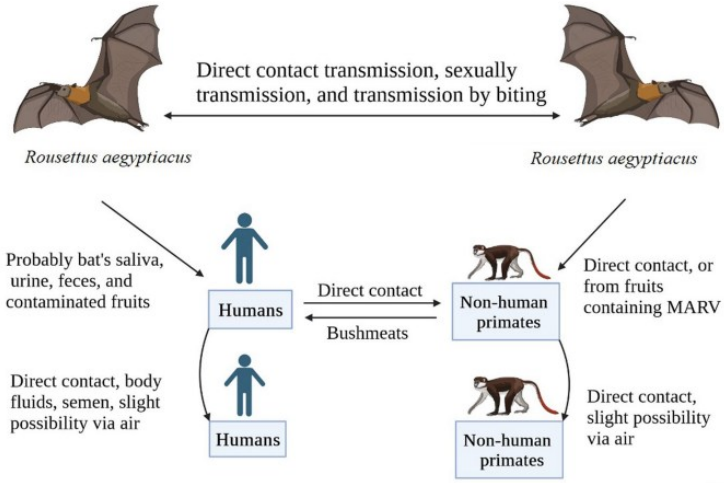

***Figure 15**. MARV transmission (Srivastava S et al., 2023).*

From 1967 until 2024, 18 outbreaks of MARV for a total of 709 reported cases and 537 associated deaths were observed (Figure 16), the case fatality rate is around 50% and has varied from 24% to 88% in past outbreaks (World Health Organization, 2025).

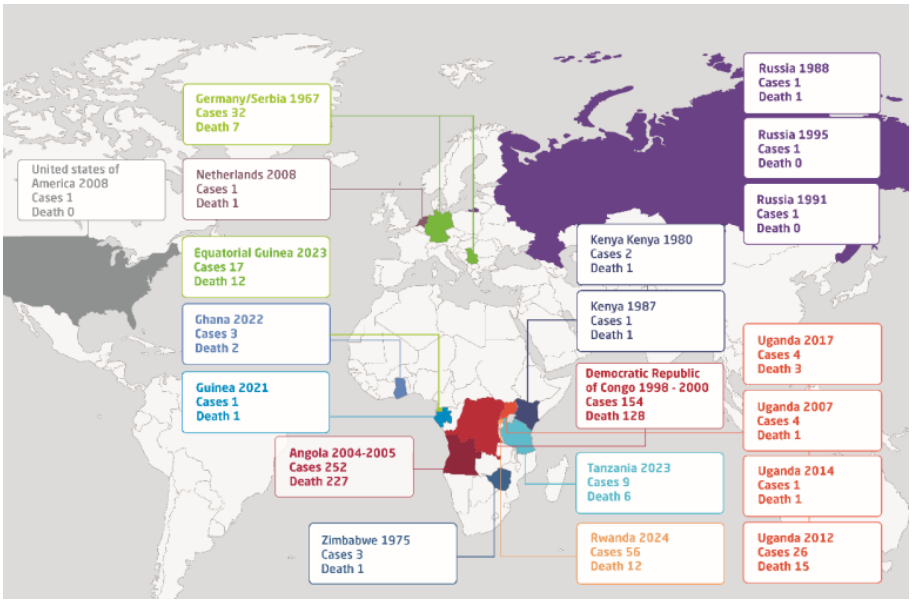

***Figure 16**. Map of MARV outbreaks (Muvunyi CM et al., 2024).*

MARV is the causative agent of Marburg virus disease (MARVD) (Figure 17): following the incubation period (3-21 days), patients show nonspecific symptoms such as fever, headache, myalgia, vomiting, diarrhea and maculopapular rash. As the disease progresses, patients may develop mucosal hemorrhage, impaired renal function and in fatal cases hypotension, shock and multiorgan failure are also observed (Kortepeter MG *et al*., 2020). MARV firstly targets monocytes, macrophages and dendritic cells, moving then forward to lymph nodes and liver for more advanced dissemination. The release of inflammatory cytokines and chemokines sets off the coagulation cascade giving rise to intravascular coagulation and blood clotting (Hunter N *et al*., 2025).

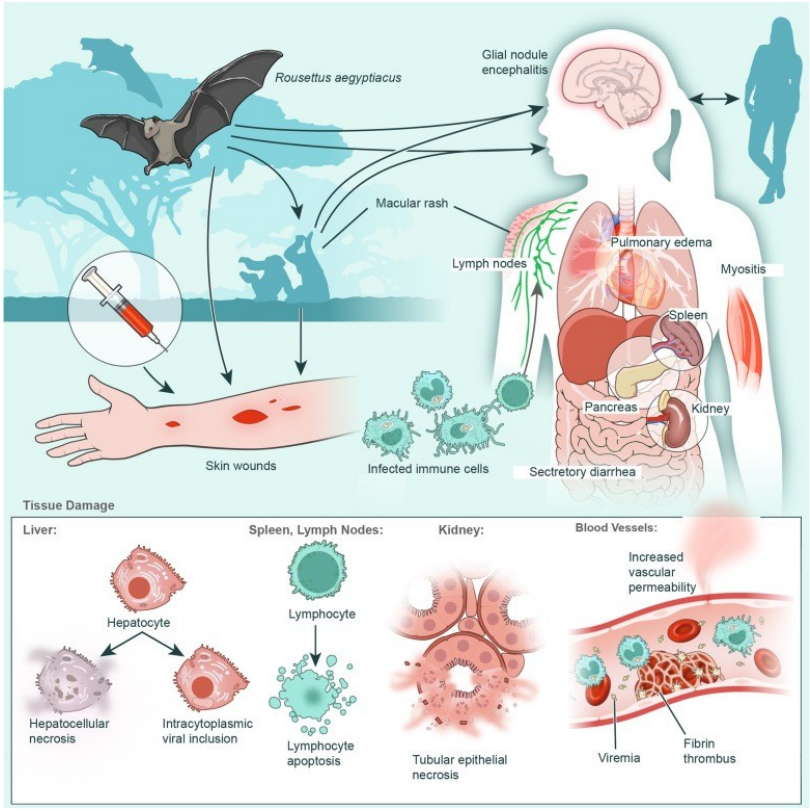

***Figure 17**. Pathophysiology of MARVD (Shifflett K et al., 2019).*

MARVD in survivors can be accompanied by a series of *sequelae*: hair loss, testicular atrophy, liver inflammation, encephalitis, skin desquamation, hyperhidrosis, amnesia and decreased libido (Nyenke CU *et al*., 2022). Currently there are no licensed vaccines nor medical drugs available against MARV (Martins KA *et al*., 2025).

3.2.4 The *Paramyxoviridae* Family

The classification of *Paramyxoviridae* (Figure 18) includes 4 subfamilies, 14 genera and 72 species. Measles virus, mumps virus, human parainfluenza viruses, and Hendra and Nipah viruses are major human pathogens (Azarm KD *et al*., 2020).

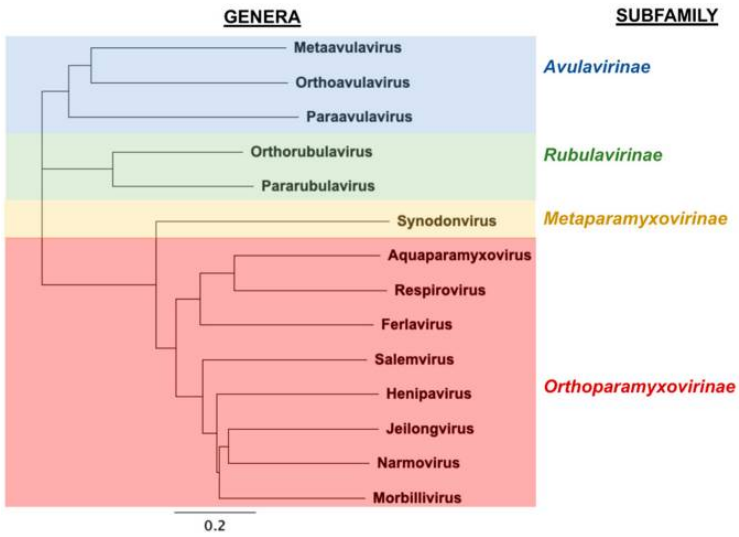

Figure 18. *Phylogenetic tree of Paramyxovirus family (Azarm KD et al., 2020).*

Virions belonging to the *Paramyxoviridae* family have spherical shape and are enveloped (Figure 17), their genome is non segmented negative sense RNA. The envelope contains two glycoproteins, one serving for receptor attachment (receptor-binding protein, designated variably as haemagglutinin–neuraminidase protein, haemagglutinin or glycoprotein) and one with fusion functions (Rima B *et al*., 2019). Figure 19 illustrates the composition of Paramyxovirus virion with a focus on the attachment and fusion proteins.

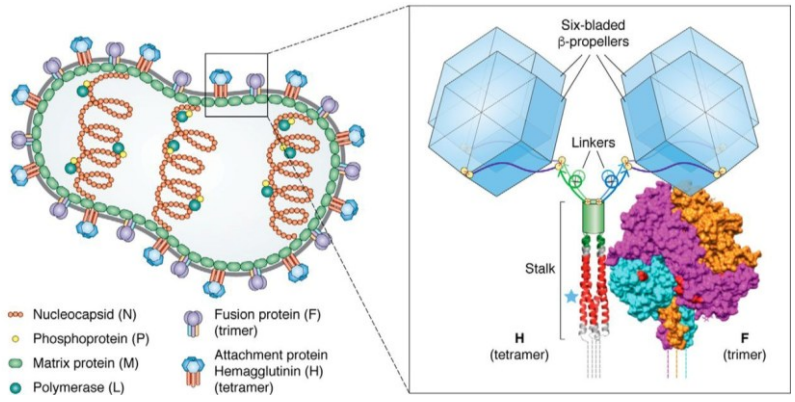

Figure 19. *Paramyxovirus structure with an up close of its envelope proteins (Navaratnarajah CK et al., 2020).*

Nipah virus

NiV was described for the first time in 1999 in Malaysia during an outbreak of encephalitis and respiratory disease in pig farmers (O'Shea H *et al*., 2019). The natural reservoir of this zoonotic viral pathogen are fruit bats (Mougari S *et al*., 2022); directly from bats humans can be infected when consuming contaminated date palm sap, indirect transmission can also occur though spillover to domesticated animals (Figure 20) (McKee CD *et al*., 2022). Person to person transmission happens through physical contact and respiratory secretion (Luby SP *et al*., 2009).

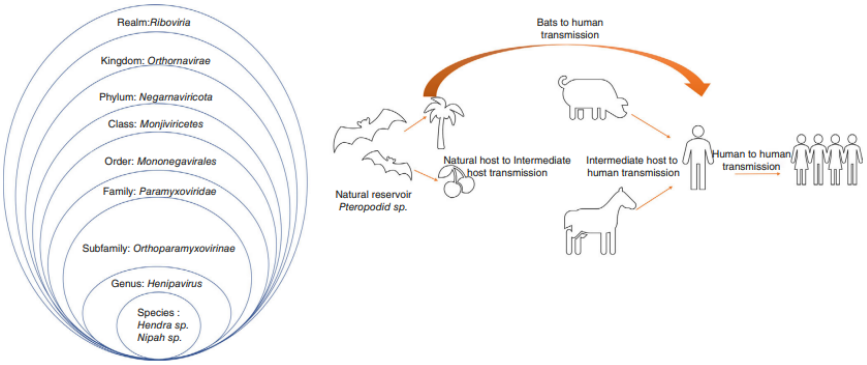

Figure 20. *NiV classification and transmission (Mishra G et al., 2023).*

From the identification of the virus until May 2024 there have been more than 700 confirmed cases (Figure 21) and around 400 deaths related to NiV infection, with an overall case fatality rate of 58% (Khan S *et al*., 2024).

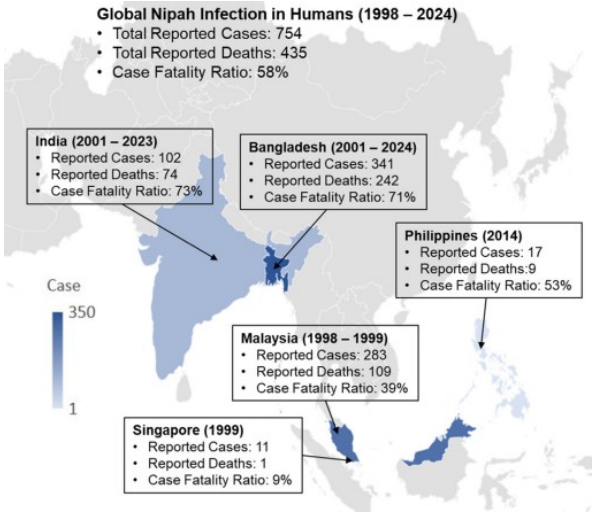

Figure 21. *Geographical distribution of NiV outbreaks (Khan S et al., 2024).*

Initial symptoms of NiV infection are common ones, such as fever, headache, dizziness and vomiting; these are followed by rapidly progressive encephalitis that can result in coma. In severe cases multiorgan impairment, gastrointestinal bleeding and renal failure are observed. Patients can also experience acute respiratory distress syndrome (Rathish B *et al*., 2023). A feature of NiV infection is the occurrence of relapses and late onset encephalitis: the longest observed gap between the end of the acute illness and the appearance of late onset encephalitis was eleven years (Abdullah S *et al*., 2012). NiV pathogenesis in humans (Figure 22) is still under investigation, endothelial cells of the respiratory tract are suggested as the primary target: NiV glycoprotein protein binds ephrin B2/B3 receptors enabling entry into host cells mediated by fusion protein. Viral replication occurs in the respiratory epithelium and spreads to the vascular endothelial cells of the lungs (Wang L *et al*., 2024).

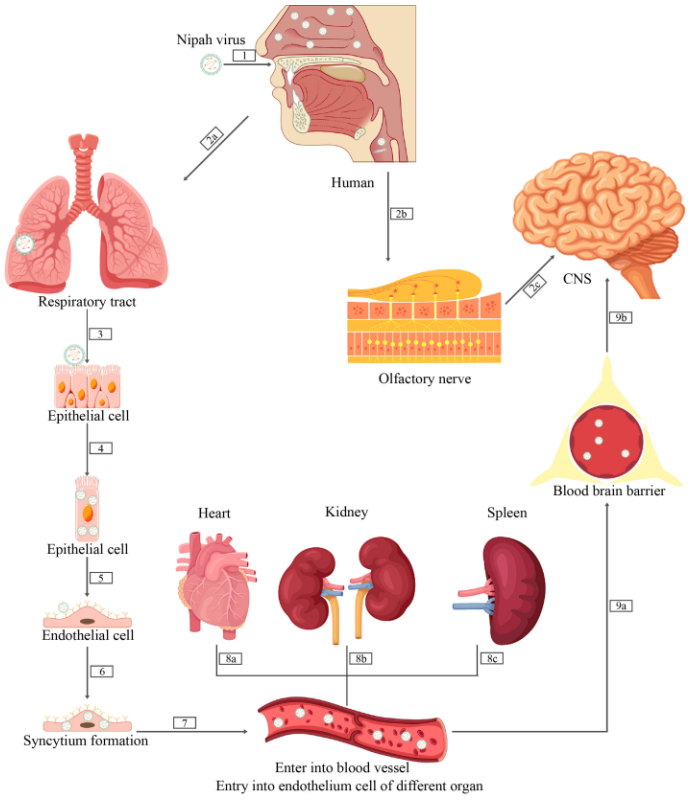

Figure 22*. NiV pathogenesis (Wang L et al., 2024).*

To date no specific medical drugs nor vaccines are approved for the treatment and prevention of NiV (Mishra G *et al*., 2023).

3.2.5 The *Togaviridae* Family

The *Togaviridae* is a family of enveloped viruses with single stranded, positive sense RNA. The family comprises the *Rubivirus* genus and the *Alphavirus* genus (Figure 23).

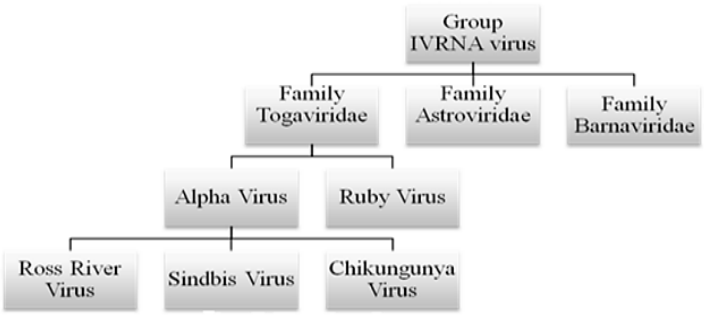

***Figure 23**. Classification of Togaviruses (Das M et al., 2021).*

The structure of Alphaviruses is reported in Figure 24, the E1-E2 envelope glycoproteins are responsible for the main steps of viral entry into host cell: E2 is involved in receptor binding, while E1 concurs to membrane fusion (Vaney MC *et al*., 2013).

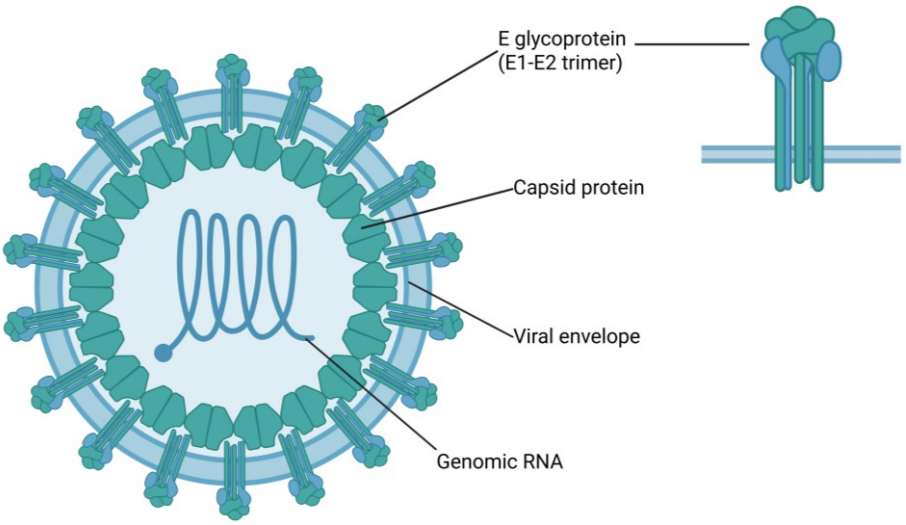

***Figure 24.** Alphavirus structure (created with Biorender.com, adapted from Mandary MB et al., 2019).*

Chikungunya virus

CHICKV was observed for the first time in Makonde (Tanzania) during a febrile illness outbreak (Cunha RVD *et al*., 2017). The primary hosts of CHICKV, that also function as vectors for disease transmission, are mosquitoes; the virus undergoes two different life

cycles (Figure 25): a sylvatic cycle that involves mosquitoes and non-human primates and an urban transmission cycle affecting humans (Madariaga M *et al*., 2016).

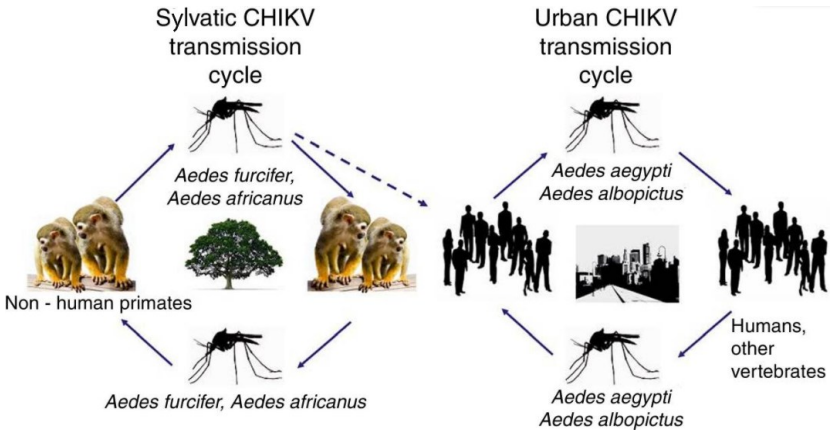

***Figure 25**. CHICK transmission (Madariaga M et al., 2016).*

The fast proliferation of mosquitoes in temperate regions and their adaptation to colder environment promote the worldwide spread of CHICKV (Figure 26): consecutive outbreaks have occurred in America, Asia, Africa and Europe with an estimation of 1,3 billion people at risk of contracting the virus (Wang M *et al*., 2024). CHICKV is a pathogen of global health concern, causing approximately 1 million infections worldwide each year (Zhang D *et al*., 2025). The data available regarding the case fatality rates are limited (Brito C *et a*l., 2025); a matched cohort study showed that CHICKV disease is associated with an increased risk of death for up to 84 days after symptom onset (Cerqueira-Silva T *et al*., 2024).

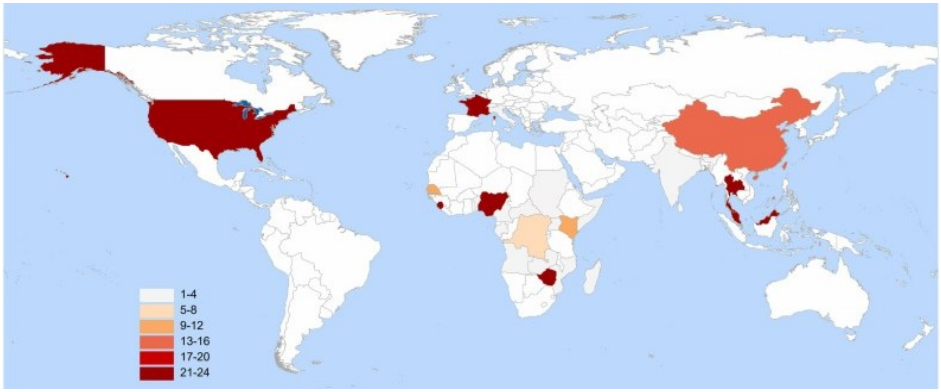

***Figure 26**. CHICKV geographical distribution, the scale indicates for how many years each country reported CHIKV cases. (Zhang D et al., 2025).*

CHICKV mostly causes symptomatic infections: Chikungunya fever begins with sudden

onset of high fever, typically maculopapular rashes are observed, arthralgia and arthritis are also associated with the disease together with fatigue, nausea, vomiting, and conjunctivitis, moreover neurologic complications, myocarditis and hepatitis have been observed (Vu DM *et al*., 2017). About 40% of patients experience long term *sequelae* such as persistent arthralgia and arthritis, about 37% of individuals with persistent arthralgia also suffer severe pain (de Lima Cavalcanti TYV *et al*., 2022). Chronic pain also has a deep impact in the surroundings of the affected individual resulting in reduced workforce productivity and increased burden for the healthcare system (Kawai K *et al*., 2017). The pathogenesis of CHICKV infection (Figure 27) is still under investigation, but evidence suggests that an infected mosquito's bite can deliver the virus directly into the bloodstream or within dermal tissue, where the virus replicates in dermal fibroblasts. Through antigen-presenting cells in the skin, CHICKV travels through the lymphatics into the bloodstream from where it disseminates systemically to secondary sites of replication: connective tissue, muscle, peripheral joints, and tendons (Freppel W *et al*., 2024).

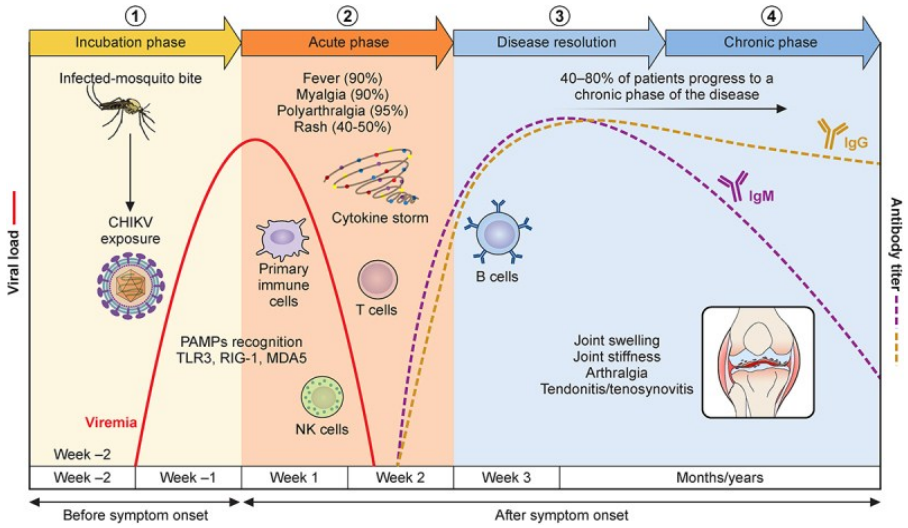

***Figure 27**. CHICKV pathogenesis (Freppel W et al., 2024).*

No specific antiviral treatment is approved for Chikungunya fever, clinical management is supportive and consists of symptomatic treatment (Centers for Disease Control and Prevention, 2024). Regarding prevention, Ixchiq (VLA1553), a single dose live attenuated vaccine, is the first one approved by the FDA (Irfan H *et al*., 2024).

3.3 Significance of Viral Pseudotypes

The evolution of global economies, along with rising international travel, shifting climates and altered human demographics, is leading to the emergence and re-emergence of different viral pathogens. Many of them are highly pathogenic and have a strong negative impact on public health. To engage basic research and therapeutic development, many of these viruses require handling by highly trained staff in BSL -3/4 laboratories, which are usually not available to most R&D communities. To avoid the strict biosafety requirement, the development of non-pathogenic pseudotyped viruses represents an effective solution, allowing the study of virus biology in a low containment biosafety level laboratory (Bentley EM *et al*., 2015).

A viral pseudotype (PV) is a recombinant viral particle composed of a structural core derived from one virus and envelope proteins derived from a different one. More specifically, pseudoviruses are based on the modified genome of different viruses, for example Vesicular Stomatitis virus (VSV), Human Immunodeficiency virus-1 (HIV-1) and Murine Leukemia virus (MLV). Here, the envelope protein genes designated for host cell infection are replaced by reporter genes that can be used for in vitro detection, such as green fluorescent protein or luciferase genes. At the same time, plasmids are used to express the envelope protein of the high-risk virus in object. Pseudoviruses are capable of infecting susceptible cell lines and completing only one replication cycle in the host cell. Pseudoviruses are safer to handle compared to wild type viruses and are also easier to manipulate, nevertheless their surface proteins' structure bears high similarity to the one of wild type viruses, mediating host cell infection (Li Q *et al*., 2018).

As previously mentioned, according to the origin of the core genome, pseudoviruses can be roughly divided into three types (Figure 28): HIV-1 based pseudotypes (lentiviral pseudotypes), VSV based pseudotypes, and MLV pseudotypes.

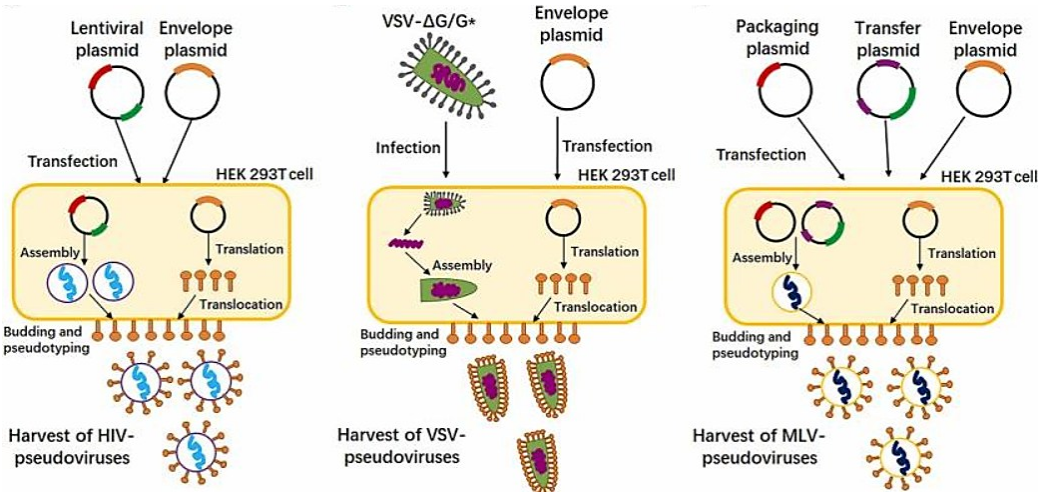

***Figure 28**. Pseudotyped-viruses based on different packaging systems (Xiang Q et al., 2022).*

Lentiviral vectors are mainly derived from HIV-1 (*Retroviridae* family, genus *Lentivirus*), a single stranded RNA virus which simple genome structure (comprising less than 10.000 bases) is convenient for genetic manipulation (Toon K *et al*., 2021). The HIV-1 based lentiviral pseudotyping system is considered a useful tool for basic science and preclinical research application, owing to some interesting features such as its large packaging capacity and efficient gene transfer capabilities (Sinn PL *et al*., 2017). The HIV pseudoviral system is the most widely used method. To avoid homologous recombination *in vitro* leading to the formation of complete HIV, some regulatory genes such as *nef* (critical for in vivo replication and pathogenesis) are deleted. Depending on the number of plasmids used, the HIV based system can be classified into two-plasmids, three-plasmids, and four-plasmids platforms. The two-plasmids platform consists of an expression plasmid encoding for the viral protein of the pathogen of interest, and of a packaging plasmid encoding for gag-pol proteins with structural and enzymatic functions (Xiang Q *et al*., 2022). The pNL4-3 packaging plasmid is the most widely used for in vitro development of two plasmid system HIV based pseudotypes (Abmad ML *et al*., 2004). In the three-plasmids system (Figure 29) the capsid plasmid encodes for the structural and enzymatic proteins (gag-pol), while the reporter plasmid encodes for packaging signal (Ψ) and the reporter (such as luciferase or green fluorescent protein). Finally, the expression plasmid encodes for the envelope protein of the virus of interest (Toon N *et al*.,2021).

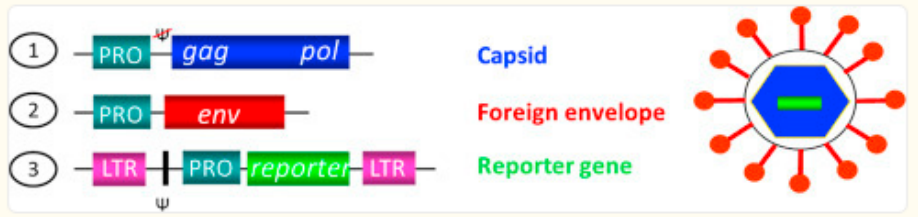

***Figure 29**. Three plasmid system for lentiviral pseudotypes development (Bentley EM et al., 2015).*

VSV is a prototypic non-segmented, negative-stranded RNA virus that belongs to the family *Rhabdoviridae*, genus *Vesiculovirus* (Ahmed MM *et al*., 2024). Early studies have shown that when cells are coinfected with VSV and other enveloped viruses, VSV pseudotypes form promptly (Huang AS *et al*., 1974). In this context, pseudotypes formation (Figure 30) is probably related to VSV budding, which does not require the glycoprotein G. Therefore, non-infectious VSV particles with the G protein sequence replaced by a reporter gene are generated. When a heterologous glycoprotein from a different enveloped virus is momentarily expressed in cells that are also infected with VSV-ΔG-LUC*G, pseudotyped particles are released efficiently (Whitt MA, 2010). Once obtained, the infectivity of the VSV based pseudotypes can be quantitatively evaluated by measurement of the reporter gene activity (Tani H *et al*., 2012).

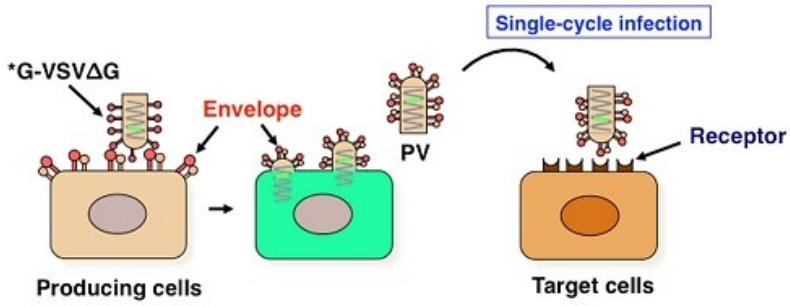

***Figure 30**. Workflow of VSV based pseudotype production (Tani H et al., 2012).*

Major threats to human health with socioeconomic impact have arisen from epidemics involving pathogenic human viruses such as influenza viruses, MERS-CoV, EBOV, CHICKV, NiV, and recently SARS-CoV-2. To enhance pandemics prevention, comprehensive studies of these viruses are needed. For this matter, pseudotyped viruses can be applied for a wide range of purposes instead of highly pathogenic wild type live viruses (Cui Q *et al*., 2023).

Receptor recognition and following interactions are the initialization of viral entry into host cells. Pseudotypes expressing the same envelope proteins as “live” viruses can be used for the exploration of the mechanisms of viral infectivity and pathogenesis, in terms of identification of target receptors (Sinn PL *et al*., 2003) and tissue tropism (Zhang F *et al*., 2021).

The effectiveness of antiviral medications that prevent viral entry into host cells can be assessed using pseudotyped virus-based inhibition tests. Pseudotyped viruses are simple to generate, suitable for automated assays, and facilitate efficient screening. As a result, several high-throughput screening platforms utilizing pseudotyped viruses have been created and employed to discover entry inhibitors for LASV (Zhang X *et al*., 2020), EBOV (Côté *et al*., 2011), and more recently, SARS-CoV-2 (González-Maldonado P *et al*., 2022).

Point mutations contribute to genetic diversity and play a key role in viral evolution, as well as in the development of new viral strains. For viruses that exhibit high genetic variability and fast mutation rates, pseudotyped virus technology enables the rapid production of different mutants, offering a more controlled and safer alternative to working with live viruses. Analyzing how mutations in amino acids impact viral infectivity and antigenic properties can offer crucial insights into anticipating the effectiveness of antibodies against new variants. As a result, pseudotyped viruses are now commonly utilized in vitro research to evaluate the antigenicity of viral mutants. (Cai M *et al.*,2022). Glycosylation is an important and thoroughly examined post-translational modification found in many proteins. Viral envelope glycoproteins often undergo extensive glycosylation. Understanding the role of these modifications is vital for gaining insights into viral infection mechanisms, host cell entry, receptor interaction, and immune system evasion. Envelope-based pseudotyped viruses serve as a useful tool for studying how glycosylation affects the function of viral glycoproteins. Many studies have utilized pseudotyping assays to explore glycosylation-related mutations in emerging viruses within natural environments. (Zhu X *et al.*, 2021).

In vivo models of viral infection are essential for understanding the mechanisms of infection. Traditional methods for studying host-pathogen interactions involve euthanizing laboratory animals at various time points, allowing for the analysis of different infection stages and the quantification of pathogen levels in various tissues. Alternatively to wild type viruses, pseudotyped viruses were applied to study SARS-CoV-2 respiratory infections in a hamster

model. Because of the single-round infectious virus, the model can be used to analyze the steps from viral binding to entry, which could serve as a base for future research on SARS-CoV-2 entry without using live SARS-CoV-2 or transgenic animals (Yamada H *et al*., 2022). Regarding the *in vivo* assessment of antiviral drugs, pseudo-filovirus-infection mouse models were constructed for filoviral entry studies in BSL-2 conditions, such models were validated with two known filovirus entry inhibitors: clomiphene and toremiphene. The study showed that Ebola and Marburg pseudoviruses not only are infectious in vitro but also provide a secure and efficient platform for screening and assessing anti-filovirus agents in BSL-2 facilities using mouse models (Chen Q *et al*., 2018).

Pseudotype neutralization assays are strong and reliable tools to study functional antibody responses against viruses in low containment laboratories (Ferrara *et al*., 2018). *In vitro* pseudoviral based neutralization assays follow the principle that neutralizing antibodies can inhibit pseudotyped viruses from infecting host cells and the antibody titer is positively correlated with the decline of the pseudotype's reporter gene signal. According to this concept, it is possible to use viral pseudotypes in neutralization analysis to evaluate the efficacy of vaccines by testing serum samples of actively immunized/convalescent patients or to screen and validate monoclonal antibodies. The mechanism of *in vitro* Pseudotype-Based Neutralization Assay (PBNA) is illustrated in Figure 31. In this context, the ability to assess the neutralizing capacity of serum samples provides insights into the effectiveness of virus-specific humoral immunity. Such data can be valuable for monitoring partial protection in asymptomatic individuals, evaluating the efficacy of both current and new vaccines against emerging viral threats, and, more broadly, advancing our understanding of immunity to viral infections (Cruz-Cardenas JA *et al*., 2022). Moreover, the *in vitro* effectiveness of monoclonal antibodies has been evaluated using both live virus assays and the PBNA, with the results from both methods showing strong correlation. For this reason, the PBNA can be considered as a valid alternative for the screening of therapeutic monoclonal antibodies, offering distinct benefits over binding activity in assessing potency (Kalkery R *et al*.,2021).

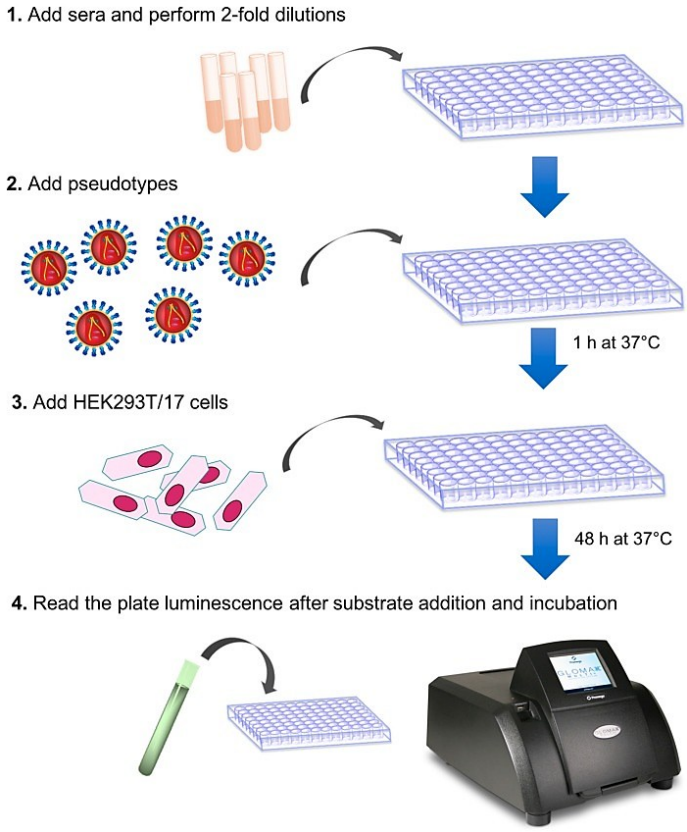

***Figure 31**. PBNA workflow (Ferrara F et al., 2018).*

4 THESIS OBJECTIVES

Highly pathogenic human RNA viruses that have a global impact on public health are highlighting society's need for robust epidemic and pandemic research preparedness. However, R&D on these high-risk viruses is significantly impaired by their stringent biocontainment requirements. Pseudotyped viruses offer a compelling solution to circumvent the challenges of handling authentic pathogens. This work addresses the limitations related to "live" pathogens through three core objectives.

A primary objective is the development of a viral pseudotype library for selected WHO priority pathogens. This resource will be made readily accessible for research purposes within a controlled biosafety level 2 laboratory, broadening research opportunities while significantly mitigating inherent risks.

Concurrently, a second key objective involves comparing via pseudotype titration assays, the production yield of each pseudotype across the three different employed systems: the two-plasmid lentiviral platform, the three-plasmid lentiviral platform, and the VSV-based platform. This analysis aims to optimize efficient and scalable production.

Furthermore, characterization of each produced viral pseudotype through PBNAs will determine their susceptibility to neutralization with specific positive controls. This critical validation step will confirm their functional integrity in mimicking authentic viral entry and will be essential to evaluate their possible application in neutralization studies.

The broader picture is to design a robust and reproducible strategy leveraging the application of viral pseudotypes in the medical field. This project aims to establish them as safe, effective, and versatile tools for the essential testing of vaccine candidates, to study immunological responses and to evaluate novel therapeutic approaches against the identified target pathogens.

5 MATERIALS AND METHODS

5.1 Materials

5.1.1 Cell culture

- 175 cm² tissue culture (T175) flask for adherent cells with filter cap (Sarstedt).
- Cell culture plate, 96 well, flat base (Sarstedt).
- DMEM, high glucose, no glutamine, no phenol red (Gibco).
- Dulbecco's modified essential medium (DMEM) high glucose, pyruvate (Gibco).
- Dulbecco's phosphate-buffered saline (DPBS) 1X no calcium, no magnesium (Gibco).
- Fetal Bovine Serum (FBS) South America origin EU Approved- Highly Tested Heat Inactivated (Euroclone).
- Gelatin from bovine skin (Merck).
- Human embryonic kidney (HEK) 293T/17-EPHRINB2 stable cell (Editgene).
- HEK293T-ACE2-TMPRSS2 stable cell line (Nibsc, catalog number: 101008).
- HEK293T/17 cells (ATCC, catalog number CRL-11268).
- L-Glutammine (L-GLUT) (Euroclone).
- Penicillin-streptomycin (PEN-STREP) (Euroclone).
- Puromycin dihydrochloride (Thermo Fisher Scientific).
- Tissue culture dish for adherent cells, 100 x 20 mm, with slip-on lid (Sarstedt).
- Trypsin-EDTA (0.05%), phenol red (Gibco).

5.1.2 Plasmid amplification

- E-Gel™ 1 Kb Plus DNA Ladder (Thermo FIsher Scientific).
- E-Gel™ Agarose Gels with SYBR™ Safe DNA Gel Stain (Thermo Fisher Scientific).
- E-Gel™ Power Snap Electrophoresis Device (Thermo Fisher Scientific).
- E-Gel™ Sample Loading Buffer, 1X (Thermo Fisher Scientific).
- LB Agar (Lennox L Agar), powder (Thermo Fisher Scientific).
- Petri dish, 92 x 16 mm, transparent (Sarstedt).
- Qiaprep Spin Miniprep Kit (Qiagen).
- SmartDropX UV-visible spectrophotometer (Accuris Instruments).

- Subcloning Efficiency™ DH5α Competent Cells (Thermo Fisher Scientific).
- Super Optimal broth with Catabolite repression (SOC) medium (Thermo Fisher Scientific).
- Terrific Broth (Gibco).

5.1.3 Viral pseudotypes production

- EndoFectin™ Lenti Transfection Reagent (GeneCopoeia).
- Lipofectamine™ 2000 Transfection Reagent (Thermo Fisher Scientific).
- Minisart® Syringe Filter, Polyethersulfone (PES), pore size 0.45 µm, sterile (Sartorius).
- Opti-MEM™ I Reduced Serum Medium (Thermo Fisher Scientific).
- PEI transfection reagent (MedChem Express).
- Packaging constructs are kindly provided by Professor Nigel Temperton (Viral Pseudotype Unit of the Medway School of Pharmacy, University of Kent, and scientific advisor for VisMederi):

    - Reporter vector HIV-1 NL4-3 ΔEnv Vpr Luc (pNL4-3.Luc.R-E-). Plasmid pNL4-3.Luc.R-E- (Figure 32) is a modified variant of the first generation pNL4-3 vector where the *env* and *vpr* genes have inhibitory frame shifts and a firefly luciferase gene is inserted into the *nef* gene (Carnell GW *et al*., 2015). This vector provides *gag* and *pol* genes for viral core assembly. The firefly luciferase is the reporter system employed, for which relative luminescence units (RLU) are measured as output to detect viral pseudotypes yield. In this work pNL4-3.Luc.R-E- is referred to also as pNL4.3.

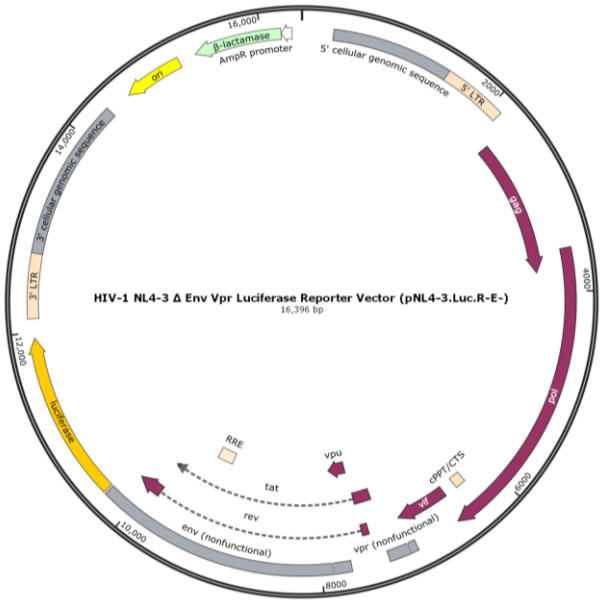

***Figure 32**. pNL4-3.Luc.R-E- map (SnapGene software)*

- Second generation vector p8.91. Plasmid p8.91 (Figure 33) is a modified HIV-1 construct lacking *env*, *nef*, *vpu* and *vpr* genes along with Ψ packaging signal. p8.91 supplies the essential genes for viral core assembly (HIV-1 *gag* and *pol*), while the packaging and regulatory elements (Ψ, LTRs and RRE) are carried by a separate plasmid named pCSFLW (Figure 34), which also bears the reporter gene firefly luciferase (Carnell GW *et al*., 2015).

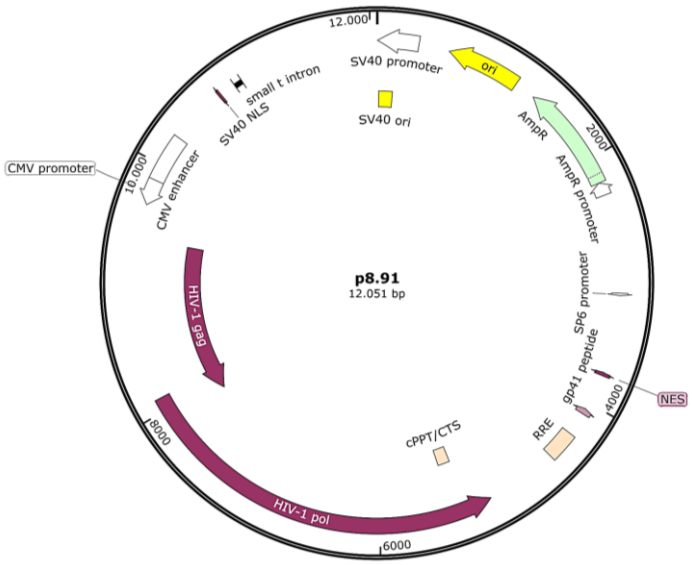

***Figure 33**. p8.91 map (SnapGene software).*

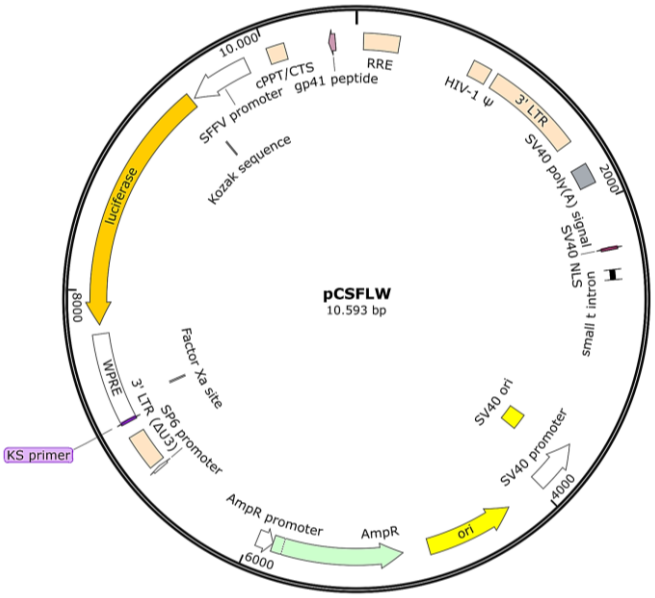

***Figure 34**. pCSFLW map (SnapGene software).*

- Viral envelope proteins:
    - LASV (strain Josiah) glycoprotein (Sino Biological, catalog number VG-40079-UT), SARS-CoV-2 wild type spike protein (Sino Biological, catalog number: VG40589-UT) and MERS (strain Jordan) spike protein (Sino Biological, catalog number: VG40069-G-N) are all expressed into pCMV vector.
    - NiV G and F proteins are expressed into pCDNA3.1 vectors (GenScript).
    - SARS-CoV-1 spike protein, EBOV (strains Sudan and Makona), MARV (strains Angola and Congo) and CHICKV glycoproteins are all expressed into pCAGGS vectors. These plasmids are kindly provided by Professor Nigel Temperton.
- G complemented VSV-ΔG helper virus expressing luciferase gene (VSV-ΔG-LUC*G) (Vector Builder, catalog number: VB900106-5669rxz). Figure 35 shows the genome and graphic structure of the helper VSV expressing the luciferase gene.

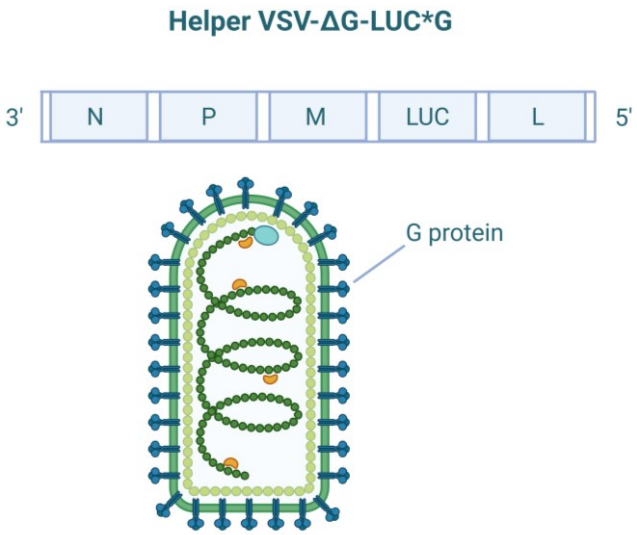

Figure 35. *VSV-ΔG-LUC*G general structure (created with Biorender.com, adapted from Zettl F et al., 2020).*

5.1.4 Pseudotypes titration assays and PBNAs

- Antibody Ab01401-10.0 Anti-VSV-G [8G5F11] (Ab anti-VSV-G) (Absolute Antibody, clone number: 8G5F11).
- Anti-MARV GP Macaque derived chimeric monoclonal antibody (human IgG1) (anti-MARV mAb) (IBT Bioservices, catalog number: 0203-028).
- Bright-Glo™ Luciferase Assay System (Promega).
- First International Standard for Anti-Nipah Virus Antibodies for neutralization assays (human sera) (WHO 22/130_NT) (Nibsc code: 22/130_NT).
- First International Standard for Ebola virus (EBOV) antibodies - Sierra Leone Convalescent Plasma Pool (WHO 15/262) (NIBSC code: 15/262).
- First WHO International Standard for Anti-MERS-CoV Immunoglobulin G (Human) (WHO 19/178) (NIBSC code: 19/178).
- GloMax® Discover Microplate Reader (Promega).
- Human serum samples (donated from University of Siena).
- Immunoglobulins Depleted Human Serum (serum minus) (BBI Solutions, catalog number: SF505-2).
- Microplate for cell culture, 96 wells, clear, with flat base (Sarstedt).
- Microplate for cell culture, 96 wells, white, with flat base (Perkin Elmer).

- Mouse anti-SUDV GP mAb 16F6 (mAb 16F6) (IBT Bioservices, catalog number: 0280-001).
- Rabbit anti-EBOV VLP Polyclonal Antibody (anti-EBOV pAb) (IBT Bioservices, catalog number: 0315-001).
- SARS-CoV/SARS-CoV-2 Spike Protein S1 Recombinant Human Monoclonal Antibody clone CR3022 (mAb CR3022) (Thermo Fisher Scientific, catalog number: MA5-48311).
- Standard 20/148 from 1st WHO International Reference Panel for anti-SARS-CoV-2 immunoglobulin (WHO 20/148) (NIBSC, panel code: 20/268).
- Standard 20/228 from WHO International Reference Panel for anti-Lassa fever virus antibodies (WHO 20/228) (NIBSC code: 21/332).
- WHO International Standard Antibodies to SARS-CoV-1 for neutralization assays (human immunoglobulin) (WHO 23/242) (NIBSC code: 23/242).

5.2 Methods

5.2.1 Cell culture maintenance

For viral pseudotypes production HEK 293T/17 cells are used. The cell line is maintained in complete medium: DMEM high glucose, pyruvate, supplemented with 10% (v/v) FBS and 1% (v/v) PEN-STREP.

For Lassa, Ebola, Marburg and Chikungunya viral pseudotypes, HEK293T/17 cell line is used for titration assays and PBNAs. On the other hand, for MERS-CoV, SARS-CoV-1 and SARS-CoV-2 pseudoviruses the cell line applied in titrations and PBNAs is HEK293T-ACE2-TMPRSS2 stable cell line; for Nipah pseudoviruses HEK293T/17-EPHRINB2 stable cell line is used. To maintain the selectivity for the two stable cell lines, complete medium is supplemented with Puromycin dihydrochloride at a final concentration of 1µg/mL.

Cell lines are preserved in T175 flasks splitted two or three times per week depending on the proliferation rate. For cell passaging, the cell layer is washed with DPBS and then treated with Trypsin-EDTA. Once cells lose adherence, culture medium is added in the same amount as the trypsin and cells are collected in a 15mL sterile centrifuge tube. Cells are centrifuged for 3 minutes at 120 rcf, and the pellet is diluted as needed. Cell handling is

performed in class II biosafety cabinet. The status of cell culture is checked under inverted light microscope.

For optimal growth conditions, cell cultures are maintained in CO_2 incubator at 37±1°C, 5±1% CO_2 and ≥ 85% relative humidity.

5.2.2 Plasmid amplification

For this work, the DNA cloning procedure is not performed since functional plasmids are externally provided by Professor Nigel Temperton, or synthesized by external companies such as GenScript Biotech (https://www.genscript.com/) or Sino Biological (https://www.sinobiological.com/). In the latter case, as a generic procedure for plasmid design, the nucleotide sequence of interest is identified and selected from viral isolates uploaded in online databases, such as GenBank (NIH genetic sequence database, https://www.ncbi.nlm.nih.gov/genbank/). Afterwards, Expasy online translating tool (https://web.expasy.org/translate/) is employed for a short supplementary analysis of protein expression to confirm the presence of both START and STOP codons, to verify the absence of missense mutations and to ensure the correct reading frame, thereby minimizing the impact of possible sequencing errors. The external company may perform codon optimization to increase protein expression and consequently pseudotypes yield.

The provided plasmids are found either in a lyophilized form or spotted on paper; therefore, an amplification procedure is required.

The amplification process of each plasmid necessary for viral pseudotypes production is divided into two main steps. Firstly, transformation of DH5α competent cells is performed: frozen single-use competent cells are thawed in ice, and 1-50 ng of plasmid DNA is added. The tube containing cells-plasmid mix is incubated in ice for 30 minutes, afterwards heat-shock at 42°C with a duration of 40 seconds is performed. The tube is returned to ice for 2 minutes and then diluted with 450µL of room temperature SOC Medium. The tube is incubated for 1 hour at 37°C while shaking at 250 rpm. Transformed cells are spread onto a Petri plate containing LB agar treated with the appropriate amount of specific antibiotic, to ensure selection of those cells that have acquired the plasmid of interest. After overnight incubation at 37°C, a single colony is picked from the agar plate and inoculated in Terrific

Broth supplemented with selective antibiotic and incubated overnight at 37°C with shaking at 250rpm. Subsequently, a pellet of the transformed bacteria is obtained through centrifugation at 4°C for 10 minutes at 4000 rcf. Plasmid purification is carried out by means of Qiaprep Spin Miniprep Kit according to the user manual provided by the manufacturer. To obtain plasmid DNA concentration, Nanodrop instrument is used and both 260nm to 280nm, and 260nm to 230nm absorbance ratios are taken into consideration to assess plasmid purity (Figure 36). Plasmid quality is further examined by performing DNA gel electrophoresis using precast 1% agarose gels featuring SYBR Safe DNA stains (Figure 37). Samples are mixed in a 1:1 ratio (v/v) with 1X Loading Buffer and loaded in the appropriate wells. The E-Gel™ 1 Kb Plus DNA Ladder is used as marker for each run. For each amplification experiment pUC19 DNA plasmid isolated from *E. coli* is used as a positive control of bacterial transformation, such plasmid is provided within the DH5α Competent Cells kit.

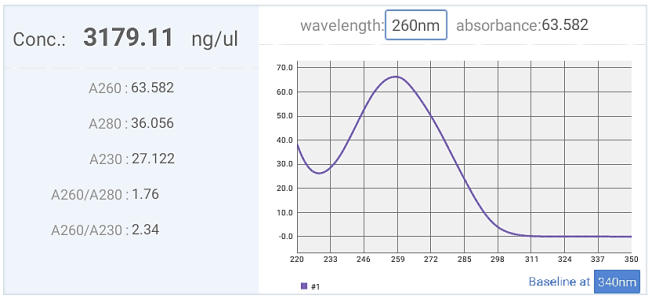

***Figure 36**. Example of plasmid DNA quantification after amplification.*
The analysis is carried out by means of SmartDrop X spectrophotometer. The output of the analysis comprises the concentration of plasmid in object expressed (ng/µL), as well as protein (A260/A280) and alcoholic (A260/230) contamination. A graphic summary of the spectral absorbance permits a qualitative evaluation of the obtained results.

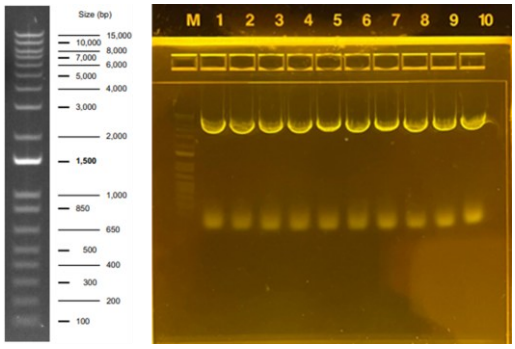

***Figure 37**. Example of DNA gel electrophoresis.*
On the left side of the figure a representative image of the DNA ladder is reported. On the right side a commercial 1% agarose gel with SYBR Safe DNA stains is used to run amplified plasmid DNAs. The absence of smeared bands indicates that the DNA sample is intact and that degradation did not occur.

5.2.3 Viral pseudotypes production

Lentiviral based pseudotypes

In this paragraph, complete growth medium refers to DMEM without phenol red supplemented with 10% (v/v) FBS, 1% (v/v) PEN-STREP, 1% (v/v) L-GLUT. When 5% growth medium is indicated, it refers to DMEM without phenol red, supplemented with 5% (v/v) FBS, 1% (v/v) PEN-STREP, 1% (v/v) L-GLUT.

The production of viral pseudotypes based on lentiviral platform is performed with both two- and three-plasmids systems; the overall process takes place during five days and is divided into three main phases. On day one, tissue culture dish is incubated for one hour at 37±1°C, 5±1% CO2 and ≥ 85% relative humidity with a layer of 0,1% (v/v) bovine gelatin. The gelatin solution is then washed with DPBS and $3{,}5x10^6$ HEK293T/17 cells/plate are seeded in complete growth medium.

Eighteen to twenty-four hours after cell seeding, cells are checked to have ~ 80% confluence (Figure 38) and transfection reaction is carried out.

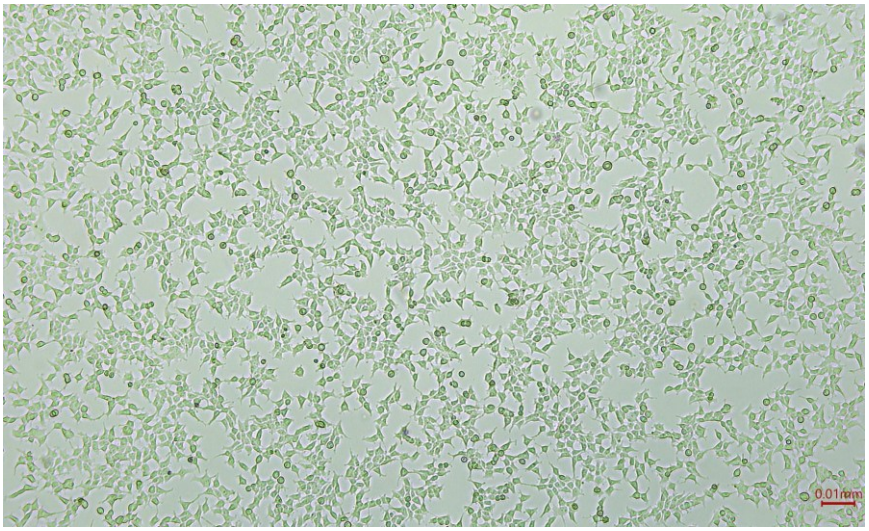

***Figure 38**. HEK293T/17 cells at day of transfection for lentiviral based pseudotypes production (zoom 10X).*

Two tubes, one for the transfection reagent and one for the plasmid mix are prepared, each one filled with 500µL of Opti-MEM. In the transfection reagent tube, EndoFectin™ Lenti Transfection Reagent or, alternatively, Lipofectamine™ 2000 Transfection Reagent, is added and then incubated according to the user manual. In the plasmid mix tube, for the

two plasmids system transfection method, the envelope protein of the virus of interest together with pNL4-3.Luc.R-E are added. Alternatively, for the three plasmids system, the envelope protein is transfected together with p8.91 and pCSFLW. Once the transfection reagent incubation is over, the plasmid mix is added to the transfection reagent tube, and the final mix is incubated at room temperature for the time reported in the transfection reagent user manual. The transfection reagent-plasmid mix is transferred to the culture dish, where the growth medium from the cell seeding was previously replaced with 5% growth medium. After 6 to 8 hours of incubation fresh complete growth medium is added to the dish.

Seventy-two hours post cell transfection, viral pseudotypes harvest is conducted: the medium is collected from the culture plate, centrifuged for 10 minutes at 4°C and 180 rcf and then filtered by means of PES syringe filters. The filtered solution is then aliquoted into siliconized microtubes and stored at -80°C.

In the case of Nipah virus pseudotypes a different harvesting method is performed: medium and cells are collected together and undergo three freezing and thawing (F&T) cycles. Afterwards, centrifuge and filtering steps are done as mentioned above. Then the filtered solution is concentrated via a 3-hour centrifugation at 4°C and 8000rcf. The pellet that has formed is carefully resuspended with 1-2mL of supernatant (according to pellet dimension) and stored at -80°C.

As a negative control (Δenvelope) for lentiviral pseudotype production cells are transfected with pUC19 DNA plasmid instead of the envelope protein of the virus of interest, following the same transfection conditions.

VSV based pseudotypes

In this paragraph, complete growth medium refers to DMEM without phenol red supplemented with 10% (v/v) FBS, 1% (v/v) PEN-STREP, 1% (v/v) L-GLUT; 5% growth medium refers to DMEM without phenol red, supplemented with 5% (v/v) FBS, 1% (v/v) PEN-STREP, 1% (v/v) L-GLUT; and 0% growth medium refers to DMEM without phenol red and without any supplements.

To produce viral pseudotypes based on VSV platform, day 1 is performed as explained in the previous paragraph (Lentiviral based pseudotypes) with the difference that $4{,}5 \times 10^6$

HEK293T/17 cells are seeded in each dish.

The day after cell seeding, cells are to be 90% confluent (Figure 39), if so, transfection reaction takes place.

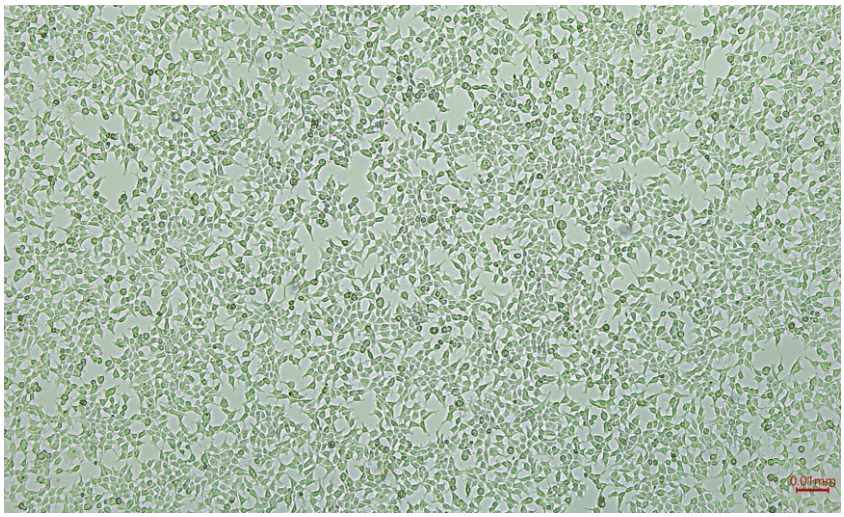

***Figure 39**. HEK293T/17 cells at day of transfection for VSV based pseudotypes production (zoom 10X).*

In the same way as described for lentiviral based pseudotypes transfection reaction is performed but in this case PEI Transfection Reagent is employed following the instructions provided by the user manual. Twenty-four hours post transfection cells are infected with VSV-ΔG vector expressing luciferase gene (VSV-ΔG-LUC*G): 5% growth medium used for transfection is removed from the plate and the VSV solution in 0% growth medium is added to the cells. After 2 hours of incubation the plate is washed several times with DPBS, and then complete growth medium is added. Twenty-four hours post infection, viral pseudotypes are harvested. Collection and storage follow the same process as described for lentiviral based pseudotypes.

As a negative control (Δenvelope) for VSV based pseudotype production the envelope protein of the virus of interest is replaced with pUC19 DNA plasmid, whilst the other PV production conditions are maintained.

5.2.4 Viral pseudotypes titration assay

Pseudotypes titration is performed by incubating the pseudotype particles with the target cell line: this assay allows to obtain the titer of the pseudotyped virus in RLUs/mL, necessary

to determine the amount of pseudotypes in a working solution to be used in pseudotype based microneutralization assays.

The titration assay is performed with target cells used in suspension. The growth medium used in titration assay is DMEM without phenol red supplemented with 10% (v/v) FBS, 1% (v/v) PEN-STREP, 1% (v/v) L-GLUT.

The volumes that will be indicated are used to perform a two-fold dilution curve of the pseudovirus. Each pseudovirus is tested in duplicate.

The titration assay is performed in a sterile, white, flat bottomed 96 well microplate. Here, 50µL of growth medium are added to all wells except for column 1, where 100µL of neat pseudotype are added. Serial dilution (1:2) is performed until column 9 (the final 50µL are discarded). Afterwards, 50 µl of target cells solution are added to each well, for a total of $1x10^7$ cells/plate. The plate is incubated at 37°C, 5% CO_2 for 72 hours (for lentiviral pseudotypes) or 24 hours (for VSV pseudotypes).

Following the same overall procedure the helper VSV-ΔG-LUC*G was titrated with two differences: the helper was tested pre-diluted 1:1000 and 1:10000, and 3-fold diluted.

The optimal target cells confluence at the time of plate readout is shown in Figure 40.

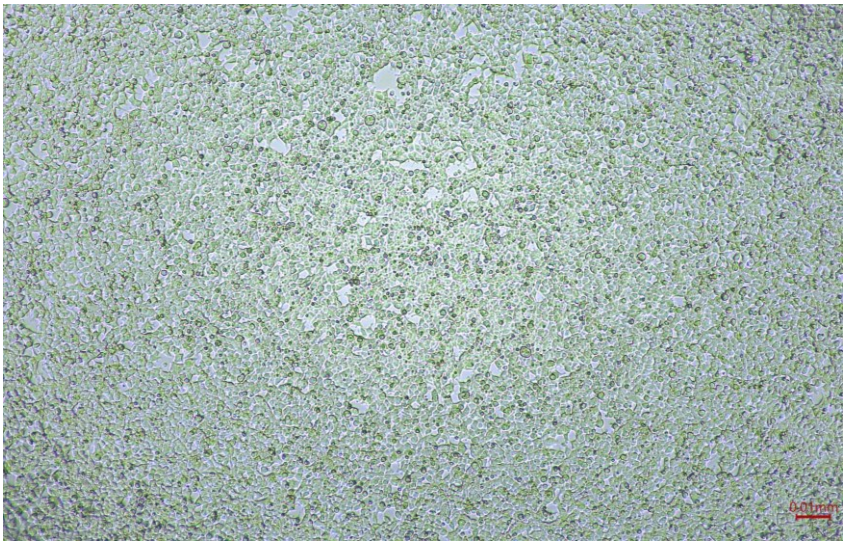

***Figure 40**. Example of the expected appearance of target cells on the day of plate readout (zoom 10X).*

The pseudoviral titration plate layout is represented in Figure 41.

For each titration assay a sterile, clear, 96 well microplate is used for seeding target cells at the same concentration as the assay. This allows the state and confluency of the cells to be checked under the microscope.

After the incubation time, 24 or 72 hours according to the pseudotype platform used, plate readout is conducted. The plate is removed from the incubator and 50µL of previously prepared Bright-Glo™ Luciferase Assay System solution are added to the wells. The plate is then incubated in the dark for 5 minutes at 500rpm. Read out is conducted by means of GloMax® Discover microplate reader luminometer, with an integration time of 0,3 seconds.

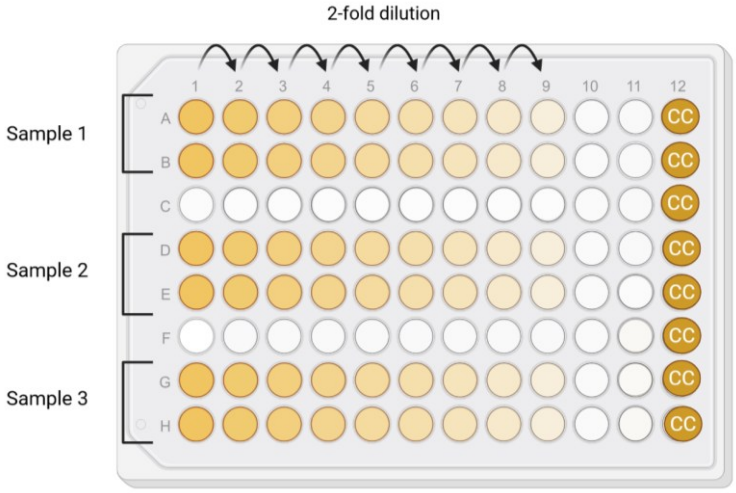

***Figure 41**. Pseudoviral titration plate layout (created with Biorender.com).*
The sample refers to the batch of pseudotypes that are tested in duplicate and serially diluted with a 2-fold dilution from column 1 to 9. Column 12 corresponds to the cell control (CC).

Data analysis for titration assays

From the RLUs obtained for each well in which the pseudotype is present, the mean of cell control RLUs (column 12) is subtracted, and the result is multiplied by the dilution factor of that well. In this way, the RLU value for 50µL is obtained and converted into RLU/mL. Since the pseudovirus is tested in duplicate, the final titer in RLU/mL will be given by the average between the mean of the 9 RLU/mL values from the first replicate and the mean of the 9 RLU/mL values from the second replicate. Through these analyses it is possible to derive the pseudoviral dose input (µL/plate) to be used for the PBNAs. From previous experiments, gold-standard doses for PBNAs regarding this work were determined to be $1x10^6$ or $5x10^5$ RLU/well.

As a practical example, in case the wanted dose input is $1x10^6$ RLU/well, the PV dose to be used in the PBNA working solution is calculated as follows:

$$\frac{1 \times 10^6\ (RLU/well) \times 100\ well}{pseudotype\ titre\ (RLU/mL)} \times 1000 = PV\ dose\ (\mu l/plate)$$

The PV dose is to be added to the final volume of PV working solution which corresponds to 50 µL per well, for a total of 5000 µL/plate.

For internal quality control, it was assessed a cell control mean lower or equal to $1x10^4$, if the assay does not meet this criterion, the titration is to be repeated.

Data analysis for pseudotype titration assays is based on the publication “Pseudotype Neutralization Assays: From Laboratory Bench to Data Analysis” (Ferrara *et al*., 2018).

5.2.5 Pseudotype-based neutralization assays

Neutralization assays are performed to determine the neutralization titer for a given serum sample or compound with respect to the previously titrated pseudoviral particle.

The growth medium used in these assays is DMEM without phenol red supplemented with 10% (v/v) FBS, 1% (v/v) PEN-STREP, 1% (v/v) L-GLUT.

Samples are tested in duplicate with a starting dilution of 1:20 and 2-fold diluted. Target cells are used in suspension. The assays are performed in a sterile, white, flat bottomed 96 well microplate; while a sterile, clear, 96 well microplate is used as before to check the cells throughout the duration of the experiment.

In the neutralization assay, 50µL of growth medium are added to all wells of the microplate, except for column 1, where 90µL are added instead. Ten microliters of the sample are added to column 1 and a 2-fold serial dilution is performed until column 9, the last 50µL are discarded. The pseudotype working solution is prepared according to the titration and 50µL are added to each well up to column 9 and to wells from E11 to D11 which correspond to pseudotype control. Moreover, 50µL of growth medium are added to the leftover wells so that the final volume of the plate is evenly distributed. The plate is now incubated 1 hour at 37±1°C, 5±1% CO2 and ≥ 85% relative humidity. When the incubation time is over, 50µL of

target cell suspension ($1x10^7$ cells in a final volume of 5mL) are added to each well. The plate is incubated at 37±1°C, 5±1% CO2 and ≥ 85% relative humidity for 72 hours (for lentiviral pseudotypes) or 24 hours (for VSV pseudotypes).

The PBNA plate layout is highlighted in Figure 42.

After the incubation time, 24 or 72 hours according to the pseudotype platform used, plate readout is conducted. The plate is removed from the incubator and 50µL of previously prepared Bright-Glo™ Luciferase Assay System solution are added to the wells. The plate is then incubated in the dark for 5 minutes at 500rpm. Read out is conducted by means of GloMax® Discover microplate reader luminometer, with an integration time of 0,3 seconds.

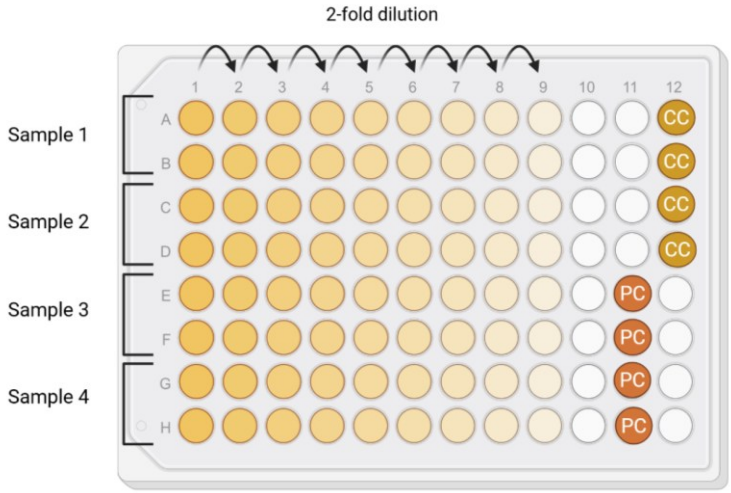

***Figure 42**. PBNA plate layout (created with Biorender.com).*
Samples are tested in duplicates and serially diluted with a 2-fold dilution from column 1 to 9. Wells E-H of column 11 correspond to the pseudotype control (PC); wells A-D of column 12 correspond to the cell control (CC).

Data analysis for pseudotype based neutralization assays

Calculation of the half maximal inhibitory concentration (IC_{50}) of the tested samples is obtained by means of GraphPad Prism. Data analysis is carried out by performing data normalization according to cell control mean value and pseudotype control mean value, followed by the application of a non-linear regression model. The procedure is described in detail on “Pseudotype Neutralization Assays: From Laboratory Bench to Data Analysis” (Ferrara *et al.*, 2018).

6 RESULTS

6.1 Viral pseudotypes production

6.1.1 Two plasmid system lentiviral pseudotypes

To produce pseudotyped viruses based on lentiviral vector with the two plasmids system, the optimal and standardized transfection condition is as follows.

- Plasmid concentration for each cell culture dish: 4,5µg of pNL4-3.Luc.R-E- plasmid and 4,5µg of the envelope protein plasmid for the virus of interest.
- Transfection reagent volume for each culture dish: 20µL of EndoFectin™ Lenti Transfection Reagent, or 20µL of Lipofectamine™ 2000 Transfection Reagent.

Figure 43 shows the status of HEK293T/17 cells throughout the process of viral pseudotype production: it is possible to observe how the cells producing the viral pseudotype are irregular in shape and growth over time when compared to the negative control.

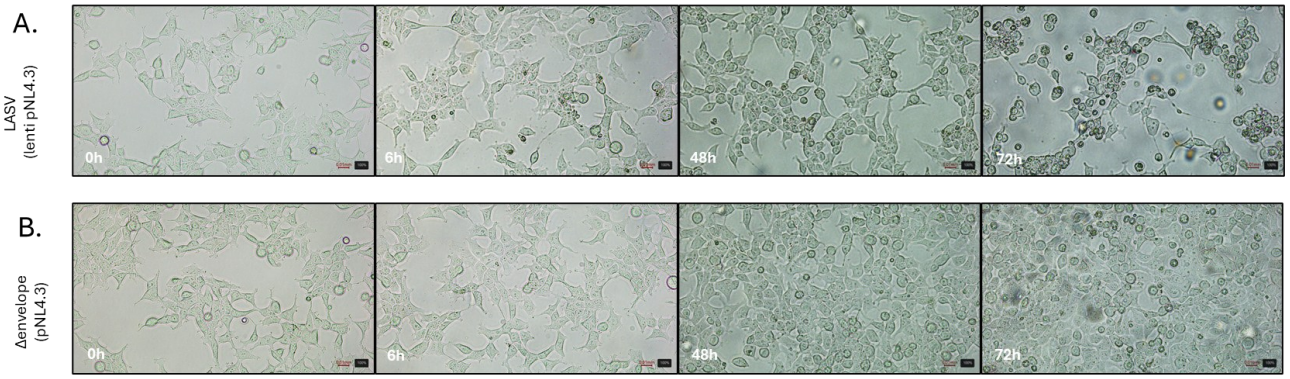

Figure 43. *Timeline of HEK293T/17 appearance during the course of LASV PV production (zoom 20X). Aspect of HEK293T/17 throughout LASV PV production with lentiviral two plasmids system (A) in comparison with that of HEK293T/17 transfected with pNL4.3 only (B). Each image corresponds to a different timepoint starting from the day after cell seeding before transfection (0h) until the time of harvest (72h post transfection).*

6.1.2 Three plasmid system lentiviral pseudotypes

To produce pseudotyped viruses based on lentiviral vector with the three plasmids system, the optimal and standardized transfection condition is as follows.

- Plasmid concentration for each cell culture dish: 3µg of p8.91 plasmid, 4,5µg of pCSFLW plasmid and 3µg of the envelope protein plasmid for the virus of interest.
- Transfection reagent volume for each culture dish: 25µL of EndoFectin™ Lenti Transfection Reagent, or 25µL of Lipofectamine™ 2000 Transfection Reagent.

6.1.3 VSV based pseudotypes

To produce pseudotyped viruses based on the VSV system, the optimal and standardized transfection condition is as follows.

- Plasmid concentration for each cell culture dish: 9µg of the envelope protein plasmid for the virus of interest.
- Transfection reagent volume for each culture dish: 60µL of PEI transfection reagent.
- Multiplicity of Infection (MOI) at which VSV-ΔG-LUC*G is used for each culture dish: 0,1 number of infectious virus particles / the number of target cells, considering the seeding cell number on day 1.
- The titer of VSV-ΔG-LUC*G is reported within the certificate of analysis provided by VectorBuilder company

6.2 Viral pseudotypes characterization

Viral pseudotypes titration assays

A PV titer is considered positive when, according to the equation described previously in Data analysis for titration assays (paragraph 5.2.4 Viral pseudotypes titration assay) the PV dose necessary for obtaining the pseudoviral working solution for PBNA is lower or equal to 5000µl, which is the total volume required for one plate. To meet this criterion, the lowest acceptable titer of a PV can be calculated as follows:

$$\frac{1 \times 10^8 (RLU/plate)}{titer\ threshold\ (RLU/mL)} \times 1000 = 5000\ (\mu l/plate)$$

This equation refers to the condition of $1x10^6$ RLU/well pseudoviral dose input. Therefore, in case the pseudoviral dose input for PBNA corresponds to $1x10^6$ RLU/well, the PV titer threshold will be $2x10^7$ RLU/mL. If the chosen pseudoviral dose input for PBNA is of $5x10^5$ RLU/well, the PV titer threshold will correspond to $1x10^7$ RLU/mL. A PV titer lower than the

indicated threshold will be considered negative, as the PV dose necessary to prepare the pseudoviral working solution for one plate will be higher than 5000 µl.

For each produced pseudotype, a Δenvelope transfection is performed in parallel. The Δenvelope represent the negative control of PV production, therefore, as expected, their titers never meet the threshold of titer acceptability.

Pseudotype-based neutralization assays

To characterize the produced viral pseudotypes, PBNAs are performed using positive control and negative control. For those pseudoviruses where a specific WHO international standard is not available, alternatives able to provide a protective titer such as neutralizing antibodies or serum samples, are used. The IgG/IgA/IgM depleted human serum (serum minus) is used as negative control.

Specific pseudotype generation is confirmed when positive and negative control provide a protective and non-protective titer, respectively. Neutralization titers are expressed as continuous half-maximal inhibitory concentration (IC_{50}) titers; when the IC_{50} is lower than 20, corresponding to the first dilution point, the sample is considered non-neutralizing (negative).

6.2.1 LASV pseudotypes

LASV pseudotypes are produced with lentiviral two- and three-plasmids systems and with the VSV system. The mean PV titers of each production are $7{,}24 \times 10^{8}$ RLU/mL, $1{,}16 \times 10^{11}$ RLU/mL and $1{,}8 \times 10^{10}$ RLU/mL, respectively. Figure 44 illustrates the comparison between LASV PV titers and that of the corresponding Δenvelope. The LASV PV doses necessary for obtaining PBNAs working solutions are shown in Table 2.

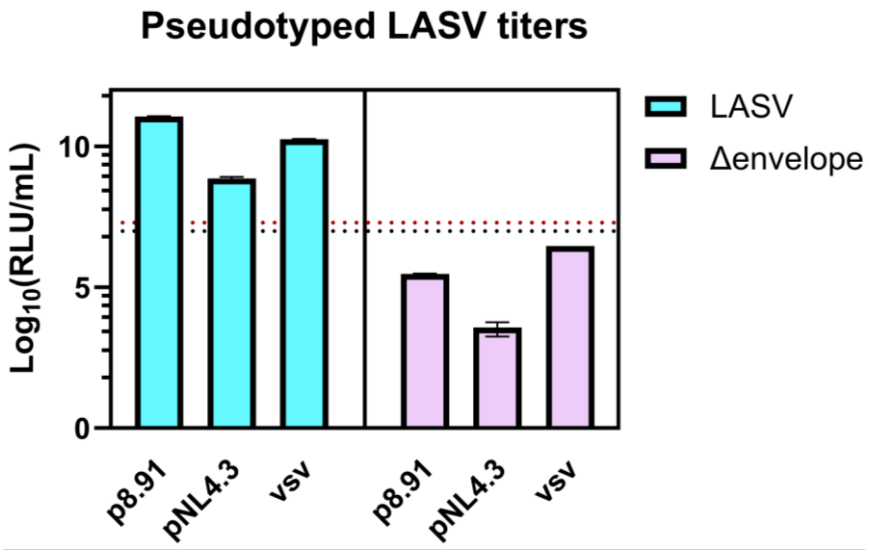

***Figure 44**. Log10 transformed titers (RLU/ml) of LASV PV and their corresponding Δenvelope conditions. Dotted red and black lines represent the threshold between positive and negative titer for 1x10⁶ and 5x10⁵ RLU/well, respectively.*

		LASV		
		lenti p8.91	lenti pNL4.3	vsv
pseudoviral working solution (ul/plate)	1.000.000 RLU/well dose input	0,86	138,3	5,6
	500.000 RLU/well dose input	0,43	69,2	2,8

***Table 2.** LASV PV doses (µl/plate) necessary for obtaining PBNA working solution (created with Biorender.com).*
The doses are calculated for each packaging construct and for a dose input of both 1x10⁶ and 5x10⁵ RLU/well.

LASV PBNAs

International standard WHO 20/228 is tested against LASV pseudotypes produced with the lentiviral two- and three-plasmids systems and with the VSV system. The respective IC_{50} values are 581, 746 and 395; therefore WHO 20/228 is able to neutralize the three LASV pseudotypes. On the contrary the serum minus is not neutralizing. The graphs in Figure 45 provide a comparison between the three neutralizations of the PVs.

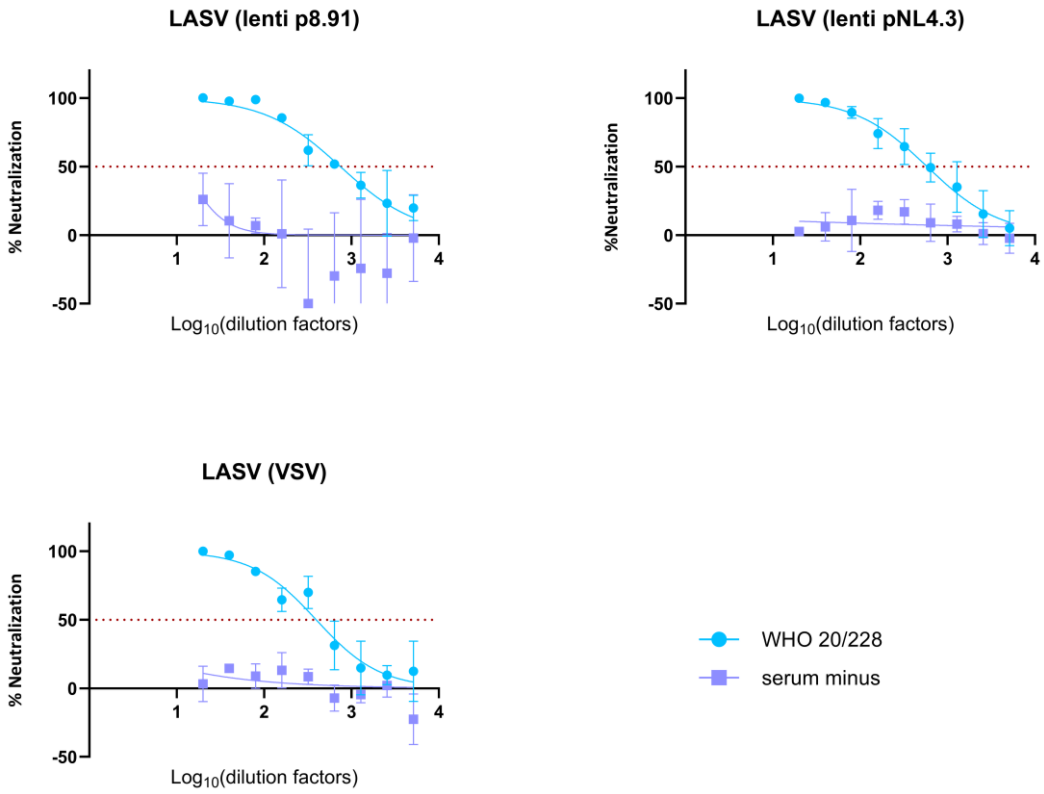

Figure 45. *Neutralization curves of LASV PBNAs performed with positive and negative controls. On the Y axis of the graphs the percentage of neutralization of the PV signal is reported and the X axis reports the Log10 transformed dilution factors of the controls indicated in the legend. The dotted red line is to highlight the point at which 50% of PV signal is neutralized. International standard WHO 20/228 is able to neutralize LASV PVs produced with both lentiviral systems (p8.91 and pNL4.3 based) and with the VSV system, whereas the serum minus does not have a protective titer.*

6.2.2 Betacoronaviruses pseudotypes

Betacoronaviruses pseudotypes are produced with lentiviral two- (pNL4.3 and envelope protein) and three- (p8.91, pCSFLW and envelope protein) plasmids systems as well as with the VSV system.

MERS-CoV pseudotypes

The mean MERS-CoV PV titers are $2{,}6x10^6$ RLU/mL, $6{,}1x10^8$ RLU/mL and $1{,}1x10^8$ RLU/mL, for the two and three plasmids lentiviral systems and for the VSV system respectively. According to the previously reported equation (paragraph 6.2 Viral pseudotypes titers) MERS-CoV PV titers obtained with lentiviral two plasmids system do not reach the threshold of acceptability; therefore, as an attempt to increase the titer, the same PV is produced using Lipofectamine™ 2000 Transfection Reagent. In this case the mean PV titer is $4{,}5x10^6$ RLU/mL, which is still under the threshold of titer acceptability.

SARS-CoV-1 pseudotypes

SARS-CoV-1 PV mean titers are $1{,}1x10^8$ RLU/mL, $1{,}6x10^8$ RLU/mL and $4{,}9x10^9$ RLU/mL, for the two- and three-plasmids lentiviral systems and for the VSV system respectively.

SARS-CoV-2 pseudotypes

SARS-CoV-2 PV mean titers are $4{,}6x10^8$ RLU/mL, $1{,}9x10^{10}$ RLU/mL and $1{,}8x10^8$ RLU/mL, for the two- and three-plasmids lentiviral systems and for the VSV system respectively.

Figure 46 illustrates the comparison between betacoronaviruses PV titers and that of the corresponding Δenvelope. The betacoronaviruses PV doses necessary for obtaining PBNAs working solutions are shown in Table 3.

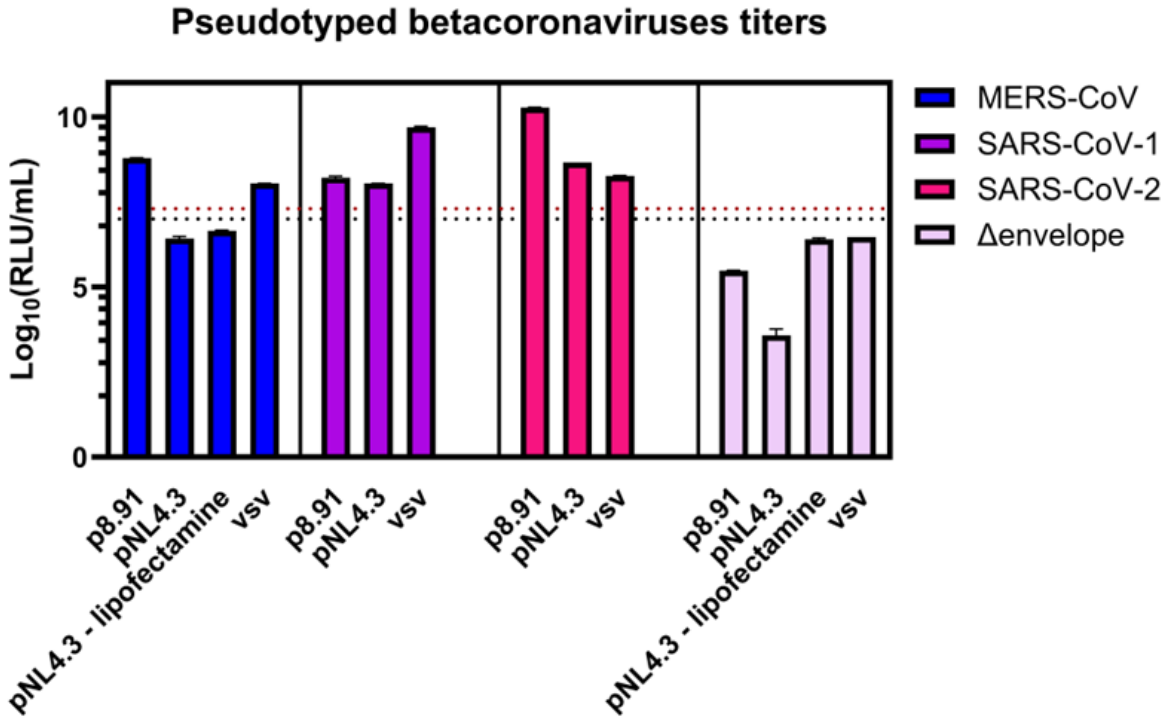

Figure 46. *Log10 transformed titers (RLU/ml) of betacoronaviruses PV and their corresponding Δenvelope conditions.*
MERS-CoV PV produced with pNL4.3, does not reach the titer of threshold acceptability, therefore is not usable in PBNA with either $1x10^6$ a $5x10^5$ RLU/well dose input. Dotted red and black lines represent the threshold between positive and negative titer for $1x10^6$ and $5x10^5$ RLU/well, respectively.

		BETACORONAVIRUSES			
	MERS-CoV	lenti p8.91	lenti pNL4.3	lenti pNL4.3 lipofectamine	vsv
pseudoviral working solution (µl/plate)	1.000.000 RLU/well dose input	164,9	> 5000	> 5000	2404,7
	500.000 RLU/well dose input	82,5	> 5000	> 5000	1202,4
	SARS-CoV-1	lenti p8.91	lenti pNL4.3	vsv	
pseudoviral working solution (µl/plate)	1.000.000 RLU/well dose input	622	913,7	20,5	
	500.000 RLU/well dose input	311	456,9	10,2	
	SARS-CoV-2	lenti p8.91	lenti pNL4.3	vsv	
pseudoviral working solution (µl/plate)	1.000.000 RLU/well dose input	5,3	219,8	547,3	
	500.000 RLU/well dose input	2,7	110	273,7	

Table 3. *Betacoronaviruses PV doses (µl/plate) necessary for obtaining PBNA working solution (created with Biorender.com).*
The doses are calculated for each packaging construct and for a dose input of both $1x10^6$ and $5x10^5$ RLU/well. When the required dose is more than 5000 µl/plate it means that the PV in object is not usable for PBNA, as it exceeds the volume of PBNA pseudoviral solution which is 5 mL/plate.

BETACORONAVIRUSES PBNAs

MERS-CoV pseudotypes

The titer MERS-CoV PV produced with the lentiviral two plasmids system did not meet the threshold of acceptability, therefore international standard WHO 20/228 is tested against MERS-CoV PVs obtained with the lentiviral three plasmids system and VSV based system. In the former case, the IC_{50} value is 1742, while in the latter case it is 2809. The serum minus is not neutralizing. Figure 47 illustrates the two neutralizations.

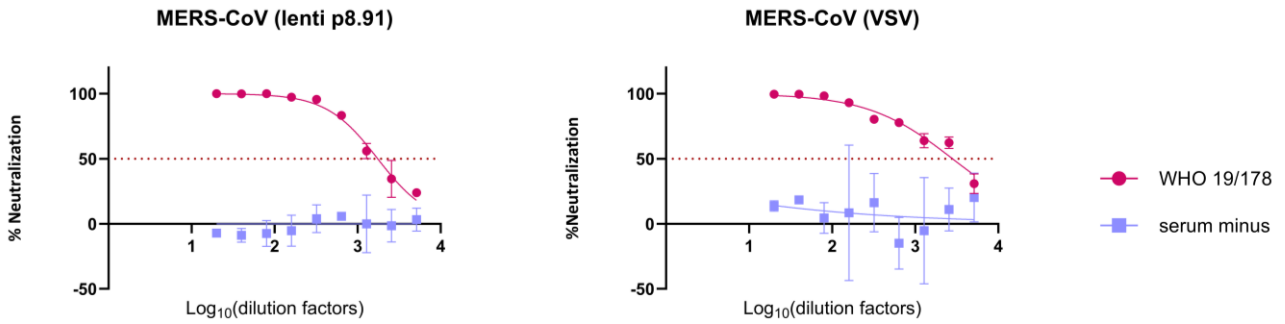

Figure 47. *Neutralization curves of MERS-CoV PBNAs performed with positive and negative controls. On the Y axis of the graphs the percentage of neutralization of the PV signal is reported and the X axis reports the Log10 transformed dilution factors of the controls indicated in the legend. The dotted red line highlights the point at which 50% of PV signal is neutralized. International standard WHO 19/178 is able to neutralize MERS-CoV PVs produced with both lentiviral system (p8.91) and with the VSV system, whereas the serum minus does not have a protective titer.*

SARS-CoV-1 pseudotypes

International standard WHO 23/242 and recombinant mAb CR3022 are tested against SARS-CoV-1 pseudotypes produced with the lentiviral two and three plasmids systems and with the VSV system. For WHO 23/242 the respective IC_{50} values are 942, 196 and 317; while for mAb CR3022 they are 179, 65 and 80. Both WHO 20/228 and mAb CR3022 are able to neutralize SARS-CoV-1 pseudotypes. On the contrary the serum minus is not neutralizing. Graphs reported in Figure 48 allow a visual comparison of the three neutralizations of the PVs.

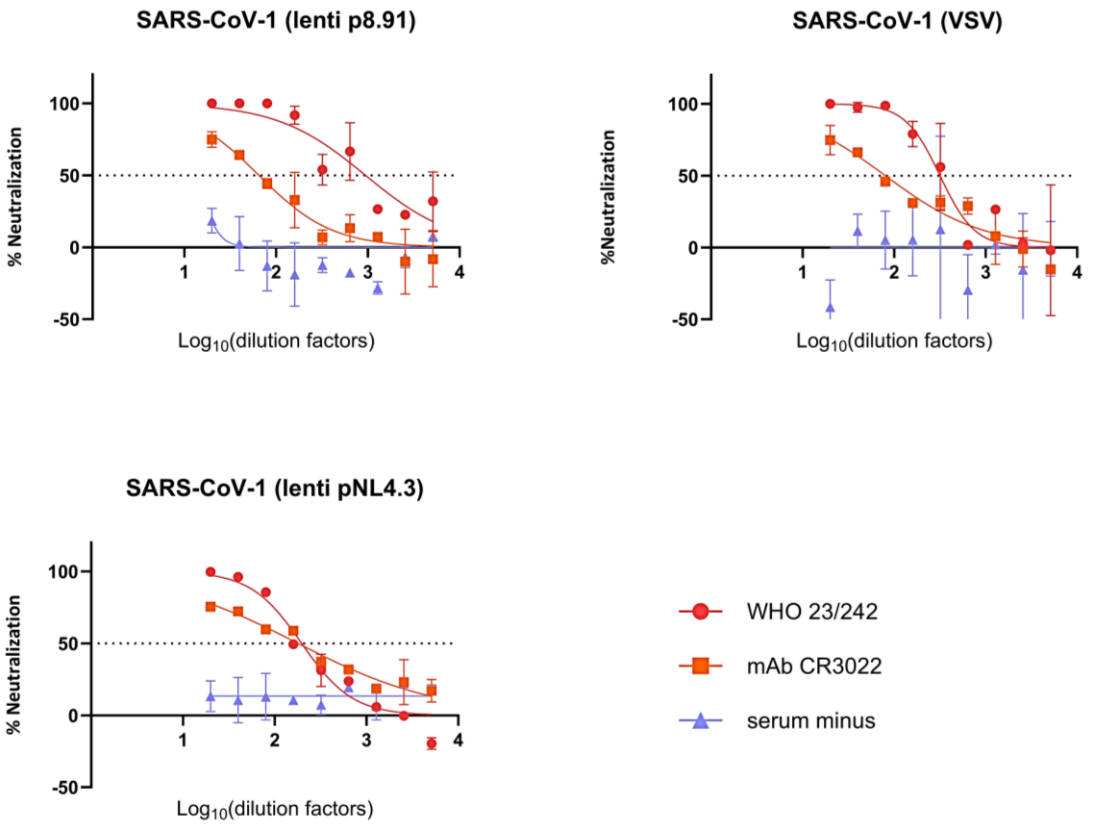

Figure 48. *Neutralization curves of SARS-CoV-1 PBNAs performed with positive and negative controls. On the Y axis of the graphs the percentage of neutralization of the PV signal is reported and the X axis reports the Log10 transformed dilution factors of the controls indicated in the legend. The dotted red line is to highlight the point at which 50% of PV signal is neutralized. International standard WHO 23/242 and mAb CR3022 are able to neutralize SARS-CoV-1 PVs produced with both lentiviral systems (p8.91 and pNL4.3 based) and with the VSV system, whereas the serum minus does not have a protective titer.*

SARS-CoV-2 pseudotypes

International standard WHO 20/148 and serum minus are tested against SARS-CoV-1 pseudotypes produced with the lentiviral two and three plasmids systems and with the VSV system. Serum minus does not provide a neutralization of PVs signal. Regarding international standard WHO 20/148, the IC_{50} values are 306 (lentiviral two plasmids system), 380 (lentiviral three plasmids system) and 190 (VSV system). Graphs reported in Figure 49 permit a visual comparison of the different neutralization curves.

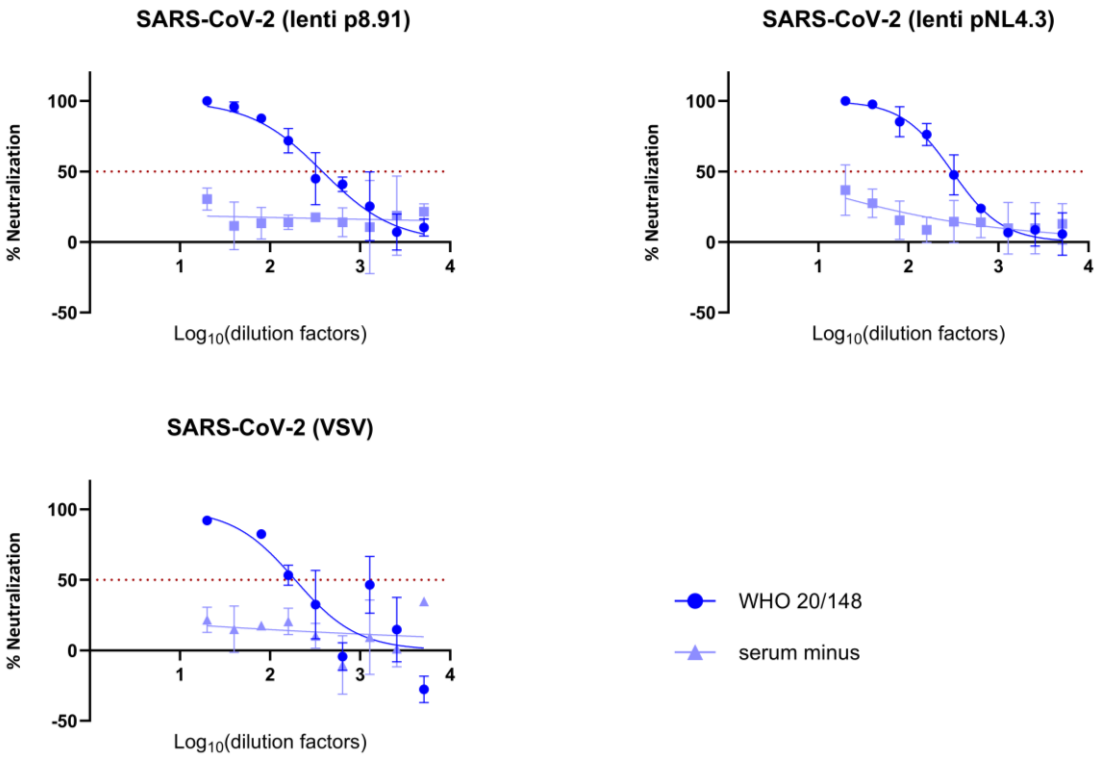

Figure 49. *Neutralization curves of SARS-CoV-2 PBNAs performed with positive and negative controls. On the Y axis of the graphs the percentage of neutralization of the PV signal is reported and the X axis reports the Log10 transformed dilution factors of the controls indicated in the legend. The dotted red line is to highlight the point at which 50% of PV signal is neutralized. International standard WHO 20/148 is able to neutralize SARS-CoV-2 PVs produced with lentiviral systems (p8.91 and pNL4.3 based) and with the VSV system, whereas the serum minus does not have a protective titer.*

6.2.3 Filoviruses pseudotypes

Filoviruses pseudotypes are produced with lentiviral two (pNL4.3 and envelope protein) and three (p8.91, pCSFLW and envelope protein) plasmids systems as well as with the VSV system.

EBOV pseudotypes: strains Sudan and Makona

The mean EBOV-Sudan PV titers are $2{,}2 \times 10^6$ RLU/mL, $4{,}7 \times 10^9$ RLU/mL and $1{,}8 \times 10^8$ RLU/mL, for the two and three plasmids lentiviral systems and for the VSV system respectively; while for EBOV-Makona the mean PV titers are $6{,}5 \times 10^5$ RLU/mL, $6{,}4 \times 10^8$ RLU/mL and $2{,}4 \times 10^8$ RLU/mL. According to the equation described in Viral pseudotypes titers (paragraph 6.2 Viral pseudotypes titers) EBOV PV titers of either strain obtained with lentiviral two plasmids system do not reach the threshold of acceptability; therefore, as an attempt to increase the titer, the same PV are produced using Lipofectamine™ 2000

Transfection Reagent. In this case the mean PV titer for EBOV-Sudan and EBOV-Makona are $3x10^5$ RLU/mL and $1,7x10^5$ RLU/mL respectively; however, both are still under the threshold of titer acceptability.

MARV pseudotypes: strains Angola and Congo

The mean MARV-Angola PV titers are $9x10^7$ RLU/mL, $2,2x10^{10}$ RLU/mL and $7,9x10^9$ RLU/mL, for the two and three plasmids lentiviral systems and for the VSV system respectively; while for MARV-Congo the mean PV titers are $2,2x10^8$ RLU/mL, $4x10^{10}$ RLU/mL and $1,2x10^9$ RLU/mL.

Figure 50 illustrates the comparison between filoviruses PV titers and that of the corresponding Δenvelope. The filoviruses PV doses necessary for obtaining PBNAs working solutions are shown in Table 4.

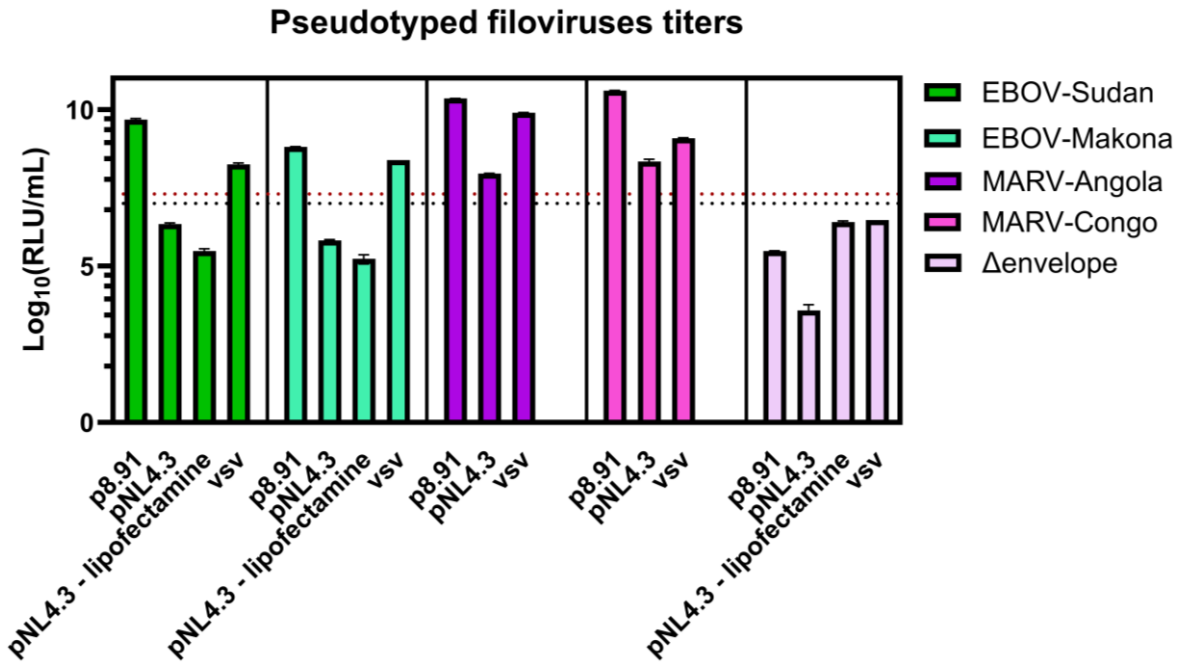

Figure 50. *Log10 transformed titers (RLU/ml) of filoviruses PV and their corresponding Δenvelope conditions. EBOV PV strains produced with pNL4.3, did not reach the titer of threshold acceptability, therefore are not usable in PBNA with either $1x10^6$ a $5x10^5$ RLU/well dose input. Dotted red and black lines represent the threshold between positive and negative titer for $1x10^6$ and $5x10^5$ RLU/well, respectively.*

		FILOVIRUSES			
pseudoviral working solution (µl/plate)	EBOV - Sudan	lenti p8.91	lenti pNL4.3	lenti pNL4.3 lipofectamine	vsv
	1.000.000 RLU/well dose input	21,3	> 5000	> 5000	572,5
	500.000 RLU/well dose input	10,7	> 5000	> 5000	286,3
pseudoviral working solution (µl/plate)	EBOV - Makona	lenti p8.91	lenti pNL4.3	lenti pNL4.3 lipofectamine	vsv
	1.000.000 RLU/well dose input	156,8	> 5000	> 5000	410,5
	500.000 RLU/well dose input	78,4	> 5000	> 5000	205,3
pseudoviral working solution (µl/plate)	MARV - Congo	lenti p8.91	lenti pNL4.3	vsv	
	1.000.000 RLU/well dose input	2,5	460,2	83,3	
	500.000 RLU/well dose input	1,3	230,1	41,6	
pseudoviral working solution (µl/plate)	MARV - Angola	lenti p8.91	lenti pNL4.3	vsv	
	1.000.000 RLU/well dose input	4,5	1110,6	12,6	
	500.000 RLU/well dose input	2,2	555,3	6,3	

Table 4. *Filoviruses PV doses (µl/plate) necessary for obtaining PBNA working solution (created with Biorender.com).*
The doses are calculated for each packaging construct and for a dose input of both $1x10^6$ and $5x10^5$ RLU/well. When the required dose is more than 5000 µl/plate it means that the PV in object is not usable for PBNA as it exceeds the volume of PBNA pseudoviral solution which is 5 mL/plate.

FILOVIRUSES PBNAs

EBOV pseudotypes: strains Sudan and Makona

As the titers of EBOV (both Sudan and Makona strains) PVs produced with the lentiviral two plasmids system did not meet the threshold of acceptability, international standard WHO 15/262 is tested against EBOV PVs obtained with the lentiviral three plasmids system and VSV based system. Moreover, mAb 16F6 was used in PBNAs with the Sudan strain, while anti-EBOV pAb was used with Makona strain. Regarding the international standard WHO 15/262 tested against EBOV PVs produced with lentiviral platform the IC_{50} values 2210 (strain Sudan) and 298 (strain Makona); while in the case EBOV PVs produced with VSV system the IC_{50} values are 141 (strain Sudan) and 91 (strain Makona). The IC_{50} of mAb 16F6 are 4436 (EBOV-Sudan lentiviral system) and 7566 (EBOV-Sudan VSV system). The IC_{50} of anti-EBOV pAb are 2773 (EBOV-Makona lentiviral system) and 880 (EBOV-Makona VSV system). All the described neutralization curves can be observed in Figure 51.

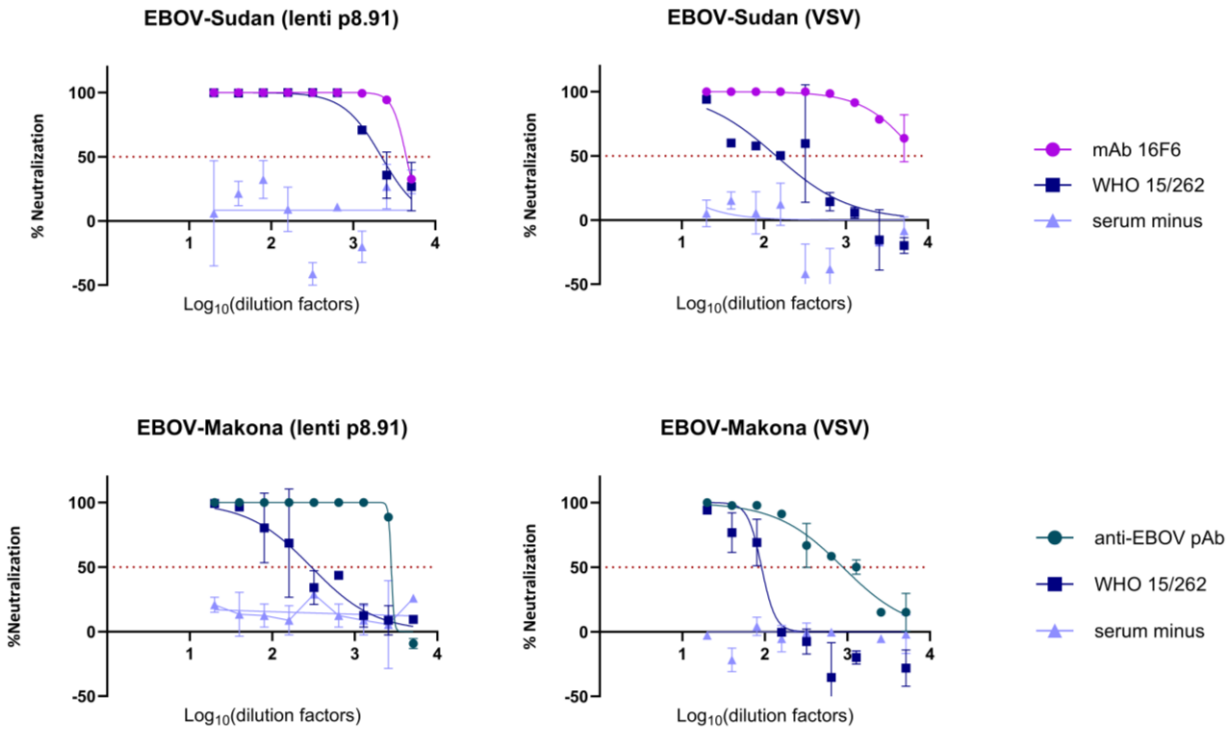

Figure 51. *Neutralization curves of EBOV PBNAs performed with positive and negative controls. On the Y axis of the graphs the percentage of neutralization of the PV signal is reported and the X axis reports the Log10 transformed dilution factors of the controls indicated in the legend. The dotted red line is to highlight the point at which 50% of PV signal is neutralized. International standard WHO 15/262 is able to neutralize all EBOV PVs; mAb 16F6 neutralizes EBOV PVs strain Sudan while anti-EBOV pAb neutralizes EBOV PVs strain Makona. The serum minus does not have a protective titer.*

MARV pseudotypes: strains Angola and Congo

Anti-MARV mAb and serum minus are tested against MARV pseudotypes (strains Angola and Congo) produced with the lentiviral two and three plasmids systems and with the VSV system. For anti-MARV mAb, tested against MARV-Angola, the respective IC_{50} values are 558, 646 and 1802. As for anti-MARV mAb, tested against MARV-Congo, the respective IC_{50} values are 2995, 3553 and 2211. Serum minus does not provide a neutralization of the PVs signal. Graphs in Figure 52 report the different neutralization curves.

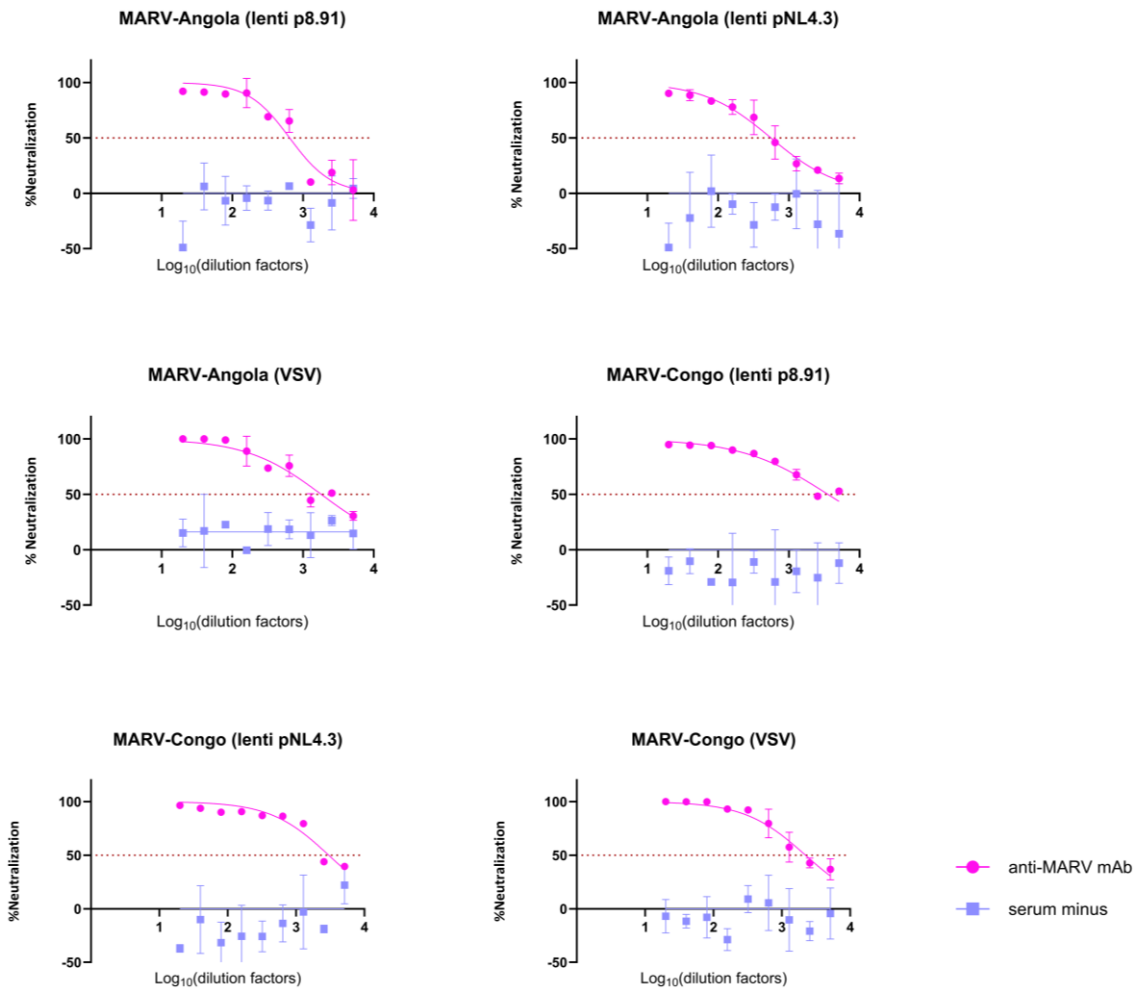

Figure 52. *Neutralization curves of MARV PBNAs performed with positive and negative controls. On the Y axis of the graphs the percentage of neutralization of the PV signal is reported and the X axis reports the Log10 transformed dilution factors of the controls indicated in the legend. The dotted red line is to highlight the point at which 50% of PV signal is neutralized. Anti-MARV mAb is able to neutralize all MARV PVs. The serum minus does not have a protective titer.*

6.2.4 NiV pseudotypes

For the production of NiV PVs two distinct envelope proteins are necessary: the G protein (receptor-binding protein) and the F protein (fusion protein). In this case, HEK293T/17 cells are transfected with a plasmid coding for the full-length envelope G protein plus a different plasmid coding for the truncated FΔct3 protein (Khetawat A *et al*., 2010), apart from the usual backbone.

NiV pseudotypes are produced with lentiviral two (pNL4.3 and envelope protein) and three (p8.91, pCSFLW and envelope protein) plasmids systems and with the VSV system. The mean PV titers of each production are $5{,}1x10^5$ RLU/mL, $4{,}8x10^6$ RLU/mL and $4{,}3x10^6$

RLU/mL, respectively. Since the closer titer to the threshold of acceptability is obtained with the lentiviral three plasmid system, the same production is performed and, in this case, at the time of harvest, the producing cells together with the medium undergo F&T steps for three times; this process improves the titer to 9,1x10^6 RLU/mL. After the F&T, the solution is concentrated through 3-hour centrifugation at 4°C and 8000rcf, and the pellet resuspended with 1mL of supernatant has a mean titer of 7,5x107 RLU/mL, which is above both threshold of acceptability.

Figure 53 illustrates the comparison between NiV PV titers and that of the corresponding Δenvelope. The NiV PV doses necessary for obtaining PBNAs working solutions are shown in Table 5.

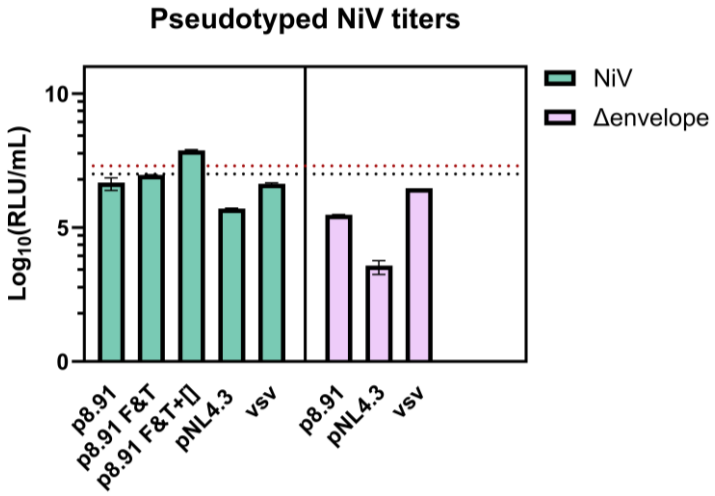

Figure 53. *Log10 transformed titers (RLU/ml) of NiV PV and their corresponding Δenvelope conditions. Only NiV PV that undergoes F&T and centrifuge concentration (indicated with symbol []) processes reaches the titer of threshold acceptability and can be used in PBNA with either 1x10^6 a 5x10^5 RLU/well dose input. Dotted red and black lines represent the threshold between positive and negative titer for 1x10^6 and 5x10^5 RLU/well, respectively.*

		NiV				
		lenti p8.91	lenti p8.91 F&T	lenti p8.91 F&T + []	lenti pNL4.3	vsv
pseudoviral working solution (ul/plate)	1.000.000 RLU/well dose input	> 5000	> 5000	1336,4	> 5000	> 5000
	500.000 RLU/well dose input	> 5000	> 5000	668,2	> 5000	> 5000

Table 5. *NiV PV doses (µl/plate) necessary for obtaining PBNA working solution (created with Biorender.com). The doses are calculated for each packaging construct and for a dose input of both 1x10^6 and 5x10^5 RLU/well. When the required dose is more than 5000 µl/plate it means that the PV in object is not usable for PBNA as it exceeds the volume of PBNA pseudoviral solution which is 5 mL/plate.*

NiV PBNAs

International standard WHO 22/130_NT is tested against NiV pseudotypes produced with the lentiviral three plasmids systems. The IC_{50} value is 795, therefore WHO 22/130_NT is able to neutralize NiV PV produced with the lentiviral three plasmids system. Serum minus is not neutralizing. The graph in Figure 54 illustrate the neutralization curve of NiV PBNA.

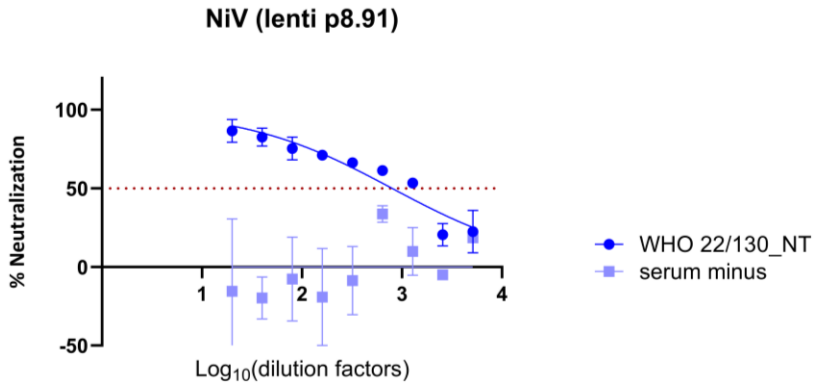

Figure 54. *Neutralization curves of NiV PBNA performed with positive and negative controls. On the Y axis of the graphs the percentage of neutralization of the PV signal is reported and the X axis reports the Log10 transformed dilution factors of the controls indicated in the legend. The dotted red line is to highlight the point at which 50% of PV signal is neutralized. WHO 22/130_NT is able to neutralize NiV PV. The serum minus does not have a protective titer.*

6.2.5 CHICKV pseudotypes

CHICKV pseudotypes are produced with lentiviral two (pNL4.3 and envelope protein) and three (p8.91, pCSFLW and envelope protein) plasmids systems and with the VSV system. The mean PV titers of each production are $3{,}9x10^7$ RLU/mL, $4{,}4x10^9$ RLU/mL and $3{,}9x10^9$ RLU/mL, respectively. Figure 55 illustrates the comparison between CHICKV PV titers and that of the corresponding Δenvelope. The CHICKV PV doses necessary for obtaining PBNAs working solutions are shown in Table 6.

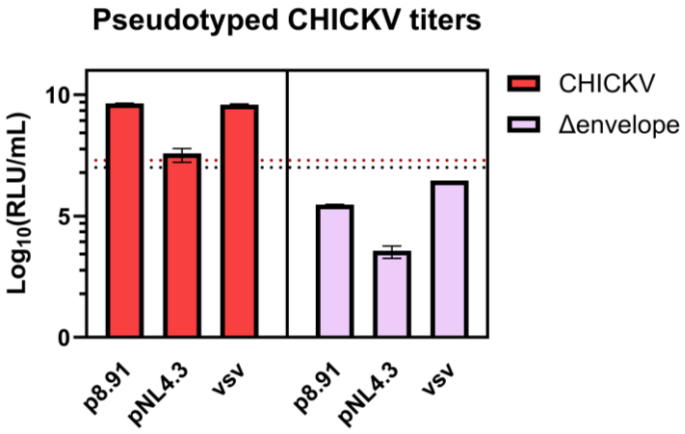

Figure 55. *Log10 transformed titers (RLU/ml) of CHICKV PV and their corresponding Δenvelope conditions. A visual comparison of the bars permits to observe that all the productions lacking LASV envelope protein did not reach the titer of threshold acceptability, therefore are not usable in PBNA with either 1x10⁶ a 5x10⁵ RLU/well dose input. Dotted red and black lines represent the threshold between positive and negative titer for 1x10⁶ and 5x10⁵ RLU/well, respectively.*

		CHICKV		
		lenti p8.91	lenti pNL4.3	vsv
pseudoviral working solution (ul/plate)	1.000.000 RLU/well dose input	22,8	2589,1	25,5
	500.000 RLU/well dose input	11,4	1294,5	12,7

Table 6. *CHICKV PV doses (µl/plate) necessary for obtaining PBNA working solution (created with Biorender.com).*
The doses are calculated for each packaging construct and for a dose input of both 1x10⁶ and 5x10⁵ RLU/well.

CHICKV PBNAs

PBNAs of CHICKV are performed with pseudotypes produced with the lentiviral two- and three-plasmids systems and with the VSV system. Human serum samples from Africa, are donated from the University of Siena and used as positive controls as they resulted positive for IgG against CHICKV in an unpublished comparative study of commercial ELISAs. These samples are identified as samples 189, 216, 251 and 009. When tested against CHICK PV produced with the lentiviral two plasmids system the IC_{50} values of the respective samples are 164, 85, 64 and 84. When tested against CHICK PV produced with the lentiviral three plasmids system the IC_{50} values of the respective samples are 4205, 3344, 1376 and 2696. Finally, when tested against CHICK PV produced with the VSV system the IC_{50} values of the respective samples are 7676, 7137, 4689 and 4610. Serum minus is not neutralizing. The graphs in Figure 56 illustrate the neutralization curves of CHICKV PBNAs.

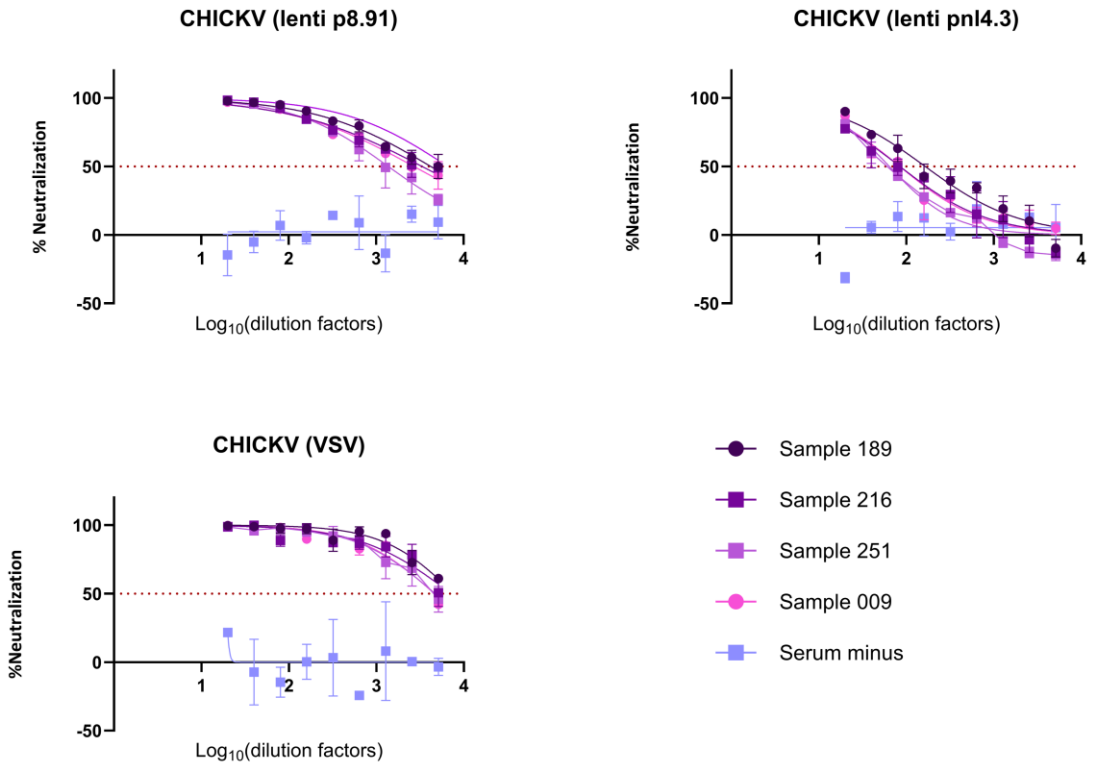

***Figure 56**. Neutralization curves of CHICKV PBNAs performed with positive and negative controls. On the Y axis of the graphs the percentage of neutralization of the PV signal is reported and the X axis reports the Log10 transformed dilution factors of the controls indicated in the legend. The dotted red line is to highlight the point at which 50% of PV signal is neutralized. Serum samples from PATH project are able to neutralize all CHICKV PVs. The serum minus does not have a protective titer.*

6.2.6 Helper VSV-ΔG-LUC*G

The titers of the helper virus VSV-ΔG-LUC*G are expected to be high therefore, to obtain a usable titer for PBNA, the VSV-ΔG-LUC*G was pre diluted 1:1000 and 1:10000 before being titrated with a 3-fold dilution. The mean titers, normalized to the pre dilution of the helper and the 3-fold dilution performed on plate, are $1x10^{13}$ RLU/mL and $3,5x10^{12}$ RLU/mL respectively. Figure 57 illustrates the comparison between the two titers. Table 7 shows the VSV-ΔG-LUC*G doses necessary for obtaining PBNAs working solutions, in this case pre-diluted does not refer to the neat helper vector but to its pre diluted state.

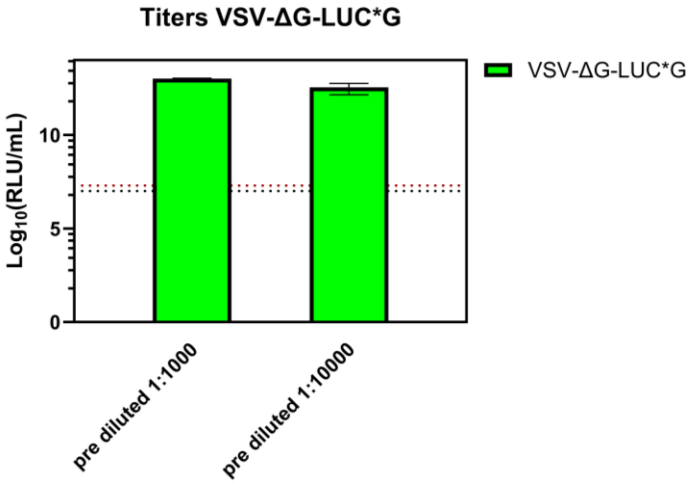

Figure 57. *Log10 transformed titers (RLU/ml) of VSV-ΔG-LUC*G pre diluted 1:1000 and 1:10000 and 3-fold titrated.*
Dotted red and black lines represent the threshold between positive and negative titer for 1x10^6 and 5x10^5 RLU/well, respectively.

		Helper VSV-ΔG-LUC	
		pre diluted 1:1000	pre diluted 1:10000
pseudoviral working solution (ul/plate)	1.000.000 RLU/well dose input	9,6	79,1
	500.000 RLU/well dose input	4,8	39,5

Table 7. *VSV-ΔG-LUC*G doses (µl/plate) necessary for obtaining PBNA working solution (created with Biorender.com).*
The doses are calculated for a dose input of both 1x10^6 and 5x10^5 RLU/well, the corresponding values do not refer to the neat helper vector but to its mentioned pre dilution state.

Evaluation of proper integration of target envelope proteins into the VSV backbone

With regard to the pseudotypes produced through the VSV platform, in order to verify the correct incorporation of the target envelope protein into the VSV backbone, and to observe any interference by the VSV helper in PBNAs, neutralization assays of VSV-ΔG-LUC*G are initially performed with Ab anti-VSV-G. Such antibody, either pre-diluted 1:10 and 1:100 is able to neutralize the “naked” VSV helper virus. The neutralization curve is shown in Figure 58.

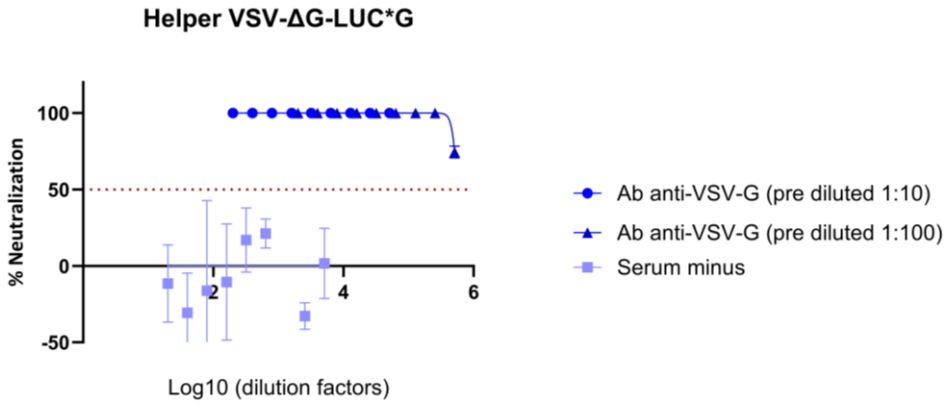

Figure 58. *Neutralization curves of helper vector VSV-ΔG-LUC*G obtained through neutralization assays performed using positive and negative controls.*
*On the Y axis of the graph the percentage of neutralization of helper VSV-ΔG-LUC*G signal is reported and the X axis reports the Log10 transformed dilution factors of the controls indicated in the legend. The dotted red line is to highlight the point at which 50% of PV signal is neutralized. Ab anti-VSV-G, pre diluted 1:10 and 1:100, is able to neutralize VSV helper vector in either case. The serum minus does not have a protective titer.*

Subsequently, neutralization assays were performed on all pseudotypes produced with the VSV platform, using Ab anti-VSV-G pre-diluted 1:100 and serum minus. The Ab anti-VSV-G in this case did not produce a neutralizing titer against any pseudotype, and neither did the serum minus. The histogram shown in Figure 59 illustrates the difference in IC_{50} of the Ab anti-VSV-G and serum minus used against VSV helper vector and VSV-based pseudotypes.

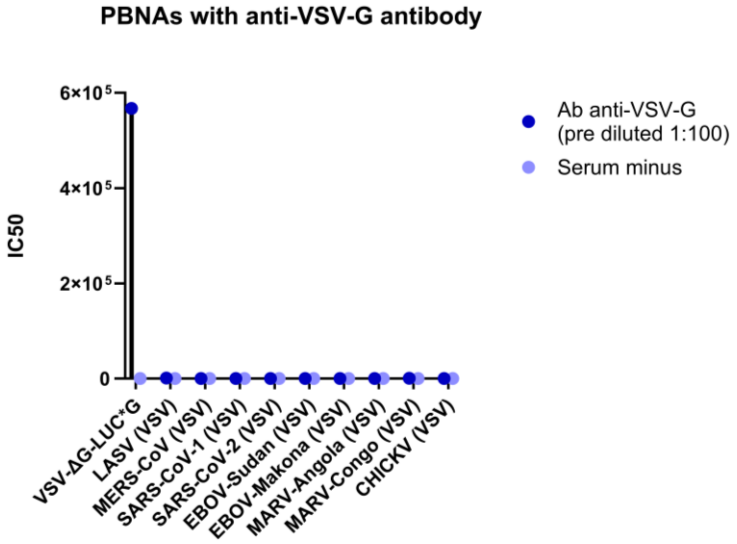

Figure 59. *IC_{50} values of Ab anti-VSV-G.*
*The X axis of the histogram reports the VSV helper virus and the pseudotypes produced with the VSV platform against which the Ab anti-VSV-G (pre-diluted 1:100) and serum minus are tested. The Y axis shows the IC50 values obtained from the neutralization assays: a neutralizing titer is observed only when the anti-VSV-G antibody is tested against helper virus VSV-ΔG-LUC*G. The antibody is not neutralizing against any VSV-based pseudotypes, nor is serum minus.*

7 DISCUSSION AND CONCLUSION

The danger posed by RNA viruses represents significant global health concern, as humanity consistently faces the risk of emerging and re-emerging pandemics caused by these pathogens. Recent history has demonstrated their devastating impact through outbreaks of viruses such as the Middle East Respiratory Syndrome Coronavirus and Ebola, all of which have led to severe public health crises across the globe. Another notable example like SARS-CoV-2, the causative agent of COVID-19, has resulted in millions of cases and fatalities worldwide. The inherent danger of RNA viruses stems from several characteristics, including their genomes' capacity for genetic recombination, which frequently leads to the formation of new viral variants. Furthermore, many of these viruses originate from vertebrate animal reservoirs and possess the ability to jump species barriers, crossing into new hosts, including humans, where they can cause fatal diseases. This capacity for rapid evolution, marked by high mutation rates and short replication cycles, enables RNA viruses to generate new subtypes and variants, posing substantial challenges to effective surveillance and control efforts (Chen Y *et al*., 2024; Ameni G *et al*., 2024).

Among RNA viruses, LASV, MERS-CoV, SARS-CoV-1 and SARS-CoV-2, EBOV, MARV, NiV and CHIKV represent a group of pathogens sharing several commonalities. These are all enveloped viruses which use their surface protein to initiate host cell infection, moreover, surface proteins are key target for neutralizing antibodies. Due to their highly pathogenic nature these viruses must be handled in high containment level laboratories, typically BSL-3 or BSL-4, to ensure safety and prevent accidental exposure and spread. Infection with these pathogens often leads to fatalities in humans, and survivors frequently experience severe long-term *sequelae*. Consequently, these pathogens are recognized as urgent priorities by the WHO R&D Blueprint for Epidemics (Mandl JN *et al*., 2015; Husby ML *et al*., 2021; Nnaji ND *et al*., 2021; Brake DA *et al*., 2022; Hewson R, 2024).

Given the inherent dangers posed by RNA viruses, robust pandemic preparedness is not merely a precautionary measure but an urgent global imperative. Lessons gleaned from previous outbreaks, particularly the profound impact of COVID-19, underscore the critical need for comprehensive strategies implemented during inter-pandemic periods. Effective preparedness aims to drastically reduce transmission, minimize cases and fatalities, sustain

essential health services, and mitigate the socio-economic fallout of future pandemics. Pandemic preparedness involves expanded surveillance systems to enable earlier detection of novel threats, alongside the development of stronger plans that go beyond traditional approaches. Furthermore, successful preparedness hinges on public perception and engagement, requiring transparent communication and addressing behavioral barriers like vaccine hesitancy to ensure public cooperation and adherence to health measures. Proactive investment in research, rapid data sharing, and the establishment of clear frameworks for prompt responses to early warning signals are crucial to mitigate the devastating impact of the next potential RNA virus pandemic (Williams BA *et al*., 2023; İzmir O *et al*., 2025).

Viral pseudotypes serve as crucial tools in virology and vaccine development due to their ability to enable the study of highly pathogenic viruses with minimized safety risks. Viral pseudotypes' limitation to a single round of replication makes them non-pathogenic. Consequently, the primary advantage of viral pseudotypes over authentic viruses lies in their enhanced safety profile, which allows for their handling in lower containment biosafety level 2 laboratory facilities, circumventing the need for BSL-3/4. This enables broader access for researchers globally to investigate dangerous viruses, including those difficult to propagate in vitro. (Bentley EM *et al*., 2015; Sedgwick RL *et al*., 2024; Rizatdinova SN *et al*., 2025).

This work describes the generation of a viral pseudotype library for LASV, MERS-CoV, SARS-CoV-1 and SARS-CoV-2, EBOV, MARV, NiV and CHIKV. Such library is based on both lentiviral two- and three-plasmid systems and on the VSV platform.

All viral pseudotypes, depending on the employed platform, are produced and harvested maintaining the same experimental conditions. The fact that plasmid concentration for cell transfection and incubation time before PVs collection does not change according to the viral strain, facilitates workflow and renders stable the methodology. The only exception is represented by NiV PV as in this case harvest is not performed by simply collecting and clarifying supernatant: in this case the transfected cells are also collected before undergoing three freeze and thaw cycles, clarification and finally a three hour long centrifugation. Since the pellet formed post centrifugation is resuspended in a small volume the production yield is lower than the other pseudotypes.

Overall, the lentiviral three-plasmids system and the VSV platform outperformed in terms of produced pseudotypes yield. Specifically, LASV, Sars-CoV-1 and Sars-CoV-2, MARV and CHICKV PVs reached an acceptable titer with all three production systems. EBOV and MERS did not reach acceptable titer when produced with pNL4.3. NiV only reached acceptable titer when produced with p8.91 and only with the harvest method performed from cell layer. The signal obtained with the titration of the negative control represents the background of the assay.

Regarding the lentiviral pseudotypes production system general considerations are to be addressed. First of all, plasmid size affects the efficiency of nuclear uptake, in fact cell transfection with larger plasmids is less efficient than that performed with smaller plasmids (Ribeiro S *et al*., 2012). This is confirmed in this work, since lentiviral pseudotypes produced with pNL4.3 resulted in lower titers in comparison to the ones produced with the smaller p8.91 plasmid. Even though with the use of pNL4.3 in the transfection reaction the ratio between gag-pol and luciferase is maintained stable as they are both unified in the same construct, the application of p8.91 together with pCSFLW might offer an enhanced biosafety profile, as the genes compartmentalization across multiple plasmids mitigates the risk of recombination events (Pauwels K *et al*., 2009; Tareen SU *et al*., 2013).

The main advantage of applying the VSV platform for viral pseudotypes generation is that it represents a time-saving procedure. In practical terms, when producing lentiviral pseudotypes from the day of cell seeding until readout of PVs titer a total of 8 days go by. On the other hand, titer readout of VSV based pseudotypes is within 5 days from cell seeding. Assay times are reduced due to cytoplasmic VSV replication, which allows reporter expression to be detected within 24 hours after transduction (Jayakar HR *et al*., 2004; Toon K *et al*., 2021). Moreover, in titration and neutralization assays an appropriate target cell line is necessary, therefore the backbone can determine whether the PV is able to infect the required cell line. As an example, the VSV system represents an alternative for the production of those PV that require monkey derived cells which are resistant to HIV-1 infection (Toon K *et al*., 2021). Overall, having two different available platforms for viral pseudotypes production allows flexibility for those envelope proteins that show preferential pseudotyping with a specific backbone (Toon K *et al*., 2021).

Conspicuously, when the VSV platform is used for PVs production, it is possible that VSV

virus residual mixes with the pseudovirus. This may complicate titration and neutralization assays as the G protein of the helper virus could reassemble on the newly produced particles causing background noise; for this reason, it is necessary to use the least possible amount of helper VSV for pseudoviral production (Li Q *et al*., 2018; Xiang Q *et al*., 2022). With the purpose of demonstrating that residual VSV-ΔG-LUC*G does not contaminate the resulting titer of those PVs produced with the VSV platform, neutralization assays are performed with anti-VSV-G antibody. Since the anti-VSV-G antibody does not have a neutralizing titer against the PVs produced with the VSV platform, it is possible to deduce that excess VSV does not interfere with pseudovirus-based assay.

Neutralization assays are essential tools for quantifying the presence of functional neutralizing antibodies within serum samples. For viruses classified as Category 3 and 4 biosafety level pathogens, pseudotyped viruses enable extensive and widespread serum/plasma screening for the detection of antibodies against viral entry, to be conducted safely in a BSL-2 laboratory. Neutralization assays performed with viral pseudotypes have consistently demonstrated a robust correlation with those utilizing authentic, live viruses, thereby establishing their validity as critical tools in virological and immunological research (D'Apice L *et al*., 2022; Fantoni T *et al*., 2023). Recent studies have underscored this concordance across various viral systems. For example, a comprehensive systematic review and meta-analysis confirmed a high level of correlation between pseudotyped virus and authentic virus neutralization assays (Cantoni D *et al*., 2023). In the context of SARS-CoV-2, comparative analyses assessing vaccine immunogenicity against variants have shown PBNAs to have sensitivities and specificities exceeding 90%, with accuracy rates approaching 99% when compared to live virus neutralization assays (Gao C *et al*., 2025). This strong correlation and functional mimicry validate the use of pseudotyped viruses as reliable surrogates that enable standardized and rapid assessment of neutralizing antibody responses in clinical and research settings.

The usage of an international standard, incorporating a common unit and value for neutralizing antibody titers and antibody responses, is crucial for ensuring comparable diagnostic results in neutralization studies. There is a large variety of available neutralization antibody tests and comparing outcomes from different assays remains challenging. Moreover, variations in experimental results across different laboratories can arise from

disparities in interpretation, detection equipment, and protocols. Therefore, international standards for viral diagnosis are indispensable to calibrate measurements obtained from diverse methods or laboratories (Liu KT *et al*., 2022). Furthermore, the ability to evaluate vaccine candidates using harmonized assays with a reference reagent will support the identification and prioritization of the most promising options for progression into large-scale and expensive phase III clinical trials. Incorporating standards into assays can also help streamline the regulatory approval process. In fact, WHO guidance recommends that, when available, International Standard should be used for calibrating assays and reporting results (Mattiuzzo G *et al*., 2019).

In this work, the pseudotype-based neutralization assays study consistently delivered the anticipated outcomes, thereby validating the integrity and utility of the developed pseudotype system. All selected positive controls exhibited robust neutralization activity against their respective viral pseudotype confirming the effective blocking of PVs entry. Conversely, the absence of any detectable neutralization activity in the serum-minus controls ruled out non-specific inhibitory effects. These cumulative results affirm the functional integrity of the produced pseudotypes library, supporting its promising application in different serological studies, including vaccine efficacy assessment and epidemiological surveillance.

8 Bibliography

Abad ML, Verdura T, Vela A, et al. *Construction and characterization of a minimized version of the HIV-1 pNL4-3 plasmid and its application for pseudotyping HIV-1 vectors*. Mol Biotechnol. 2004;28(2):87-95. doi:10.1385/MB:28:2:087

Abdelazim M, Abdelkader R, Ali A, et al. *A longitudinal study of Middle East respiratory syndrome coronavirus (MERS-CoV) in dromedary camels*. BMC Vet Res. 2023;19(1):228. Published 2023 Nov 2. doi:10.1186/s12917-023-03769-z

Abdelrahman Z, Li M, Wang X. *Comparative Review of SARS-CoV-2, SARS-CoV, MERS-CoV, and Influenza A Respiratory Viruses*. Front Immunol. 2020;11:552909. Published 2020 Sep 11. doi:10.3389/fimmu.2020.552909

Abdullah S, Chang LY, Rahmat K, Goh KJ, Tin C, Lumpur K. *Late-onset Nipah virus encephalitis 11 years after the initial outbreak: a case report*. Neurology Asia. 2012;17(1):71. https://neurologyasia.org/articles/neuroasia-2012-17(1)-071.pdf

Ahmad B, Sagide M, Ntamwinja S, et al. *National burden of Ebola virus disease in Democratic Republic of the Congo: the urgency to act*. Ann Med Surg (Lond). 2024;86(8):4579-4585. Published 2024 Jun 21. doi:10.1097/MS9.0000000000002213

Ahmed MM, Okesanya OJ, Ukoaka BM, Ibrahim AM, Lucero-Prisno DE 3rd. *Vesicular Stomatitis Virus: Insights into Pathogenesis, Immune Evasion, and Technological Innovations in Oncolytic and Vaccine Development*. Viruses. 2024;16(12):1933. Published 2024 Dec 18. doi:10.3390/v16121933

Al-Tawfiq JA, Al Johani S, Memish ZA. *MERS-CoV remains a persistent threat amid global events*. J Infect Public Health. 2024;17(8):102487. doi:10.1016/j.jiph.2024.102487

Ameni G, Zewude A, Tulu B, et al. *A Narrative Review on the Pandemic Zoonotic RNA Virus Infections Occurred During the Last 25 Years*. J Epidemiol Glob Health. 2024;14(4):1397-1412. doi:10.1007/s44197-024-00304-7

Antonelli R, Forconi V, Molesti E, et al. *A validated and standardized pseudotyped microneutralization assay as a safe and powerful tool to measure LASSA virus neutralising*

antibodies for vaccine development and comparison. F1000Res. 2024;13:534. Published 2024 Oct 14. doi:10.12688/f1000research.149578.2

Arienzo A, Gallo V, Tomassetti F, Pitaro N, Pitaro M, Antonini G. *A narrative review of alternative transmission routes of COVID 19: what we know so far*. Pathog Glob Health. 2023;117(8):681-695. doi:10.1080/20477724.2023.2228048

Artik Y, Cesur NP, Laçin N. *SARS-COV-2 mutations, diagnosis and their concern*. Archives of Molecular Biology and Genetics. 2022;1(2). doi:10.33696/genetics.1.008

Asogun DA, Günther S, Akpede GO, Ihekweazu C, Zumla A. *Lassa Fever: Epidemiology, Clinical Features, Diagnosis, Management and Prevention*. Infect Dis Clin North Am. 2019;33(4):933-951. doi:10.1016/j.idc.2019.08.002

Assiri A, McGeer A, Perl TM, et al. *Hospital outbreak of Middle East respiratory syndrome coronavirus* [published correction appears in N Engl J Med. 2013 Aug 29;369(9):886]. N Engl J Med. 2013;369(5):407-416. doi:10.1056/NEJMoa1306742

Azarm KD, Lee B. *Differential Features of Fusion Activation within the Paramyxoviridae*. Viruses. 2020;12(2):161. Published 2020 Jan 30. doi:10.3390/v12020161

Barbiero VK. *Ebola: A Hyperinflated Emergency*. Glob Health Sci Pract. 2020;8(2):178-182. Published 2020 Jun 30. doi:10.9745/GHSP-D-19-00422

Baseler L, Chertow DS, Johnson KM, Feldmann H, Morens DM. *The Pathogenesis of Ebola Virus Disease*. Annu Rev Pathol. 2017 Jan 24;12:387-418. doi: 10.1146/annurev-pathol-052016-100506. PMID: 27959626.

Bentley EM, Mather ST, Temperton NJ. *The use of pseudotypes to study viruses, virus sero-epidemiology and vaccination*. Vaccine. 2015;33(26):2955-2962. doi:10.1016/j.vaccine.2015.04.071.

Besson ME, Pépin M, Metral PA. *Lassa Fever: Critical Review and Prospects for Control*. Trop Med Infect Dis. 2024;9(8):178. Published 2024 Aug 14. doi:10.3390/tropicalmed9080178

Brake DA, Kuhn JH, Marsh GA, Beer M, Fine JB. *Challenges and Opportunities in the Use of High and Maximum Biocontainment Facilities in Developing and Licensing Risk Group 3 and Risk Group 4 Agent Veterinary Vaccines*. ILAR J. 2022;61(1):46-61. doi:10.1093/ilar/ilab004

Brauburger K, Hume AJ, Mühlberger E, Olejnik J. *Forty-five years of Marburg virus research*. Viruses. 2012;4(10):1878-1927. Published 2012 Oct 1. doi:10.3390/v4101878

Breman JG, Heymann DL, Lloyd G, et al. *Discovery and Description of Ebola Zaire Virus in 1976 and Relevance to the West African Epidemic During 2013-2016*. J Infect Dis. 2016;214(suppl 3):S93-S101. doi:10.1093/infdis/jiw207

Brito C, Falcão MB, De Fatima Pessoa Militão De Albuquerque M, Cerqueira-Silva T, Teixeira MG, De Oliveira Franca RF. *Chikungunya: From hypothesis to evidence of increased severe disease and fatalities*. Viruses. 2025;17(1):62. doi:10.3390/v17010062

Cai M, Liu H, Jiang F, et al. *Analysis of the evolution, infectivity and antigenicity of circulating rabies virus strains*. Emerg Microbes Infect. 2022;11(1):1474-1487. doi:10.1080/22221751.2022.2078742

Cantoni D, Wilkie C, Bentley EM, et al. *Correlation between pseudotyped virus and authentic virus neutralisation assays, a systematic review and meta-analysis of the literature*. Front Immunol. 2023;14:1184362. Published 2023 Sep 18. doi:10.3389/fimmu.2023.1184362

Carnell GW, Ferrara F, Grehan K, Thompson CP, Temperton NJ. *Pseudotype-based neutralization assays for influenza: a systematic analysis*. Front Immunol. 2015;6:161. Published 2015 Apr 29. doi:10.3389/fimmu.2015.00161

Centers for Disease Control and Prevention (CDC). *Treatment and Prevention of Chikungunya Virus Disease*. Chikungunya Virus. Published May 15, 2024. https://www.cdc.gov/chikungunya/hcp/treatment-prevention/index.html. Date Accessed: 27 March 2025.

Cerqueira-Silva T, Pescarini JM, Cardim LL, et al. *Risk of death following chikungunya virus disease in the 100 Million Brazilian Cohort, 2015–18: a matched cohort study and self-controlled case series*. The Lancet Infectious Diseases. 2024;24(5):504-513.

doi:10.1016/s1473-3099(23)00739-9

Chaudhary M, Cutland CL, Bonet M, et al. *Burden of Lassa fever disease in pregnant women and children and options for prevention*. Vaccine. Published online November 1, 2024. doi:10.1016/j.vaccine.2024.126479

Chen Q, Tang K, Zhang X, Chen P, Guo Y. *Establishment of pseudovirus infection mouse models for in vivo pharmacodynamics evaluation of filovirus entry inhibitors* [published correction appears in Acta Pharm Sin B. 2020 Aug;10(8):1586-1587. doi: 10.1016/j.apsb.2020.06.010]. Acta Pharm Sin B. 2018;8(2):200-208. doi:10.1016/j.apsb.2017.08.003

Chen Y, Wang P, Zhang FN, et al. *Sensors for surveillance of RNA viruses: a One Health perspective*. Lancet Microbe. 2025;6(6):101029. doi:10.1016/j.lanmic.2024.101029

Chung YS, Lam CY, Tan PH, Tsang HF, Wong SC. *Comprehensive Review of COVID-19: Epidemiology, Pathogenesis, Advancement in Diagnostic and Detection Techniques, and Post-Pandemic Treatment Strategies*. Int J Mol Sci. 2024;25(15):8155. Published 2024 Jul 26. doi:10.3390/ijms25158155

Côté M, Misasi J, Ren T, et al. *Small molecule inhibitors reveal Niemann-Pick C1 is essential for Ebola virus infection*. Nature. 2011;477(7364):344-348. Published 2011 Aug 24. doi:10.1038/nature10380

Cruz-Cardenas JA, Gutierrez M, López-Arredondo A, et al. *A pseudovirus-based platform to measure neutralizing antibodies in Mexico using SARS-CoV-2 as proof-of-concept*. Sci Rep. 2022;12(1):17966. Published 2022 Oct 26. doi:10.1038/s41598-022-22921-7

Cucinotta D, Vanelli M. *WHO Declares COVID-19 a Pandemic*. Acta Biomed. 2020;91(1):157-160. Published 2020 Mar 19. doi:10.23750/abm.v91i1.9397

Cui Q, Huang W. *Application of Pseudotyped Viruses*. Adv Exp Med Biol. 2023;1407:45-60. doi:10.1007/978-981-99-0113-5_3

Cunha RVD, Trinta KS. *Chikungunya virus: clinical aspects and treatment - A Review*. Mem Inst Oswaldo Cruz. 2017;112(8):523-531. doi:10.1590/0074-02760170044

D'Apice L, Trovato M, Gramigna G, et al. *Comparative analysis of the neutralizing activity against SARS-CoV-2 Wuhan-Hu-1 strain and variants of concern: Performance evaluation of a pseudovirus-based neutralization assay*. Front Immunol. 2022;13:981693. Published 2022 Sep 26. doi:10.3389/fimmu.2022.981693

Das M, Chakraborty U, Sinha M, Kool A, Parveen S, Das S. *Newer Conventional and Nonconventional Treatment Strategy of Chikungunya Fever along with a Review of its Virology and Epidemiology*. Acta Scientific Pharmaceutical Sciences. 2021;5(3):13-23. doi:10.31080/asps.2021.05.0675

de Lima Cavalcanti TYV, Pereira MR, de Paula SO, Franca RFO. *A Review on Chikungunya Virus Epidemiology, Pathogenesis and Current Vaccine Development*. Viruses. 2022;14(5):969. Published 2022 May 5. doi:10.3390/v14050969

Du J, Lang HM, Ma Y, et al. *Global trends in COVID-19 incidence and case fatality rates (2019-2023): a retrospective analysis*. Front Public Health. 2024;12:1355097. Published 2024 Jul 29. doi:10.3389/fpubh.2024.1355097

Dupuy LC, Spiropoulou CF, Towner JS, Spengler JR, Sullivan NJ, Montgomery JM. *Filoviruses: Scientific Gaps and Prototype Pathogen Recommendation*. J Infect Dis. 2023;228(Suppl 6):S446-S459. doi:10.1093/infdis/jiad362

Fantoni T, Bissoli M, Stefani C, et al. *Pseudotyped Viruses As a Molecular Tool to Monitor Humoral Immune Responses Against SARS-CoV-2 Via Neutralization Assay*. J Vis Exp. 2023;(201):10.3791/65658. Published 2023 Nov 21. doi:10.3791/65658

Ferrara F, Temperton N. *Pseudotype Neutralization Assays: From Laboratory Bench to Data Analysis*. Methods Protoc. 2018;1(1):8. Published 2018 Jan 22. doi:10.3390/mps1010008

Forni D, Sironi M. *Population structure of Lassa Mammarenavirus in West Africa*. Viruses. 2020;12(4):437. Published 2020 Apr 13. doi:10.3390/v12040437

Freppel W, Silva LA, Stapleford KA, Herrero LJ. *Pathogenicity and virulence of chikungunya virus*. Virulence. 2024;15(1):2396484. doi:10.1080/21505594.2024.2396484

Fung TS, Liu DX. *Human Coronavirus: Host-Pathogen Interaction*. Annu Rev Microbiol.

2019;73:529-557. doi:10.1146/annurev-micro-020518-115759

Gao C, Yi J, Baidoo A, et al. *Comparative analysis of neutralization assays performed using live SARS-CoV-2 virus and pseudovirus to assess immunogenicity of a bivalent SARS-CoV-2 protein vaccine in humans*. Front Immunol. 2025;16:1650083. Published 2025 Sep 23. doi:10.3389/fimmu.2025.1650083

Garry RF. *Lassa fever - the road ahead*. Nat Rev Microbiol. 2023;21(2):87-96. doi:10.1038/s41579-022-00789-8-

Garry RF. *Lassa Virus Structural Biology and Replication*. Curr Top Microbiol Immunol. 2023;440:147-164. doi:10.1007/82_2023_262

Golke A, Piekarska K, Dzieciątkowski T. *Coronaviruses - a new old menace*. Postepy Biochem. 2021;66(4):303-308. Published 2021 Jan 5. doi:10.18388/pb.2020_357

González-Maldonado P, Alvarenga N, Burgos-Edwards A, et al. *Screening of Natural Products Inhibitors of SARS-CoV-2 Entry*. Molecules. 2022;27(5):1743. Published 2022 Mar 7. doi:10.3390/molecules27051743

Goodsell DS. *Ebola virus proteins*. RCSB Protein Data Bank. September 2014. doi:10.2210/rcsb_pdb/mom_2014_10

Gozalo AS, Clark TS, Kurtz DM. *Coronaviruses: Troubling Crown of the Animal Kingdom*. Comp Med. 2023;73(1):6-44. doi:10.30802/AALAS-CM-21-000092

Grant DS, Samuels RJ, Garry RF, Schieffelin JS. *Lassa Fever Natural History and Clinical Management. Curr Top Microbiol Immunol*. 2023;440:165-192. doi:10.1007/82_2023_263

Groseth A, Hoenen T. *Novel filoviruses: indication of a global threat or cause to reassess our risk perception?*. Npj Viruses. 2024;2:38. Published 2024 Aug 21. doi:10.1038/s44298-024-00050-4

Guito JC, Kirejczyk SGM, Schuh AJ, et al. *Coordinated inflammatory responses dictate Marburg virus control by reservoir bats*. Nat Commun. 2024;15(1):1826. Published 2024 Feb 28. doi:10.1038/s41467-024-46226-7

Günther S, Lenz O. *Lassa virus*. Crit Rev Clin Lab Sci. 2004;41(4):339-390. doi:10.1080/10408360490497456

Gupta SK, Minocha R, Thapa PJ, Srivastava M, Dandekar T. *Role of the Pangolin in Origin of SARS-CoV-2: An Evolutionary Perspective*. Int J Mol Sci. 2022;23(16):9115. Published 2022 Aug 14. doi:10.3390/ijms23169115

Harne R, Williams B, Abdelal HFM, Baldwin SL, Coler RN. *SARS-CoV-2 infection and immune responses*. AIMS Microbiol. 2023;9(2):245-276. Published 2023 Mar 29. doi:10.3934/microbiol.2023015

Hastie KM, Melnik LI, Cross RW, et al. *The Arenaviridae Family: Knowledge Gaps, Animal Models, Countermeasures, and Prototype Pathogens*. J Infect Dis. 2023;228(Suppl 6):S359-S375. doi:10.1093/infdis/jiac266

Hewson R. *Understanding Viral Haemorrhagic Fevers: Virus Diversity, Vector Ecology, and Public Health Strategies*. Pathogens. 2024;13(10):909. Published 2024 Oct 18. doi:10.3390/pathogens13100909

Hingorani KS, Bhadola S, Cervantes-Arslanian AM. *COVID-19 and the brain*. Trends Cardiovasc Med. 2022;32(6):323-330. doi:10.1016/j.tcm.2022.04.004

Hoffmann M, Kleine-Weber H, Schroeder S, et al. *SARS-CoV-2 Cell Entry Depends on ACE2 and TMPRSS2 and Is Blocked by a Clinically Proven Protease Inhibitor*. Cell. 2020;181(2):271-280.e8. doi:10.1016/j.cell.2020.02.052

Hollingshead CM, Swinkels HM, Shah SU. *Ebola Virus Disease*. In: StatPearls. Treasure Island (FL): StatPearls Publishing; March 1, 2024.

Huang AS, Palma EL, Hewlett N, Roizman B. *Pseudotype formation between enveloped RNA and DNA viruses*. Nature. 1974;252(5485):743-745. doi:10.1038/252743a0

Hunter N, Rathish B. *Marburg Virus Disease*. In: StatPearls. Treasure Island (FL): StatPearls Publishing; February 6, 2025.

Husby ML, Stahelin RV. *Negative-sense RNA viruses: An underexplored platform for examining virus-host lipid interactions*. Mol Biol Cell. 2021;32(20):pe1. doi:10.1091/mbc.E19-09-0490

Igarashi M, Hirokawa T, Takadate Y, Takada A. *Structural Insights into the Interaction of Filovirus Glycoproteins with the Endosomal Receptor Niemann-Pick C1: A Computational Study*. Viruses. 2021;13(5):913. Published 2021 May 14. doi:10.3390/v13050913

Irfan H, Ahmed A. *Advancements in chikungunya virus management: FDA approval of ixchiq vaccine and global perspectives*. Health Sci Rep. 2024;7(6):e2183. Published 2024 Jun 21. doi:10.1002/hsr2.2183

İzmir O, Lebcir RM, Oypan O. *Exploring pandemic preparedness through public perception and its impact on health service quality, attitudes, and healthcare image*. Sci Rep. 2025;15(1):17545. Published 2025 May 20. doi:10.1038/s41598-025-95488-8

Izudi J, Bajunirwe F. *Case fatality rate for Ebola disease, 1976-2022: A meta-analysis of global data*. J Infect Public Health. 2024;17(1):25-34. doi:10.1016/j.jiph.2023.10.020

Jacob ST, Crozier I, Fischer WA 2nd, et al. *Ebola virus disease*. Nat Rev Dis Primers. 2020;6(1):13. Published 2020 Feb 20. doi:10.1038/s41572-020-0147-3

Jarczak D, Nierhaus A. *Cytokine Storm-Definition, Causes, and Implications*. Int J Mol Sci. 2022;23(19):11740. Published 2022 Oct 3. doi:10.3390/ijms231911740

Jayakar HR, Jeetendra E, Whitt MA. *Rhabdovirus assembly and budding*. *Virus Res*. 2004;106(2):117-132. doi:10.1016/j.virusres.2004.08.009

Kaiser Family Foundation (KFF). *The U.S. Government and the World Health Organization*, June 13, 2024, https://www.kff.org/global-health-policy/fact-sheet/the-u-s-government-and-the-world-health-organization/ . Date Accessed: 23 October 2024.

Kalkeri R, Cai Z, Lin S, Farmer J, Kuzmichev YV, Koide F. *SARS-CoV-2 Spike Pseudoviruses: A Useful Tool to Study Virus Entry and Address Emerging Neutralization Escape Phenotypes*. Microorganisms. 2021;9(8):1744. Published 2021 Aug 16. doi:10.3390/microorganisms9081744

Kamorudeen RT, Adedokun KA, Olarinmoye AO. *Ebola outbreak in West Africa, 2014 - 2016: Epidemic timeline, differential diagnoses, determining factors, and lessons for future response*. J Infect Public Health. 2020;13(7):956-962. doi:10.1016/j.jiph.2020.03.014

Kannan S, Subbaram K, Ali S, Kannan H. *Molecular Characterization and Amino Acid Homology of Nucleocapsid (N) Protein in SARS-CoV-1, SARS-CoV-2, MERS-CoV, and Bat Coronavirus*. J Pure Appl Microbiol. 2020;14(suppl 1):757-763. doi: 10.22207/JPAM.14.SPL1.13

Kawai K, Kawai AT, Wollan P, Yawn BP. *Adverse impacts of chronic pain on health-related quality of life, work productivity, depression and anxiety in a community-based study*. Fam Pract. 2017;34(6):656-661. doi:10.1093/fampra/cmx034

Kayem ND, Benson C, Aye CYL, et al. *Ebola virus disease in pregnancy: a systematic review and meta-analysis*. Trans R Soc Trop Med Hyg. 2022;116(6):509-522. doi:10.1093/trstmh/trab180

Keshta AS, Mallah SI, Al Zubaidi K, et al. *COVID-19 versus SARS: A comparative review*. J Infect Public Health. 2021;14(7):967-977. doi:10.1016/j.jiph.2021.04.007

Khan S, Akbar SMF, Mahtab MA, et al. *Twenty-five years of Nipah outbreaks in Southeast Asia: A persistent threat to global health*. IJID Reg. 2024;13:100434. Published 2024 Aug 26. doi:10.1016/j.ijregi.2024.100434

Khetawat D, Broder CC. *A functional henipavirus envelope glycoprotein pseudotyped lentivirus assay system*. *Virol J*. 2010;7:312. Published 2010 Nov 12. doi:10.1186/1743-422X-7-312

King B, Temperton NJ, Grehan K, et al. *Technical considerations for the generation of novel pseudotyped viruses*. Future Virology. 2016;11(1):47-59. doi:https://doi.org/10.2217/fvl.15.106

Kirtipal N, Bharadwaj S, Kang SG. *From SARS to SARS-CoV-2, insights on structure, pathogenicity and immunity aspects of pandemic human coronaviruses*. Infect Genet Evol. 2020;85:104502. doi:10.1016/j.meegid.2020.104502

Kortepeter MG, Dierberg K, Shenoy ES, Cieslak TJ; Medical Countermeasures Working Group of the National Ebola Training and Education Center's (NETEC) Special Pathogens Research Network (SPRN). *Marburg virus disease: A summary for clinicians*. Int J Infect Dis. 2020;99:233-242. doi:10.1016/j.ijid.2020.07.042

Kuehn R, Ryan H, Okwaraeke KC, et al. *Vaccines for preventing Ebola virus disease*. Cochrane Database Syst Rev. 2024;11(11):CD015828. Published 2024 Nov 19. doi:10.1002/14651858.CD015828

Kuhn JH, Amarasinghe GK, Basler CF, et al. *ICTV Virus Taxonomy Profile: Filoviridae*. J Gen Virol. 2019;100(6):911-912. doi:10.1099/jgv.0.001252

Languon S, Quaye O. *Impacts of the Filoviridae family*. Curr Opin Pharmacol. 2021;60:268-274. doi:10.1016/j.coph.2021.07.016

Li Q, Liu Q, Huang W, Li X, Wang Y. *Current status on the development of pseudoviruses for enveloped viruses*. Rev Med Virol. 2018;28(1):e1963. doi:10.1002/rmv.1963

Li X, Mi Z, Liu Z, Rong P. *SARS-CoV-2: pathogenesis, therapeutics, variants, and vaccines*. Front Microbiol. 2024;15:1334152. Published 2024 Jun 13. doi:10.3389/fmicb.2024.1334152

Liu KT, Han YJ, Wu GH, Huang KA, Huang PN. *Overview of Neutralization Assays and International Standard for Detecting SARS-CoV-2 Neutralizing Antibody*. Viruses. 2022;14(7):1560. Published 2022 Jul 18. doi:10.3390/v14071560

Løkke FB, Hansen KS, Dalgaard LS, Öbrink-Hansen K, Schiøttz-Christensen B, Leth S. *Long-term complications after infection with SARS-CoV-1, influenza and MERS-CoV - Lessons to learn in long COVID?*. Infect Dis Now. 2023;53(8):104779. doi:10.1016/j.idnow.2023.104779

Luby SP, Gurley ES, Hossain MJ. *Transmission of human infection with Nipah virus*. Clin Infect Dis. 2009;49(11):1743-1748. doi:10.1086/647951

Madariaga M, Ticona E, Resurrecion C. *Chikungunya: bending over the Americas and the rest of the world*. Braz J Infect Dis. 2016;20(1):91-98. doi:10.1016/j.bjid.2015.10.004

Mandary MB, Masomian M, Poh CL. *Impact of RNA Virus Evolution on Quasispecies Formation and Virulence*. Int J Mol Sci. 2019;20(18):4657. Published 2019 Sep 19. doi:10.3390/ijms20184657

Mandl JN, Ahmed R, Barreiro LB, et al. *Reservoir host immune responses to emerging zoonotic viruses*. Cell. 2015;160(1-2):20-35. doi:10.1016/j.cell.2014.12.003

Martins KA, Wolfe DN. *Marburg Virus Medical Countermeasures*. Methods Mol Biol. 2025;2877:25-43. doi:10.1007/978-1-0716-4256-6_2

Mattiuzzo G, Bentley EM, Page M. *The Role of Reference Materials in the Research and Development of Diagnostic Tools and Treatments for Haemorrhagic Fever Viruses*. Viruses. 2019;11(9):781. Published 2019 Aug 24. doi:10.3390/v11090781

McKee CD, Islam A, Rahman MZ, et al. *Nipah Virus Detection at Bat Roosts after Spillover Events, Bangladesh, 2012-2019*. Emerg Infect Dis. 2022;28(7):1384-1392. doi:10.3201/eid2807.212614

Mishra G, Prajapat V, Nayak D. Advancements in Nipah virus treatment: Analysis of current progress in vaccines, antivirals, and therapeutics. Immunology. 2023;171(2):155-169. doi:10.1111/imm.13695

Mohd HA, Al-Tawfiq JA, Memish ZA. *Middle East Respiratory Syndrome Coronavirus (MERS-CoV) origin and animal reservoir*. Virol J. 2016;13:87. Published 2016 Jun 3. doi:10.1186/s12985-016-0544-0

Mougari S, Gonzalez C, Reynard O, Horvat B. *Fruit bats as natural reservoir of highly pathogenic henipaviruses: balance between antiviral defense and viral toleranceInteractions between Henipaviruses and their natural host, fruit bats*. Curr Opin Virol. 2022;54:101228. doi:10.1016/j.coviro.2022.101228

Muratov EN , Amaro R , Andrade CH , et al. *A critical overview of computational approaches employed for COVID-19 drug discovery*. Chem Soc Rev. 2021;50(16):9121-9151. doi:10.1039/d0cs01065k

Muvunyi CM, Ngabonziza JC, Bigirimana N, et al. *Emerging threat of Marburg virus disease:*

Epidemiology, clinical management, and the One Health Strategy for prevention and Control. Preprints. Published online October 11, 2024. doi:10.20944/preprints202410.0942.v1

Navaratnarajah CK, Generous AR, Yousaf I, Cattaneo R. *Receptor-mediated cell entry of paramyxoviruses: Mechanisms, and consequences for tropism and pathogenesis*. *J Biol Chem*. 2020;295(9):2771-2786. doi:10.1074/jbc.REV119.009961

Nicastri E, Kobinger G, Vairo F, et al. *Ebola Virus Disease: Epidemiology, Clinical Features, Management, and Prevention*. Infect Dis Clin North Am. 2019;33(4):953-976. doi:10.1016/j.idc.2019.08.005

Nnaji ND, Onyeaka H, Reuben RC, Uwishema O, Olovo CV, Anyogu A. *The deuce-ace of Lassa Fever, Ebola virus disease and COVID-19 simultaneous infections and epidemics in West Africa: clinical and public health implications*. Trop Med Health. 2021;49(1):102. Published 2021 Dec 30. doi:10.1186/s41182-021-00390-4

Nyenke CU, Konne FE, Nwalozie R, Precious-Ogbueri R. *Marbug virus disease: an overview*. Asian Journal of Research in Infectious Diseases. September 2022:15-21. doi:10.9734/ajrid/2022/v11i2213

O'Shea H, Blacklaws BA, Collins PJ, McKillen J, Fitzgerald R. *Viruses Associated With Foodborne Infections*. Reference Module in Life Sciences. 2019;B978-0-12-809633-8.90273-5. doi:10.1016/B978-0-12-809633-8.90273-5

Ohimain EI. *Ecology of Ebolaviruses*. Curr Opin Pharmacol. 2021;60:66-71. doi:10.1016/j.coph.2021.06.009

Panahi Y, Gorabi AM, Talaei S, et al. *An overview on the treatments and prevention against COVID-19*. Virol J. 2023;20(1):23. Published 2023 Feb 8. doi:10.1186/s12985-023-01973-9

Pauwels K, Gijsbers R, Toelen J, et al. *State-of-the-art lentiviral vectors for research use: risk assessment and biosafety recommendations*. Curr Gene Ther. 2009;9(6):459-474. doi:10.2174/156652309790031120

Peiris JS, Yuen KY, Osterhaus AD, Stöhr K. *The severe acute respiratory syndrome*. N Engl J Med. 2003;349(25):2431-2441. doi:10.1056/NEJMra032498

Pennington HN, Lee J. *Lassa virus glycoprotein complex review: insights into its unique fusion machinery*. Biosci Rep. 2022;42(2):BSR20211930. doi:10.1042/BSR20211930

Perrett HR, Brouwer PJM, Hurtado J, et al. *Structural conservation of Lassa virus glycoproteins and recognition by neutralizing antibodies*. Cell Rep. 2023;42(5):112524. doi:10.1016/j.celrep.2023.112524

Polgreen PM, Polgreen EL. *Emerging and Re-emerging Pathogens and Diseases, and Health Consequences of a Changing Climate*. Infectious Diseases. 2017;40-48.e2. doi:10.1016/B978-0-7020-6285-8.00004-6

Pustake M, Tambolkar I, Giri P, Gandhi C. *SARS, MERS and CoVID-19: An overview and comparison of clinical, laboratory and radiological features*. J Family Med Prim Care. 2022;11(1):10-17. doi:10.4103/jfmpc.jfmpc_839_21

Raabe V, Mehta AK, Evans JD; Science Working Group of the National Emerging Special Pathogens Training and Education Center (NETEC) Special Pathogens Research Network (SPRN). *Lassa Virus Infection: a Summary for Clinicians*. Int J Infect Dis. 2022;119:187-200. doi:10.1016/j.ijid.2022.04.004

Rabaan AA, Al-Ahmed SH, Haque S, et al. *SARS-CoV-2, SARS-CoV, and MERS-COV: A comparative overview*. Infez Med. 2020;28(2):174-184

Rabaan AA, Alenazy MF, Alshehri AA, et al. *An updated review on pathogenic coronaviruses (CoVs) amid the emergence of SARS-CoV-2 variants: A look into the repercussions and possible solutions*. J Infect Public Health. 2023;16(11):1870-1883. doi:10.1016/j.jiph.2023.09.004

Rathish B, Vaishnani K. *Nipah Virus*. In: StatPearls. Treasure Island (FL): StatPearls Publishing; April 24, 2023

Rezaverdinejad M. *A review of the epidemiology, pathogenesis and treatment of Lassa hemorrhagic fever virus*. 7th International Conference On New Findings in Medical and

Health Sciences With a Health Promotion Approach. Berlin, Germany. Published July 21, 2024. Date Accessed: 28 March 2025

Ribeiro S, Mairhofer J, Madeira C, et al. *Plasmid DNA size does affect nonviral gene delivery efficiency in stem cells*. Cell Reprogram. 2012;14(2):130-137. doi:10.1089/cell.2011.0093

Rizatdinova SN, Ershova AE, Astrakhantseva IV. *Pseudotyped Viruses: A Useful Platform for Pre-Clinical Studies Conducted in a BSL-2 Laboratory Setting*. Biomolecules. 2025;15(1):135. Published 2025 Jan 15. doi:10.3390/biom15010135

Rothan HA, Byrareddy SN. *The epidemiology and pathogenesis of coronavirus disease (COVID-19) outbreak*. J Autoimmun. 2020;109:102433. doi:10.1016/j.jaut.2020.102433

Rutten L, Gilman MSA, Blokland S, Juraszek J, McLellan JS, Langedijk JPM. *Structure-Based Design of Prefusion-Stabilized Filovirus Glycoprotein Trimers*. Cell Rep. 2020;30(13):4540-4550.e3. doi:10.1016/j.celrep.2020.03.025

Saberiyan M, Karimi E, Khademi Z, Movahhed P, Safi A, Mehri-Ghahfarrokhi A. *SARS-CoV-2: phenotype, genotype, and characterization of different variants*. Cell Mol Biol Lett. 2022;27(1):50. Published 2022 Jun 17. doi:10.1186/s11658-022-00352-6

Salam AP, Duvignaud A, Jaspard M, et al. *Ribavirin for treating Lassa fever: A systematic review of pre-clinical studies and implications for human dosing*. PLoS Negl Trop Dis. 2022;16(3):e0010289. Published 2022 Mar 30. doi:10.1371/journal.pntd.0010289

Salomon I. *Saudi Arabia's Middle East respiratory syndrome Coronavirus (MERS-CoV) outbreak: consequences, reactions, and takeaways*. Ann Med Surg (Lond). 2024;86(8):4668-4674. Published 2024 Jul 1. doi:10.1097/MS9.0000000000002336

Sedgwick RL, ElBohy O, Daly JM. *Role of pseudotyped viruses in understanding epidemiology, pathogenesis and immunity of viral diseases affecting both horses and humans*. Virology. 2024;597:110164. doi:10.1016/j.virol.2024.110164

Shifflett K, Marzi A. *Marburg virus pathogenesis - differences and similarities in humans and animal models*. Virol J. 2019;16(1):165. Published 2019 Dec 30. doi:10.1186/s12985-019-1272-z

Simons D. *Lassa fever cases suffer from severe underreporting based on reported fatalities*. Int Health. 2023;15(5):608-610. doi:10.1093/inthealth/ihac076

Sinn PL, Coffin JE, Ayithan N, Holt KH, Maury W. *Lentiviral Vectors Pseudotyped with Filoviral Glycoproteins*. Methods Mol Biol. 2017; 1628:65-78. doi:10.1007/978-1-4939-7116-9_5

Sinn PL, Hickey MA, Staber PD, et al. *Lentivirus vectors pseudotyped with filoviral envelope glycoproteins transduce airway epithelia from the apical surface independently of folate receptor alpha*. J Virol. 2003;77(10):5902-5910. doi:10.1128/jvi.77.10.5902-5910.2003

Srivastava S, Sharma D, Kumar S, et al. *Emergence of Marburg virus: a global perspective on fatal outbreaks and clinical challenges*. Front Microbiol. 2023;14:1239079. Published 2023 Sep 13. doi:10.3389/fmicb.2023.1239079

Sušac L, Vuong MT, Thomas C, et al. *Structure of a fully assembled tumor-specific T cell receptor ligated by pMHC*. Cell. 2022;185(17):3201-3213.e19. doi:10.1016/j.cell.2022.07.010

Tai W, He L, Zhang X, et al. *Characterization of the receptor-binding domain (RBD) of 2019 novel coronavirus: implication for development of RBD protein as a viral attachment inhibitor and vaccine*. Cell Mol Immunol. 2020;17(6):613-620. doi:10.1038/s41423-020-0400-4

Tani H, Morikawa S, Matsuura Y. *Development and Applications of VSV Vectors Based on Cell Tropism*. Front Microbiol. 2012;2:272. Published 2012 Jan 18. doi:10.3389/fmicb.2011.00272

Tareen SU, Nicolai CJ, Campbell DJ, et al. *A Rev-Independent gag/pol Eliminates Detectable psi-gag Recombination in Lentiviral Vectors*. Biores Open Access. 2013;2(6):421-430. doi:10.1089/biores.2013.0037

Te N, Ciurkiewicz M, van den Brand JMA, et al. *Middle East respiratory syndrome coronavirus infection in camelids*. Vet Pathol. 2022;59(4):546-555. doi:10.1177/03009858211069120

Tomori O, Kolawole MO. *Ebola virus disease: current vaccine solutions*. Curr Opin Immunol.

2021;71:27-33. doi:10.1016/j.coi.2021.03.008

Toon K, Bentley EM, Mattiuzzo G. *More Than Just Gene Therapy Vectors: Lentiviral Vector Pseudotypes for Serological Investigation*. Viruses. 2021;13(2):217. Published 2021 Jan 31. doi:10.3390/v13020217

Ukoaka BM, Okesanya OJ, Daniel FM, et al. *Updated WHO list of emerging pathogens for a potential future pandemic: Implications for public health and global preparedness*. Infez Med. 2024;32(4):463-477. Published 2024 Dec 1. doi:10.53854/liim-3204-5

Vaney MC, Duquerroy S, Rey FA. *Alphavirus structure: activation for entry at the target cell surface*. Curr Opin Virol. 2013;3(2):151-158. doi:10.1016/j.coviro.2013.04.003

Verma J, Subbarao N. *A comparative study of human betacoronavirus spike proteins: structure, function and therapeutics*. Arch Virol. 2021;166(3):697-714. doi:10.1007/s00705-021-04961-y

Vu DM, Jungkind D, Angelle Desiree LaBeaud. *Chikungunya Virus*. Clin Lab Med. 2017;37(2):371-382. doi:10.1016/j.cll.2017.01.008

Wang L, Lu D, Yang M, Chai S, Du H, Jiang H. *Nipah virus: epidemiology, pathogenesis, treatment, and prevention*. Front Med. 2024;18(6):969-987. doi:10.1007/s11684-024-1078-2

Wang M, Wang L, Leng P, Guo J, Zhou H. *Drugs targeting structural and nonstructural proteins of the chikungunya virus: A review*. Int J Biol Macromol. 2024;262(Pt 2):129949. doi:10.1016/j.ijbiomac.2024.129949

Wang Y, Zhou Z, Wu X, et al. *Pseudotyped Viruses*. Adv Exp Med Biol. 2023;1407:1-27. doi:10.1007/978-981-99-0113-5_1

Whitt MA. *Generation of VSV pseudotypes using recombinant ΔG-VSV for studies on virus entry, identification of entry inhibitors, and immune responses to vaccines*. J Virol Methods. 2010;169(2):365-374. doi:10.1016/j.jviromet.2010.08.006

Williams BA, Jones CH, Welch V, True JM. *Outlook of pandemic preparedness in a post-COVID-19 world*. NPJ Vaccines. 2023;8(1):178. Published 2023 Nov 20.

doi:10.1038/s41541-023-00773-0

World Health Organization (WHO), Research and Development Blueprint for Epidemics. *Pathogens Prioritization - A scientific framework for epidemic and pandemic research preparedness*. [Unpublished report]. June 2024. https://cdn.who.int/media/docs/default-source/consultation-rdb/prioritization-pathogens-v6final.pdf?sfvrsn=c98effa7_7&download=true . Date Accessed: 23 October 2024.

World Health Organization (WHO). *Marburg virus disease*. Published January 20, 2025. https://www.who.int/news-room/fact-sheets/detail/marburg-virus-disease . Date Accessed: 11 March 2025.

Wu C, Liu Y, Yang Y, et al. *Analysis of therapeutic targets for SARS-CoV-2 and discovery of potential drugs by computational methods*. Acta Pharm Sin B. 2020;10(5):766-788. doi:10.1016/j.apsb.2020.02.008

Xiang Q, Li L, Wu J, Tian M, Fu Y. Application of pseudovirus system in the development of vaccine, antiviral-drugs, and neutralizing antibodies. Microbiol Res. 2022;258:126993. doi:10.1016/j.micres.2022.126993

Xu RH, He JF, Evans MR, et al. *Epidemiologic clues to SARS origin in China*. Emerg Infect Dis. 2004;10(6):1030-1037. doi:10.3201/eid1006.030852

Yamada H, Sasaki SI, Tani H, et al. *A novel hamster model of SARS-CoV-2 respiratory infection using a pseudotyped virus* [published correction appears in Sci Rep. 2022 Dec 7;12(1):21138. doi: 10.1038/s41598-022-25678-1]. Sci Rep. 2022;12(1):11125. Published 2022 Jul 1. doi:10.1038/s41598-022-15258-8

Yun NE, Walker DH. *Pathogenesis of Lassa fever*. Viruses. 2012;4(10):2031-2048. Published 2012 Oct 9. doi:10.3390/v4102031

Zaki AM, van Boheemen S, Bestebroer TM, Osterhaus AD, Fouchier RA. *Isolation of a novel coronavirus from a man with pneumonia in Saudi Arabia* [published correction appears in N Engl J Med. 2013 Jul 25;369(4):394]. N Engl J Med. 2012;367(19):1814-1820. doi:10.1056/NEJMoa1211721

Zettl F, Meister TL, Vollmer T, et al. *Rapid Quantification of SARS-CoV-2-Neutralizing Antibodies Using Propagation-Defective Vesicular Stomatitis Virus Pseudotypes*. Vaccines (Basel). 2020;8(3):386. Published 2020 Jul 15. doi:10.3390/vaccines8030386

Zhang D, Qiu Z, Hao Y, et al. *Progress in the molecular epidemiology of Chikungunya Virus*. Animals and Zoonoses. Published online January 1, 2025. doi:10.1016/j.azn.2025.01.003

Zhang F, Li W, Feng J, et al. *SARS-CoV-2 pseudovirus infectivity and expression of viral entry-related factors ACE2, TMPRSS2, Kim-1, and NRP-1 in human cells from the respiratory, urinary, digestive, reproductive, and immune systems*. J Med Virol. 2021;93(12):6671-6685. doi:10.1002/jmv.27244

Zhang L, Lin D, Sun X, et al. *Crystal structure of SARS-CoV-2 main protease provides a basis for design of improved α-ketoamide inhibitors*. Science. 2020;368(6489):409-412. doi:10.1126/science.abb3405

Zhang X, Li M, Zhang N, et al. *SARS-CoV-2 Evolution: Immune Dynamics, Omicron Specificity, and Predictive Modeling in Vaccinated Populations*. Adv Sci (Weinh). 2024;11(40):e2402639. doi:10.1002/advs.202402639

Zhang X, Tang K, Guo Y. *The antifungal isavuconazole inhibits the entry of lassa virus by targeting the stable signal peptide-GP2 subunit interface of lassa virus glycoprotein*. Antiviral Res. 2020;174:104701. doi:10.1016/j.antiviral.2019.104701

Zhu X, Liu Y, Guo J, et al. *Effects of N-Linked Glycan on Lassa Virus Envelope Glycoprotein Cleavage, Infectivity, and Immune Response*. Virol Sin. 2021;36(4):774-783. doi:10.1007/s12250-021-00358-y